SOME STUDIES ON ICE SLURRY REFRIGERATION SYSTEM

By

RAJINDER SINGH
(Enrolment Number: Ph.D (DP-145/92)

Submitted

In partial fulfillment of the requirement of the degree of

DOCTOR OF PHILOSOPHY

To the

DEPARTMENT OF MECHANICAL ENGINEERING
DELHI COLLEGE OF ENGINEERING (NOW DTU)
UNIVERSITY OF DELHI
DELHI
NOVEMBER 2013

CERTIFICATE

This is to certify that the thesis entitled "**Some Studies on Ice Slurry Refrigeration System**" which is being submitted by **Mr. Rajinder Singh** (Enrolment Number - Ph.D (DP-145/92) to the Faculty of Technology, University of Delhi, Delhi, for the award of the degree of **Doctor of Philosophy** is a record of the original bonafide research work carried out by him under my guidance and supervision and has fulfilled the requirements for the submission of this thesis. The thesis, in our opinion, has attained a standard required for a Ph.D. degree of this University. The results contained in this thesis have not been submitted in part or full to any other university or institution for the award of any other degree or diploma.

Dr. S. S. Kachhwaha
Supervisor
[Associate Professor (on lien)
Mechanical Engineering Department
Delhi College of Engineering (Now DTU)
Delhi, India.]
Professor
School of Technology
Pandit Deendayal Petroleum University
Gandhinagar, India.

Dr. Raj Senani
Head of Department
Mechanical Engineering Department
Faculty of Technology,
University of Delhi, Delhi, India.

ACKNOWLEDGEMENTS

All praise to Almighty God, the creator and sustainer of the worlds. I wish to express my profound thanks to my supervisors Professor S. S. Kachhwaha for his invaluable guidance, constant motivation and moral support through out this study. It was their help and continuous encouragement in academic as well as personnel matters that has enabled this work to achieve its present form and status. It is with full humility that I desire to extend my sincere appreciation to them.

Thanks are due to Professor R.S.Mishra, Professor S. Maji, Dr. Samsher, Professor D. S. Nagesh, Dr. Amit Pal, and Dr.B.B Arora members of Research Advisory Committee for their valuable suggestions for improving the thesis.

I attribute the completion of this research work to the dedicatory prayers, moral support, and love and affection of my father, mother, elder brother, sister, mother-in-law, brother-in-law, sister -in-law and other family members. They have always been a major source of motivation and strength.

Finally, I express my sincere and hearty feelings to my wife Sumeet Kaur and son Divnit Singh for their moral support, patience and bearing with me during the crucial moments.

Rajinder Singh

ABSTRACT

Compared to commonly used brines, the application of ice slurries in indirect refrigeration systems shows interesting advantages, such as the possibility of enhanced thermal storage and the reduction of transport friction losses due to the higher volumetric heat capacity.

Among various ice slurry generation techniques, the scraped ice slurry generator is the most technologically developed and widely accepted ice slurry generation process. However, a widespread utilization of ice slurry systems has not taken place mainly attributed due to the high investment costs of commercially available ice slurry generators.

In the present research work, a scraped surface ice slurry generator test rig has been designed, developed and fabricated with the help of cost effective manufacturing processes. Initially a scraped surface ice slurry generator test rig of five litre capacity has been developed. Based on the encouraging results a scraped surface ice slurry generator of 74 litre capacity has been designed, developed and fabricated successfully through commonly used cost effective manufacturing processes employed by small and medium scale industries with a focus on collection of experimental data related to ice slurry production using 10%, 20%, 30% and 40% concentrations of antifreezes (PG, MEG and DEG). R410A (refrigerant blend having zero ODP) is used as primary refrigerant in the primary refrigeration circuit. The lowest temperatures achieved were -20.7 ^{0}C, -25.6 ^{0}C and -19.9 ^{0}C respectively for PG, MEG and DEG for 40 % depressant concentration. The COP of present ice slurry generation test rig varies between 2.30 to 3.33. Thermophysical properties are significantly different as compared to the chilled water. **Three distinct stages- cool down or chilling period, nucleation or unstable ice slurry generation period and stable ice slurry generation period were observed through historical time dependence curves.**

Experiments were conducted on a plate heat exchanger and heat transfer and pressure drop data were collected **for water to water and ice slurry to water flow. The depressants use for ice slurry production are PG and MEG. Thermo-hydraulic modeling for PHE is validated with the experimental data. The parameters included in thermo-hydraulic modeling are overall heat transfer coefficient, cooling duty and**

pressure drop. It can be concluded that the present formulation provides the relationship to predict heat transfer based on the allowable pressure drops are reasonably matching with experimental data. The thermo-hydraulic model is useful for the design of individual PHEs.

Keywords: Scraped surface ice slurry generator; Ice slurry; Depressants; Thermo-hydraulic modeling; Plate heat exchanger.

CONTENTS

List of Tables

List of Figures

NOTATIONS AND ABBREVIATIONS

Nomenclatures

A Heat transfer area, m^2

a, b, c, d Constants

b_1 Passage width, m

D_e Equivalent diameter, m

d_p Port diameter, m

f Fanning friction factor

G_p Mass velocity inside the port, $kg / m^2 s$

g Acceleration due to gravity, m / s^2

h Heat transfer coefficient, $W / m^2 K$

k_1, k_2, k_3 Constants

l Projected plate length, m

M Mass flow rate, kg / s

m Path number

m_p Mass flow rate per passage, kg / s

N Number of plates

Nu Nusselt number

n pass number

Pr Prandtl Number

Re Reynolds number

R_f Fouling factor, $m^2 K / W$

S Cross sectional area of passage, m^2

T Temperature, $^\circ$C

U Overall heat transfer coefficient, $W / m^2 K$

u Fluid velocity, m / s

V Volumetric flow rate, m^3 / s

w Plate width, m

ΔP Pressure drop, kPa

Greek symbols

δ	Plate thickness, m
ε	Thermal effectiveness
λ	Thermal conductivity, W / mK
ν	Kinematic viscosity, m^2 / s
μ	Dynamic viscosity, kg / ms
θ	Corrugation angle
σ	Coefficient
ρ	Fluid density, kg / m^3

Subscripts

1	Stream 1
2	Stream 2
in	Stream inlet
out	Stream outlet
w	Wall
elev.	Elevation
pr	Predicted

Acronyms

CFC – Chloro Fluoro Carbon

CFD - Computational Fluid Dynamics

CHS - Clathrate Hydrate Slurry

COP - Coefficient of Performance

DEG - Di-Ethylene Glycol

FDA - Food and Drug Administration

GA - Genetic Algorithm

HE - Heat Exchanger

HVAC - Heating, Ventilation, and Air Conditioning

IPF - Ice Packing Factor

LMTD- Log mean temperature difference

MATLAB - Matrix Laboratory

MEG - Mono Ethylene Glycol

MPG – Mono Propylene Glycol

N - Net Refrigerating Effect

NTU- Number of Transfer Units

NSF - National Science Foundation

ODP – Ozone Depletion Potential

PCM - Phase Change Material

PFHE - Plate-Fin Heat Exchanger

PG - Propylene Glycol

PHE - Plate heat exchanger

PVA - Poly Vinyl Alcohol

SSHE - Scraped Surface Heat Exchanger

SSISG - Scraped Surface Ice Slurry Generator

TBAB – Tetra-Butyl-Ammonium-Bromide

UDM - Ultrasonic Doppler Method

CHAPTER-I
INTRODUCTION

1.1. INDIRECT REFRIGERATION SYSTEM

Indirect refrigeration plants with secondary working fluids are frequently used all over the world. The discovery that some primary refrigerants contribute to global environmental effects has led to the phasing out of CFC refrigerants. Large primary refrigerant leaks in supermarkets and large heat pumps have focused attention on the use of indirect systems (factory built cooling units) with secondary fluids for a variety of applications. Further the primary refrigeration unit is designed as a compact chiller in a machine room with an extremely small refrigerant charge [1].

Indirect refrigeration systems are variants of the centralized direct expansion system (Figure 1.1). In a secondary system, the centralized refrigeration unit cools a secondary fluid that is circulated to the display cases and cold storage. By using indirect systems, the refrigerant charge can be reduced by 80-90%. If the refrigeration system can be located in a controlled environment (away from the application), indirect systems may use natural refrigerants, such as hydrocarbons, propane, butane or ammonia, which have negligible global warming potential. Due to the decreased refrigerant piping lengths among, some practitioners believe the emissions of refrigerants could be reduced to 2-4% of charge per year [2].

Secondary refrigeration systems are the best way to lower emissions from refrigeration plants since the charge needed to generate a certain refrigeration effect is reduced in the refrigeration system. The leakage of refrigerant is reduced by reducing the refrigerant piping lengths, the number of fittings, valves [2].

There are some drawbacks of indirect systems such as, higher investment cost for pump, additional heat exchanger and secondary fluid. Additional pumping power is required, though it can be quite small compared to the cooling capacity. In spite of

these drawbacks of indirect systems in comparison with direct ones, the earlier mentioned advantages have been main reasons for the move toward more indirect systems [1].

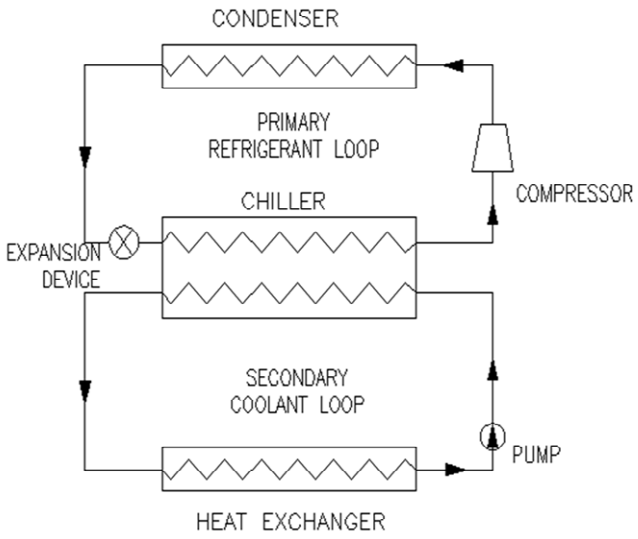

Fig 1.1 .Indirect System

.

1.2. ICE SLURRY AS SECONDARY FLUID

Ice slurry refers to a homogenous mixture of small ice particles (0.1 to 1 mm diameter) and carrier liquid. The liquid consists of a binary solution having water and a freezing point depressant. Sodium chloride, ethanol, ethylene glycol and propylene glycol are the four most commonly used freezing point depressants in industry [3]. Depending on the type of additive and additive concentration, the operating temperature for ice slurry can be chosen from 0 to at least -35ºC [2].

Ice slurry having many advantages due to latent heat of the ice. Ice slurries have higher heat transport capability than single-phase fluids. By using ice slurry it is possible to reduce the volume flow rate at a given cooling capacity; which reduces the required pipe dimensions and also allows smaller temperature changes over the cooling object, which leads to higher product quality. Using ice slurry with accumulation increases the possibility to build indirect systems without increasing the energy

consumption [2]. Ice slurry facilitates several efficiency improvements at temperatures below the freezing point of water, such as reductions in pumping energy consumption as well as reducing the required temperature difference in heat exchangers due to the beneficial thermo-physical properties of ice slurry [3].

The use of ice slurry enables the use of indirect refrigeration systems with small charge of the primary refrigerant as well as the possibility of ice slurry storage and the associated economic advantage. Further, the use of ice slurry gives the possibility of direct contact cooling and freezing of products.

Various applications of ice-slurry are comfort cooling, commercial refrigeration to industrial production processes, milk production, mine cooling, food processing and preservation; fish processing and some future applications are medical, fire fighting, ice pigging, artificial snow and transport application.

Further the existing ice slurry generator technology is energy efficient, environmental friendly and industrially viable alternative to conventional HVAC and refrigeration technologies.

Different techniques used for ice slurry generation are: scraped surface ice slurry generator, vacuum ice, direct contact generators with immiscible refrigerant, direct contact generators with immiscible liquid secondary refrigerant, supercooled brine method, hydro-scraped ice slurry generator, fluidized bed crystallizer, high-pressure ice slurry generator and recuperative ice making [4]. Among these most commonly used commercial technique is scraped surface ice slurry generator. The scraped surface ice slurry generator consists of a circular shell-and-coil type heat exchanger; where outer shell side is cooled by an evaporating refrigerant and inside surface is scraped by spring loaded rotating blades to prevent any deposition of ice crystals on the cooled surface.

1.3. OUTLINE OF THESIS

The thesis is organized into six chapters as discussed below:

Chapter 1 describes indirect refrigeration system, secondary refrigerants used in indirect refrigeration system, ice slurry as secondary fluid, and advantages of ice slurry used as secondary refrigerant.

Chapter 2 summaries the literature survey on various ice slurry generation techniques and comparative study of existing ice slurry generators, thermophysical properties of ice slurries, theoretical and experimental studies of ice slurries in plate heat exchangers. From the literature survey it emerges that:

(a) Detailed information for development and fabrication of scraped surface ice slurry generator through cost effective manufacturing processes employed by small and medium scale industries are not available in open literature.

(b) There are few experimental studies of ice slurries in plate heat exchanger with thermo-hydraulic modeling.

The present research work has, therefore, been carried out in the steps:

- Fabrication of a five litre capacity scraped surface ice slurry generator to understand the working and function for production of ice slurry mixtures.
- Based on experimental experience of five litre capacity ice slurry generator, design, development and fabrication of 74 litre capacity scraped surface ice slurry generator for commercial application through commonly used cost effective manufacturing processes employed by small and medium scale industries and collection of experimental data.
- Experimental heat transfer and pressure drop studies of ice slurries in plate heat exchanger.
- Thermo-hydraulic modeling of plate heat exchanger and validation with experimental data.

Chapter 3 summaries development and experimental data collection of small size ice slurry generator and large scraped surface ice slurry generator for industrial applications, system components, specifications, system assembly, system working and instrumentation. Experimental results, thermophysical data of ice slurry, first law analysis and economics of ice slurry generator is also discussed.

In Chapter 4, terminology of plate heat exchanger, mathematical modeling of plate heat exchanger, formulation for chilled water vs hot water and ice slurry vs hot water, formulation for thermophysical properties of ice slurry and solution methodology with the help of computer programming using MATLAB is summarized.

Chapter 5 summaries preparation of ice slurries, description of experimental setup, experimental procedure and data Collection, experimental results of chilled water vs hot water ice slurry vs hot water and comparison of ice slurry and chilled water.

Conclusions and scope for future work are given in Chapter 6. Scope for future work- system can be further optimized in future developments.

CHAPTER-II
LITERATURE REVIEW

Ice slurry generation and its industrial applications have been extensively studied by several researchers. A review of these is presented below in three major categories; viz. (a) classification of ice slurry generation techniques; (b) thermophysical properties; and (c) theoretical and experimental studies of ice slurries in plate heat exchanger.

2.1. CLASSIFICATION OF ICE SLURRY GENERATION TECHNIQUES

The most commonly used ice slurry generation technique is scraped surface ice slurry generator. This is described below.

In open literature different techniques used for ice slurry generation are: scraped surface ice slurry generator, vacuum ice, direct contact generators with immiscible refrigerant, direct contact generators with immiscible liquid secondary refrigerant, supercooled brine method, hydro-scraped ice slurry generator, fluidized bed crystallizer, high-pressure ice slurry generator and recuperative ice making [4].

2.1.1. SCRAPED SURFACE ICE SLURRY GENERATOR (SSISG)

Working principle of scraped surface ice slurry generator is shown in Fig 3.12(b): The SSISG consists of a circular shell-and-coil type heat exchanger, where outer shell side is cooled by an evaporating refrigerant and inside surface is scraped by spring loaded rotating blades to prevent any deposition of ice crystals on the cooled surface. This scraping action is required to prevent the formation of an ice layer on the inner walls of ice generator, which would otherwise introduce an additional thermal resistance and could seriously lower the heat transfer. Depressants are added to depress the freezing point of the solution to prevent the freeze-up of the ice generator walls and alternatively provide impact on the temperature driving force for heat transfer. Turbulence is mechanically induced into the ice slurry flow by the action of the rotating scarper blades

mounted in the centre of the circular cylinder, thus greatly increasing the heat transfer rates and facilitating the production of a homogeneous ice slurry mixture.

Heat transfer in presence of a high viscosity fluid may be substantially enhanced using heat exchangers supported by a mechanical agitation system that can also scrapen the exchange surface (Scraped Surface Heat Exchanger, SSHE). In this case, heat transfer efficiency depends strongly on exchanger and agitator geometries, agitation methods as well as fluid characteristics and heat transfer conditions. Heat transfer correlations for the SSHE installed in a commercial soft ice-cream machine presented by Saraceno et al. [5].

The study performed by Yataghene et al. [6] is focused on experimental analysis of the flow patterns inside scraped surface heat exchanger (SSHE) under isothermal and continuous flow conditions. Experimental flow pattern analyses are the basis for further experimental explorations of mixing and heat exchange mechanism.

Flow pattern in the tubes of an innovative scraped surface heat exchanger with reciprocating scrapers has been experimentally investigated by Solano et al. [7].

Turbulent fluid flow and related solid particle behaviour in the direct vicinity of the heat exchanging (HE) surface of a scraped heat exchanger crystallizer was studied by Pascual et al. [8]. The main goal was the design of scraper geometries that enhance heat transfer by perturbing the thermal boundary layer, and effectively scrape off particles that nucleate, grow and adhere onto the heat exchanger surface.

The heat transfer coefficient and the power consumption of a laboratory SSHE were measured by Qin et al. [9] when it was used for freezing a 10 wt. % sugar solution. Experimental results show that the heat transfer coefficient with phase change (ice formation) was about three to five times greater than that without phase change.

For ice slurries to become more widely accepted, however, more engineering information is required on fluid flow and heat transfer characteristics. An experimental study was carried out by Lakhdar et al. [10] on a scraped surface heat exchanger used for freezing of water–ethanol mixture and aqueous sucrose solution. The influence of various parameters on heat transfer intensity was established.

The basic crystallization principles and heat transfer mechanisms in current ice generators are not yet fully understood. To elucidate the heat transfer mechanisms, heat

transfer measurements are presented by Stamatiou et al. [11] in a prototype compact ice generator.

Heat transfer phenomena in two types of eutectic crystallizers have been analyzed by Vaessen et al. [12]. Both increasing and decreasing heat transfer rates have been observed in crystallizing conditions at increasing scraping rates.

Continuous heat extraction is important for the process of freeze concentration of aqueous solutions, in which water is removed as solid ice. Three typical stages of heat-transfer patterns, namely, chilling, nucleation, and crystallization were identified by Qin et al. [13] during the process of freeze concentration in a scraped surface heat exchanger.

An experimental investigation of a SSHE was undertaken by Dumon et al. [14] using visual observations and the electrochemical technique in order to study the transition between laminar and vortex flows and to evaluate the wall shear rates. It was established that flow patterns in a SSHE are noticeably different from those observed in an annular space in the same conditions.

Heat transfer from a jacketed wall of a scraped-surface heat exchanger (SSHE) numerically simulated by Baccar and Abid [15] to analyze the hydrodynamic and thermal behavior under various operating and geometrical conditions using three-dimensional form of the Navier-Stokes and energy equations. Results show that geometrical and operating parameters can strongly affect the performance of a heat exchanger. An increase in the number of scrapers contributes to a higher frequency of the scraped film which would improve heat transfer performance.

European patent, ice slurry generator granted to Lim et al. [16]. Ice generator for providing ice slurry uses stripping devices for removing ice from inside walls of parallel pipes for aqueous medium within heat exchanger, European patent, granted to Doetsch et al. [17]. European patent, slurry ice generator for cool thermal storage system, granted to Lee et al. [18]. Ice making machine and heat exchanger, U.S. Patent granted to Goldstein et al. [19].

Table 2.1. A comparative study of work done by researchers on scraped surface ice slurry generators

Authors name	**System description / Work**	**Salient features/Outcome**
Saraceno et al. (2011).	Presented heat transfer correlations for the SSHE installed in a commercial soft ice-cream machine.	Heat transfer efficiency depends strongly on exchanger and agitator geometries, agitation methods, fluid characteristics and heat transfer conditions.
Yataghene et al. (2011a)	Performed study on experimental analysis of the flow patterns inside scraped surface heat exchanger (SSHE) under isothermal and continuous flow conditions.	Experimental flow pattern analyses are the basis for further experimental explorations of mixing and heat exchange mechanism.
Solano et al. (2011b).	Investigated experimentally flow pattern in the tubes of an innovative scraped surface heat exchanger with reciprocating scrapers.	Flow pattern in the tubes of an innovative scraped surface heat exchanger with reciprocating scrapers.
Pascual et al. (2009)	Turbulent fluid flow and related solid particle behaviour in the direct vicinity of the heat exchanging (HE) surface of a scraped heat exchanger crystallizer was studied by Pascual et al. (2009).	The main goal was the design of scraper geometries that enhance heat transfer by perturbing the thermal boundary layer, and effectively scrape off particles that nucleate, grow and adhere onto the heat exchanger surface.
Qin et al. (2006)	Measured heat transfer coefficient and the power consumption of a laboratory SSHE used for freezing a 10 wt. % sugar solution.	Experimental results show that the heat transfer coefficient with phase change (ice formation) was about three to five times greater than that without phase change.
Lakhdar et al. (2005)	Carried out an experimental study on a scraped surface heat exchanger used for	The influence of various parameters on heat transfer intensity were established.

	freezing of water–ethanol mixture and aqueous sucrose solution.	
Stamatiou et al. (2005a)	Presented heat transfer measurements to elucidate the heat transfer mechanisms in a prototype compact ice generator.	Heat transfer measurements to elucidate the heat transfer mechanisms in a prototype compact ice generator.
Vaessen et al. (2004)	Analyzed heat transfer phenomena in two types of eutectic crystallizers.	Both increasing and decreasing heat transfer rates have been observed in crystallizing conditions at increasing scraping rates.
Qin et al. (2003)	Identified three typical stages of heat-transfer patterns, namely, chilling, nucleation, and crystallization during the process of freeze concentration in a scraped surface heat exchanger.	Continuous heat extraction is important for the process of freeze concentration of aqueous solutions, in which water is removed as solid ice.
Dumon et al. (2000)	Undertaken an experimental investigation of a SSHE using visual observations and the electrochemical technique in order to study the transition between laminar and vortex flows and to evaluate the wall shear rates.	It was established that flow patterns in a SSHE are noticeably different from those observed in an annular space in the same conditions.
Baccar and Abid (1997)	Numerically simulated heat transfer from a jacketed wall of a scraped-surface heat exchanger (SSHE) to analyze the hydrodynamic and thermal behavior under various operating and geometrical conditions using three-dimensional form of the Navier-Stokes and energy equations.	Results show that geometrical and operating parameters can strongly affect the performance of a heat exchanger. An increase in the number of scrapers contributes to a higher frequency of the scraped film which would improve heat transfer performance.

2.1.2. VACUUM ICE

Working principle: The most efficient means of producing ice slurry employs a direct contact heat transfer vacuum freeze process where water is used as refrigerant. In the evaporator which contains a water/ salt solution, water is evaporated and compressed to the condenser pressure. The pressure inside the evaporator is close to the triple-point of water i.e. slightly below 6 mbar vapour pressure; hence the common name vacuum ice arises for such systems.

A method for production of ice slurry from ethanol solution without using a refrigerator is proposed by Asaoka et al. [20].

A functional fluid was made by adding a small amount of additive to a water silicone-oil mixture with 90 vol % water content, and the functional fluid was transformed into an ice slurry by cooling while stirring. The new ice formation system, proposed by Matsumoto et al. [21] for ice storage based on the results of previous studies, demonstrated that the ice slurry could be formed continuously for 10 h. Experiments were carried out, varying operating conditions, and an optimal operating condition was determined to improve performance of the present system. Experiments were carried out, varying operating conditions, and an optimal operating condition was determined to improve performance of the present system.

2.1.3.DIRECT CONTACT GENERATORS WITH IMMISCIBLE REFRIGERANT

In a direct contact ice slurry generator the immiscible primary refrigerant is expanded and then injected into a tank where it evaporates. The evaporation cools and supersaturates the water and small dispersed ice particles are formed. Injection devices are required in the evaporating tank in order to distribute the primary refrigerant so that ice slurry will be formed evenly throughout the tank. The injectors should be designed so that there is no risk of ice formation on the injectors themselves. Also, injection and

evaporation have to induce enough turbulence to make sure that finely dispersed ice slurry will form.

An analytical model has been developed by Hawlader et al. [22] to predict the growth of ice around the injected supercooled coolant droplets, which involves phase change and heat transfer between layers.

The research studies on heat transfer characteristic during ice formation of a direct contact heat transfer between carbon dioxide and water mixture was conducted by Vorayos et al. [23].

The Ultrasonic Doppler Method (UDM) has been applied by Vuarnoz et al. [24] to the process of ice slurry generation by direct injection of a refrigerant into an aqueous solution. The main objective of this work has been to investigate the fluid dynamic behaviour of evaporating refrigerant drops in an immiscible fluid and the approach taken has been to evaluate how suitable the UDM technique is for such investigations.

2.1.4. DIRECT CONTACT GENERATORS WITH IMMISCIBLE LIQUID SECONDARY REFRIGERANT

The generator contains an extra cycle in which a heavy non-miscible liquid provides the heat exchange between the ice slurry loop and the primary refrigeration cycle. The liquid is cooled by the evaporator of the primary cycle and is mixed with an aqueous solution in the ejector. Because the temperature of the liquid is below the freezing temperature of the aqueous solution, the formation of ice crystals occurs. In the freeze tank, ice crystals rise upward and the heavy liquid sinks to the bottom from where it returns to the pump and the evaporator.

2.1.5. SUPERCOOLED BRINE METHOD

In this method water in the ice slurry storage tank is sent to the supercooler where it is supercooled to -2 ºC. This supercooled water runs against the inner wall of the

pipe in the releaser and undergoes a phase change to become ice slurry containing very small ice particles. The ice content within the ice slurry is 2.5 wt%. The ice slurry is fed through a piping system to the ice slurry storage tank where it is separated by the difference in density between ice and water.

The conventional ice slurry producing method using supercooled water suffers from the instability of ice block and depends heavily on electric power. A novel ice slurry producing system utilizing inner waste heat was proposed by Li et al. [25]. Compared with the conventional system, this new system can alleviate the burden on electric power and raise the efficiency.

Lasvignottes et al. [26] demonstrated the feasibility to produce ice slurry from supercooled water. This technology which does not use extra mechanical energy source to operate is a promising alternative to the actual technologies. However the design must be very accurate to control the supercooled degree at the outside of the evaporator.

2.1.6. HYDRO- SCRAPED ICE SLURRY GENERATOR

Ice slurry, especially made from carrier fluids with high concentrations of freezing point depressing additives, can be produced in conventional heat exchangers, if the evaporation temperature of the primary refrigerant and the flow rate of the ice slurry are carefully controlled. In the Hydro- Scraped Ice Slurry Generators ice particles are flushed away by the fluid flow itself, hence the name “hydro-scraped ice slurry generator”

2.1.7. SPECIAL COATING OF GENERATOR SURFACE TO AVOID ICE STICKING TO SURFACE

In order to simplify the careful operation of the hydro-scraped ice slurry generator, the heat exchangers surface on the ice slurry side can be coated with special substances preventing the growth of ice crystals on the surface.

2.1.8. FLUIDIZED BED CRYSTALLIZER

Fluidized bed heat exchangers are shell-and-tube or tube-in tube type heat exchangers. On the shell side, a primary refrigerant is evaporated, for example, ammonia, a hydrocarbon or a chemical refrigerant. Ice is formed on or near the inside surface of the tubes mounted in the shell of the heat exchanger. Insides the tubes a fluidized bed is contained, consisting of small particles made of steel or glass, with a diameter of 1 to 5 mm. The particle beds are fluidized by the upward flowing liquid phase, which is the ice slurry feed flow. When fluidized, the solid particles continuously impact on the inside walls of the tubes. Build-up of an ice layer on the heat exchanging surface is prevented in this way. Fluidized particles also continuously disturb the heat exchanging boundary layer. The thickness of this layer therefore becomes small and heat transfer rates are enhanced.

Pronk et al. [27] performed a dynamic simulation of an experimental set-up in order to predict heat transfer coefficients in a fluidised bed ice slurry generator. A comparison between experiments and results from simulations pointed out that both models overestimate heat transfer coefficients and that crystallisation does not affect the heat transfer process significantly. A possible explanation for the latter phenomenon is that the crystallisation takes place in the bulk of the fluidised bed instead of near the wall.

Five empirical correlations for the prediction of heat transfer to liquid-solid fluidized beds with three, four, five, six and seven constants were fitted to experimental data by Haid et al. [28].

2.1.9. HIGH-PRESSURE ICE SLURRY GENERATOR

In this method raising water to a high pressure causes the freezing point to reduce. The high pressure solution is cooled and after release of the pressure, ice crystals are formed.

2.1.10. RECUPERATIVE ICE MAKING

In this method cyclic removal of ice from ice banks by heat (defrosting) or with mechanical means, where ice crushing devices may be used.

2.1.11. COMPARATIVE STUDY OF EXISTING ICE SLURRY GENERATORS

A comparative study of existing ice slurry generation techniques is given in Table 2.2.

Table 2.2. A comparative study of existing ice slurry generation techniques

	1.Scraped Surface Ice Slurry Generator	**2.Vacuum Ice**	**3.Direct Contact Generators With Immiscible Refrigerant**	**4.Direct Contact Generators With Immiscible Liquid Secondary Refrigerant**	**5.Super cooled Brine Method**
Capacity and size	3 to 400 tons of ice per day (10-1400 kW) Ref. capacity (1.8-2.4m long) inner dia. 0.15m	150 kW-3 MW	Heat transfer rate per unit volume is 1000 W/m^2K		Refrigeration capacity 35 MW or more
Costs and energy consumption	Require 1-2 kW/m2 of scraper driving power	-	Uses less power than ice slurry Generators	energy consumption high	-
Economics, investments, operating costs and reliability	Cost about US$ 1500-2000 per ton of ice produced	-	Low investment costs and energy consumption	Investment cost high	-
Applications	Process chemical and food industries	Cooling of deep mines	Industrial	-	Air-Conditioning systems
Advantages	1.Offer much smaller heat transfer with reduced space, weight and power requirements. 2. mechanical agitation results in high heat transfer rates	1.Lower inefficiencies due to temperature differences 2.Water is used as refrigerant(environmental safe)	No physical boundary exists between the primary refrigerant and the ice slurry	The primary evaporating refrigerants can be used that do mix with water	Used for peak power shifts
Disadvantages and limitations	High capital cost	Temperature limited between 0 to -4°C	Due to operational problems, non uniform ice formation	The extra cycle	-

	6.Hydro- Scraped Ice Slurry Generator	7.Special Coating of Generator Surface to avoid Ice Sticking to Surface	8.Fluidized Bed Crystallizer	9.High-Pressure Ice Slurry Generator	10.Recuperative Ice Making
Capacity and size	Prototype	Capacity and size follows those from conventional shell-and-tube evaporators	Systems built small and capacities starts from a few kilowatts	-	-
Costs and energy consumption	-	Cost of Fluorinated coating is additional and energy consumption is same as conventional chillers	Low energy consumption	-	-
Economics, investments, operating costs and reliability	-	Initial and operating costs are less	Initial and operating costs are less	High economic cost	Additional evaporator surface adds to the initial cost of the device
Applications	Laboratory scale	Laboratory scale	Laboratory scale	Ceramics, semi conductors etc.	Laboratory scale
Advantages	-	Without mechanical moving parts	Without mechanical moving parts	-	Operating without any motorized moving part and load shifting capabilities, no moving parts
Disadvantages and limitations	Need careful operation	A minimum flow velocity of 1 m/s is required, below this velocity icing of the coated surface may occur	Minimum allowable temperature difference	High pressure equipment	-

2.2. THERMOPHYSICAL PROPERTIES OF ICE SLURRIES

Ice slurry refers to a homogenous mixture of small ice particles (0.1 to 1mm diameter) and carrier liquid. The liquid can be either pure fresh water or a binary solution consisting of water and a freezing point depressant are added for different purposes, such as:

- freezing point depression,
- decreasing viscosity,
- increasing the thermal conductivity of the fluid phase,
- reduction of corrosion behaviour and prevention of agglomeration.

Sodium chloride, ethanol, ethylene glycol and propylene glycol are four most commonly used freezing point depressants in industry [1].

Selection of Antifreezes

There are some problems with the various types of secondary fluid are: water freezes to ice at or near 0°C, water and the water solutions are corrosive in the presence of oxygen if effective corrosion inhibitors are not added. Flammability risk determines safety demands on the use of ethyl alcohol (ethanol) in higher concentrations (≥ 30 % by weight), The flash point [29] limits the use of ethyl alcohol – water, for temperatures above about 25ºC. Ethyl alcohol cannot be used for freezer temperatures; high viscosity at low temperatures. Chloride salts: the eutectic point and the steep freezing point curve near this point limits calcium chloride – water to about -40ºC, sodium chloride – water to about -10ºC while lithium chloride from this point of view can be used even somewhat below -50ºC. Chloride salts are strongly corrosive in the presence of oxygen. (Corrosion inhibitors with cromates viewed as a health risk, especially inhalation during the mixing process). Organic potassium salts: The freezing point [29] curve near the eutectic point is not a steep as for the chlorides. Usually the freezing point is recommended just to be chosen about 10ºC below the operation temperature limiting this temperature to -40ºC or somewhat lower for potassium acetate and potassium formate. Potassium carbonate (K2CO3). Low viscosity. Corrosive with zink, soft solering and aluminum (if effective corrosion inhibitors are not used) due to high pH-value. Risk of damage at eye contact due to high pH-value.

Glycols are well developed products that have long lifespan and low total cost for a secondary system, acceptable thermo physical properties, low corrosion activity, low purchase cost and properties that are easy to handle. A limitation with glycols are applications with low work temperatures where the viscosity becomes too high. From an environmental aspect the products [29] are acceptable, but are not produced by renewable materials and can at great spillage form ecological and biological impact. Ethylene glycol (EG) having good thermo-physical properties for cooling applications, water can be used down to the operation temperatures at about -30ºC. By propylene glycol (PG) water can be used down to the operation temperatures at about -20ºC. However, well dimensioned heat exchangers, pumps and tubes are needed for good function and acceptable energy exchange. EG and PG both are fast biologically decomposable with moderate oxygen consumption. PG is sometimes environmental glycol or green glycol. It is not toxic to consume, which in itself is a great advantage. However it has higher viscosity leading to inferior thermal properties. Ethylene glycol and its solutions [29] are toxic to consume and should be stored under safe forms. Propylene glycol is not toxic and can consequently be used in i Food stuff connected activity. There are also propylene based products that are approved by NSF and FDA, which means that they can be used in food stuff.

Melinder et al. [30] introduces properties of secondary working fluids for indirect systems, tables and charts with fluid properties, property relations of ice and of ice slurry, enthalpy-phase diagrams and related charts for sodium chloride and water, as an example.

Kumano et al. [31] measured latent heat of fusion of ice in aqueous solutions to understand latent heat of fusion of ice slurries. Propylene glycol, ethylene glycol, ethanol, NaCl and $NaNO_3$ solutions were used as aqueous solutions.

Guilpart et al. [32] compared the performance of several commonly used organic and inorganic ice slurry secondary refrigerants, based on thermo physical assessments carried out at different operating temperatures.

Melinder and Granryd [33] suggested for ice slurry applications there is a need for accurate freezing point data and for more basic thermo physical property data at low concentrations.

Ayel et al. [34] described a new type of sensor for in-line measurements of antifreeze mass fraction in aqueous solutions.

Lua et al. [35] investigated the surface morphology of ice crystals containing adsorbed poly(vinyl alcohol) (PVOH) molecules inside a cold room at -7.0 ^{0}C.

2.3. THEORETICAL AND EXPERIMENTAL STUDIES OF ICE SLURRIES IN PLATE HEAT EXCHANGERS

Plate heat exchangers (PHE's) have a high heat transfer rate and low pressure drop compared to other types of heat exchangers due to their large surface area. These are composed of a number of thin metal plates compressed together into a 'plate pack' by two pressure plates. Within a plate heat exchanger, the fluid paths alternate between plates allowing the two fluids to interact, but not mix, several times in a small area. Each plate is corrugated to increase the surface area and maximize heat transfer. Plate Heat Exchangers have a number of applications in the refrigeration and air-conditioning, pharmaceutical, petrochemical, chemical, power, industrial dairy, and food & beverage industry.

An experimental model was developed by Illa and Viedma [36] for theoretical analysis of heat exchangers performance. Ma and Zhang [37] investigated pressure drop and heat transfer characteristics of tetrabutylammoniumbromide (TBAB) clathrate hydrate slurry (CHS) as a secondary refrigerant flowing through a plate heat exchanger (PHE). Kalaiselvam et al. [38] analyzed the heat transfer and pressure drop characteristics of a tube–fin heat exchanger in ice slurry HVAC system.

The overall heat transfer coefficient and pressure drop in a plate heat exchanger was developed and the experimental results were correlated by Worck et al. [39]. From the results in plate heat exchanger investigated in this work, the transition to turbulent flow occurs at Reynolds numbers as low as 10-400. Hence even at the moderate velocities, plate heat exchangers can achieve high heat transfer coefficients, low fouling rates and reduction of overall size. With high heat transfer coefficients, high overall transfer rates can be achieved in comparatively smaller flow paths and thereby keeping the overall size and pressure drop at the minimum.

Ling et al. [40] demonstrated successful application of genetic algorithm (GA) combined with back propagation neural networks (BP) for the optimal design of plate-fin heat exchangers (PFHE). The major objectives in the PFHE design are the minimum total weight and total annual cost for a given constrained conditions. The total weight target ensures an exchanger of the smallest size with minimum capital cost, whereas the annual cost target yields the optimum pressure drops accounting for the tradeoff between power consumption and heat exchanger weight.

Pronk et al. [41] presented ice slurry melting experiments with a tube-in-tube heat transfer coil. The experimental results indicate that operating conditions such as ice slurry velocity, heat flux, solute concentration, ice fraction, and ice crystal size determine the degree of superheating.

The mathematical model of the heat-transfer phenomenon in a double-pass laminar countercurrent heat exchanger with uniform heat fluxes has been developed theoretically by Ho et al. [42]. The analytical solutions for such conjugated Graetz problem are obtained by using an eigenfunction expansion in terms of power series for the homogeneous part and an asymptotic solution for the non-homogeneous part.

Cascales et al. [43] studied refrigeration cycles in which plate heat exchangers are used as either evaporators or condensers. The performance of the cycle is studied by means of a method which consists of assessing the goodness of a calculation method by looking at representative variables such as the evaporation or the condensation temperature depending on the case evaluated. This procedure was also used to compare several heat transfer coefficients in the refrigerant side. Ice slurries can be used both for cold storage in place of chilled water or ice and as a secondary refrigerant. Despite the fact that ice slurry has now a days gaining wide acceptance, a little engineering information is available on fluid flow and heat transfer characteristics.

The flow behaviour of ice slurry has been investigated by Norgaard et al. [44] in a test rig with transparent pipes to allow visual observation of flow patterns in various single components such as fittings, valves and heat exchangers. Pressure loss coefficients in selected fittings have been measured to reveal the dependency of ice concentration.

Pinto et al. [45] presented a screening method for selecting optimal configurations for plate heat exchangers. The optimization problem formulate as the minimization of the heat transfer area, subject to constraints on the number of channels, pressure drops, flow velocities and thermal effectiveness, as well as the exchanger thermal and hydraulic models.

Zhang et al. [46] discussed the integrated optimal design of the materials, placement, size and flow-rate of a plate heat exchanger. With an input of data on the application technology, and economic and environmental parameters, a computer can be used to design the optimal placement, size and flow-rate of the PHEs.

Wang et al. [47] developed optimal design method for plate heat exchangers (PHEs).

Bellas et al. [48] reported the results of experimental investigations into the melting heat transfer and pressure drop of 5% propylene/water ice slurry flowing in a commercial plate heat exchanger. The heat transfer capacity of the heat exchanger was found to increase by more than 30 % with melting ice slurry flow compared to chilled water flow.

Crystal Growth

A physical model for simulating the heat transfer inside the small cell containing the ice slurry was developed Kousksou et al. [49].

Lu and Tassou [50] investigated several types of phase change materials for the preparation of PCM slurries which have potential for cooling applications.

Most crystallization models for ice slurries are based on the assumption of equilibrium thermodynamic approach. Che´gnimonhan et al. [51] presented results of simulations grounded on classical nucleation theory and crystal growth included in global Nakamuratype kinetics coupled with the one-dimensional nonlinear heat equation.

A bubbling device was applied by Zhang et al. [52] to an experimental dynamic ice making system to suppress ice adhesion to the cooling wall.

Thongwik et al. [53] studied the heat transfer phenomenon of melting slurry ice on external surface of a copper helical coil. The experimental results show that, with

small coil diameter, high mass flow rate of circulating water and low ice fraction, high heat transfer coefficient of the slurry ice at the warm helical coil surface is obtained.

Latent heat of fusion of ice in aqueous solutions was investigated by Kumano et al. [54] in order to understand the characteristics of ice slurries used in ice thermal energy storage systems.

Effect of poly vinyl alcohol (PVA) in inhibiting an increase in ice crystal size in isothermal ice slurries was investigated by Inada and Modak [55]. Using PVA, which exhibits thermal hysteresis, is a novel technique to completely inhibit the increase in ice crystal size in isothermal ice slurries.

Study by Guilpart et al. [56] compares the performance of several commonly used organic and inorganic ice slurry secondary refrigerants. This study was based on thermo physical assessments carried out at different operating temperatures.

A new type of sensor for in-line measurements of antifreeze mass fraction in aqueous solutions is described by Ayel et al. [57]. Its principles of operation are based on the exploitation of the temperature rise that accompanies the freezing of an undercooled solution.

For ice slurry applications there is a need for accurate freezing point data and for more basic thermo physical property data at low concentrations Melinder and Granryd [58].

Differences are attributed to geometrical crystallizer characteristics and solid content by Qin et al. [59].

Using the Laplace and inverse transform, and incorporating the initial condition of ice nucleation, an analytical solution was obtained by Qin et al. [60]

The growth pattern related to the potential for crystal growth as well as the crystal surface topography have been studied by Grandum et al. [61]. The crystal shape and size were found to be strongly dependent on the supercooling in the crystal's surrounding liquid in between a transition temperature.

Ice Slurry Flow

The effect of storage on flow and heat transfer characteristics of ice slurry was investigated experimentally by Kumano et al. [62]. After ice slurry had been stored in the storage tank, variations in ice particle size were measured using a microscope, and diameter distribution and average diameter determined. The ice packing factor, Reynolds number and storage time were varied as experimental parameters. The pressure drop and heat transfer coefficient were measured when the ice slurry flowed in the horizontal tube.

Zhang et al. [63] investigated the pressure drops and loss coefficients of a phase change material slurry-tetrabutylammonium bromide (TBAB) clathrate hydrate slurry (CHS) in pipe fittings. Furthermore, the loss coefficients of TBAB CHS flowing through the pipe fittings were obtained from the experimental results and the corresponding correlations were also developed.

Mellari et al. [64] presents an experimental and numerical investigation of the flow of ice slurry, composed of monopropylene glycol (MPG) as an additive. The objective was to demonstrate the influence of initial concentrations of this additive and the ice fraction on the rheological behavior of the corresponding ice slurry. The ice slurry flow was modeled in a continuous approach, where the fluid is assumed to behave like a single-phase fluid.

Flow characteristics of ice slurry were experimentally investigated by Kumano et al. [65] using narrow tubes. Reynolds number, the diameter of the tubes and the ice packing factor (IPF) were varied as the experimental parameters. Theoretical analysis was carried out using the experimental results.

This study by Yataghene et al. [66] is focused on experimental analysis of the flow patterns inside scraped surface heat exchanger (SSHE) under isothermal and continuous flow conditions. Experimental flow pattern analyses are the basis for further experimental explorations of mixing and heat exchange mechanism.

Langlois et al. [67] presented an ultrasonic method capable to measure precisely the particle concentration in ice slurry. To calibrate the ultrasonic measurement, they first determine the sound velocity and attenuation in two model suspensions (glass

beads/polyethylene glycol and polyethylene beads/ vaseline oil) for different particle volume fractions.

Mika et al. [68] presented the results of the experimental research on the ice slurry loss coefficient during its flow through sudden contractions. Experimental studies were conducted using a few of the most common contractions of copper pipes. Six contraction ratios were covered: 0.500, 0.615, 0.650, 0.769, 0.800 and 0.813. In the experimental research, the mass fraction of solid particles in the slurry ranged from 20 to 30 (20%, 25%, 30%). Research results allow for determining the theoretical correlation for the ice slurry, in order to calculate the loss coefficient in contractions during laminar flow.

Patrick et al. [69] investigated ice slurries, in crude oil, as a simple analogy to clathrate hydrates. A series of water-in-oil emulsions were prepared at different volume fractions of water, ranging from 0.10 to 0.70. Water used in the samples was deionized watger or a 3.5 wt% NaCl brine solution.

Effects of solute included in a sample on the specific enthalpy of ice are investigated experimentally by Kumano et al. [70]. In the experiments, ice including the solute was made from an aqueous solution, and the specific enthalpy was measured by melting the ice in the aqueous solution. Moreover, a physical model of the ice including the solute is proposed. As a result, when the concentration of the aqueous solution is set at a value equivalent to the concentration of the sample, the specific enthalpy of the sample increases with the concentration of the sample. The measurement results and the calculated values agree well, and it was found that the method for calculating the specific enthalpy of the sample is valid.

The paper Dopazo et al. [71] is concerned with the experimental analysis of a standard terminal fan-coil unit with ice slurry as coolant. The ice slurry was produced from an ethylene glycol 10 wt% aqueous solution. The pressure drop measurements are presented as a function of volumetric flow rate, ice concentration and Reynolds number. The experimental friction factors are obtained and discussed.

Ashley et al. [72] presented a review on the pressure drop in pipes for ice slurry flows. The variation of the pressure drop as a function of slurry velocity, pipe diameter as well as ice concentration in the slurry is discussed. The stratification

observed for particular flow conditions and its effects on the pressure drop as well as the role of particle diameter in the evaluation of pressure drop are addressed.

Heat transfer characteristics of ice slurry were investigated experimentally by Kumano et al. [73]. The Reynolds number, diameter of the tubes and ice packing factor (IPF) were varied as experimental parameters. For laminar flow, it was found that the ratio of the Nusselt numbers increased with the IPF, and an approximation equation of the Nusselt number could be derived using the apparent Reynolds number, IPF and the ratio of the average diameter of the ice particles to the diameter of the test tube.

Illa et al. [74] studied experimentally ice slurry flow through horizontal pipes is in order to find out its heat transfer and isothermal friction properties using 9% NaCl brine as the carrier fluid, different flow conditions are discussed with a view to analyze each involved variable.

The rheological behaviour of the ice slurry made from 9% NaCl brine has been experimentally studied by Illa et al. [75]. Starting from the dimensional analysis of pressure drop and heat transfer processes, the minimum numbers of non-dimensional parameters present in these processes have been determined. Rheological behaviour has been adjusted to the experimental data on ice slurry pressure drop.

Pressure drop behaviour of ice slurry based on ethanol–water mixture in circular horizontal tubes has been experimentally investigated by Marino et al. [76]. The secondary fluid was prepared by mixing ethyl alcohol and water to obtain initial alcohol concentration of 10.3% (initial freezing temperature -4.4 ^{0}C). The pressure drop tests were conducted to cover laminar and slightly turbulent flow with ice mass fraction varying from 0% to 30% depending on test conditions.

Evans et al. [77] presented the results of experiments and modelling carried out on ice slurries flowing in uninsulated steel pipes with a nominal diameter of 50 mm. The slurries used were formed from 4.75% NaCl aqueous solution and had ice mass fractions in the range 18–42%, with a view to the use of thick ice slurry ‘pigs’ as a pipeline clearing technique.

Beata et al. [78] presented the results of experimental research on heat transfer of ice slurry during its flow through tubes of circular, rectangular and slit cross-

sections. The work discusses the influence of solid particles, type of motion and cross-section on the changes in the heat transfer coefficient.

Wissam et al. [79] investigated ice slurry pressure drops and deposition velocity. A model for the friction factor, obtained by empirical and semi-empirical approximation. A new simple and efficient method is introduced to find the deposition velocity in an ice slurry fluid flow. Finally a variety of experimental results and some theoretical calculations of ice slurry flow patterns are shown.

Koji et al. [80] discussed analytically influences of Stefan number, initial concentration of the solution, initial solid fraction (initial IPF) and Fourier number on the thermal conductivity to improve measurement accuracy of the thermal conductivity of ice slurry in the transient line heat-source technique.

Koji et al. [81] measured shearing stress corresponding to adhesion force per unit area to remove ice from the wall surface and some reagents' contact angles on the wall and ice, varying the wall material and its surface state.

Constantin et al. [82] analyzed the thermal behaviour of a new two-phase secondary refrigerant has been. The ''stabilised ice slurry'' is a suspension in a low viscosity oil of ultraporous polymeric particles filled with water in order to determine the convective heat transfer coefficient of this secondary refrigerant with waterside phase change, an experimental set-up was built. It allows determining the local heat transfer coefficients inside two heat exchangers.

Beata et al. [83] presented results of the studies of pressure drops during laminar and turbulent flows of ice slurry produced on the basis of 10.6% ethanol solution. obtained at various ice mass fractions, include pressure drops determined in horizontal ducts of circular, rectangular, and slit cross-sections. The critical Reynolds numbers were also determined.

Jorge et al. [84] presented latent heat of fusion, melting and freezing points, and temperature- and concentration-dependent viscosity data.

Beata et al. [85] presented results of the studies of ice slurry flow in horizontal tubes. The possibility of treating the rheological parameters of ice slurry as being those of Bingham fluid was confirmed. The values of parameters (mass fraction, flow velocity) corresponding to the laminar, intermediate and turbulent flow were

determined which permits to optimize the flow in the systems working with this cooling agent. Critical flow velocity and mass fraction of ice values were determined.

Beata et al. [86] analyzed the possibility of the simulations of ice slurry flow based on the known CFD procedures, for both Bingham fluids and mulitiphase flow models (the mixture and Eulerian models). It was shown that in the laminar region, the models selected (the Bingham and mixture model) gave a correct description of momentum transfer.

Beata et al. [87] presented results of studies on heat transfer in ice slurry flows through horizontal tubes. On the basis of the energy equation and experimental results, they developed their own dimensionless relationships to determine local values of heat transfer coefficients for turbulent and laminar flows.

The heat transfer characteristics were experimentally investigated by Dong et al. [88] for ice slurry made from 6.5% ethylene glycol–water solution flow in a 13.84 mm internal diameter, 1500 mm long horizontal copper tube. The ice slurry was heated by hot water circulated at the annulus gap of the test section. Experiments of the melting process were conducted with changing the ice slurry mass flux and the ice fraction from 800 to 3500 kg/m2 s and 0–25%, respectively.

The convective heat transfer characteristics of ice slurries flowing vertically upward in a rectangular channel have been experimentally investigated by Stamatiou et al. [89]. At steady state, the local heat transfer coefficients were obtained during convective melting, and the effects of ice fraction, Reynolds number and wall heat flux were determined.

Ayel et al. [90].reviewed recent studies on rheology, flow behaviour and heat transfer of two-phase aqueous secondary refrigerants (ice slurries). The difficulties in measuring their rheological properties for which standard rheometers prove to be poorly adapted are analysed.

Andrej et al. [91] analysed the fully suspended ice-slurry flow in a horizontal pipe. The model allows us to avoid the definition on what kind of fluid ice-slurry is present. For the taken ice-particle diameter, the ice concentration profiles depending on various average velocities and pipe diameters are shown. The viscosity of the ice slurry is

presented, depending on average concentration, velocity, pipe diameter and ice-particle size.

Knodela et al. [92] investigated experimentally heat transfer and pressure drop for ice-water slurries flowing turbulently in a 24.0 mm internal diameter, 4.596 m long, horizontal, stainless steel tube. The slurry velocity of the experiments was varied from 2.8 to 5.0 m/s which encompassed the range of applicability to ice-water slurry-based district cooling systems.

Paul et al. [93] carried out comparative tests between ice slurry and flake ice for the cooling of different fish, ice slurry was found to produce faster cooling. The results show that the time required to cool the plaice down to 2 ^{0}C was more than three times faster than the time required with flake ice. Paul et al. [94] developed and manufactured ice slurry generators for commercial applications.

2.4. SUMMARY OF LITERATURE REVIEW

The review shows that a number of ice slurry generation techniques are available, some are commercially used and some are at development stage. Scraped surface ice slurry generation techniques is commercially used and vast literature is available. There is a requirement of continual upgrading in the design from the economical, environmental and practical point of view.

Ice slurry refers to a homogenous mixture of small ice particles (0.1 to 1mm diameter) and carrier liquid. The liquid can be either pure fresh water or a binary solution consisting of water and a freezing point depressant. The review shows sodium chloride, ethanol, ethylene glycol and propylene glycol are four most commonly used freezing point depressants in industry. Ice slurry having many advantages, due to latent heat of the ice, ice slurries have higher heat transport capability than single-phase fluids. Due to ice slurry it is possible to reduce the volume flow rate at a given cooling capacity; which reduces the required pipe dimensions and also allows smaller temperature changes over the cooling object, which leads to higher product quality.

The review shows that plate heat exchangers (PHE's) are most commercially used due to high heat transfer rate and low pressure drop compared to other types of heat

exchangers, having a number of applications in the refrigeration and air-conditioning, pharmaceutical, petrochemical, chemical, power, industrial dairy, and food & beverage industry.

2.5. OBJECTIVES OF PREASENT RESEARCH WORK

For the design of ice slurry generator, very little information is available regarding the ice crystallization process in scraped surface ice generators and most theories of ice crystallization mechanisms largely depend on anecdotal evidences and are somewhat speculative.

In the developing countries a widespread utilization of ice slurry systems for industrial applications has not taken place yet which is mainly attributed to the high investment costs of commercially available (only imported) ice slurry generators.

The objectives of this study are design, development and fabrication of a scraped surface ice slurry generator test rig through commonly used cost effective manufacturing processes employed by small and medium scale industries and collection of experimental data to understand ice crystallization mechanism in the microscopic scale, and heat transfer and fluid mechanics involving agitation and phase change in the macro scale for ice slurry production.

Scraped surface ice slurry generator designed, developed for commercial level, fabrication and performance testing of scraped surface ice slurry generator, application of ice slurry in plate heat exchanger.

The various objectives of the present research work are:

- Design, development and fabrication of a scraped surface ice slurry generator test rig through commonly used cost effective manufacturing processes.
- Collection of experimental data to understand ice crystallization mechanism in the microscopic scale, and heat transfer and fluid flow involving agitation and phase change in the macro scale for ice slurry production.

- Thermohydraulic modeling and experimental validation for plate heat exchanger applications.
- Thermo-economic analysis and optimization of ice slurry system

CHAPTER-III

EXPERIMENTAL STUDIES OF ICE SLURRY GENERATOR

This chapter describes the design, development and fabrication techniques of scraped surface ice slurry generators. Initially a five litre capacity generator was fabricated and ice slurry generation data were collected. Based on the satisfactory experimental results of five litre capacity generator, a 74 litre capacity scraped surface ice slurry generator was designed and fabricated for industrial application point of view, using cost effective manufacturing processes employed by small and medium scale industries.

3.1. DEVELOPMENT OF FIVE LITRE CAPACITY ICE SLURRY GENERATOR TEST RIG

A scraped surface ice slurry generator test rig of five litre capacity has been designed, developed and fabricated successfully through commonly used manufacturing processes employed by small and medium scale industries. Experimental data were collected to understand ice crystallization mechanism in the microscopic scale, and heat transfer and fluid mechanics involving agitation and phase change in the macro scale for ice slurry production using freezing point depressants [Propylene Glycol (PG) and Mono Ethylene Glycol (MEG)] with water based solution at different solute concentrations. Experimental data have been collected on a prototype to explore the possibility for development of a large capacity ice slurry generation machine for industrial applications.

3.1.1 DETAILS OF COMPONENTS

The components of ice slurry generator consist of circular shell and tube heat exchanger, scraper assembly, primary refrigeration system and secondary system. The details of these components are discussed below:

(a) Circular shell and tube heat exchanger

The main features of circular shell and tube heat exchanger are inner shell, spiral shape coil and outer shell covered with insulation. The inner shell is fabricated by

bending a stainless steel sheet in a circular shape (150 mm inner diameter, 3 mm thickness and 300 mm length) and ends of sheet are joined by electric arc welding (Fig.3.1 and Fig. 3.2). Inner surface of the inner shell is smoothed by grinding process. The material selection for inner shell is stainless steel (SS-304) to make it rust proof. Stainless steel is the preferred material of construction because it offers good thermal properties, strength and corrosion resistance. Extruded materials can also be used to minimize the overall cost. Spiral shape coil around the outer surface of inner shell is made of copper (0.93 cm diameter with 16 numbers of turns). This copper tube is soldered with the outer periphery of the cylinder for proper contact to enhance the heat transfer effect. The total 40 feet length of copper tube was consumed. Around the copper tube coil, polyurethane foam insulation of thickness 60 mm is provided and inserted in the outer shell. The two concentric shells are connected by welding top and bottom plates. This type of evaporator ensures proper turbulence for the refrigerant. As shown in Figures 3.1 and 3.2, the refrigerant enters from the bottom and after absorbing the heat of depressant solution from the inner shell, exits from the top. The total volume of the inner shell is five litres.

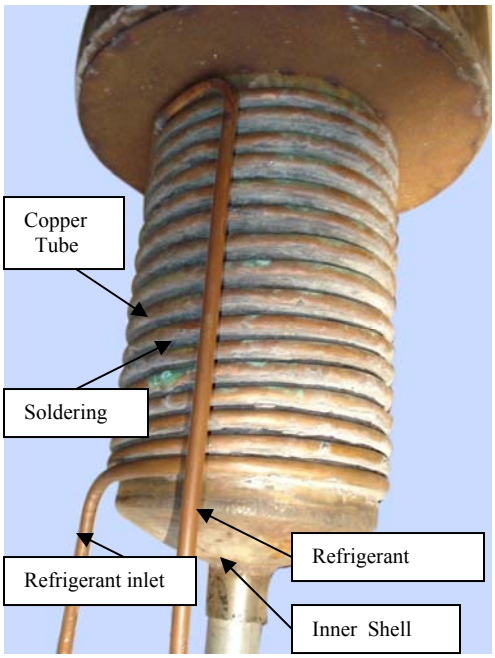

Fig.3.1 Photograph of coil of shell and coil type evaporator

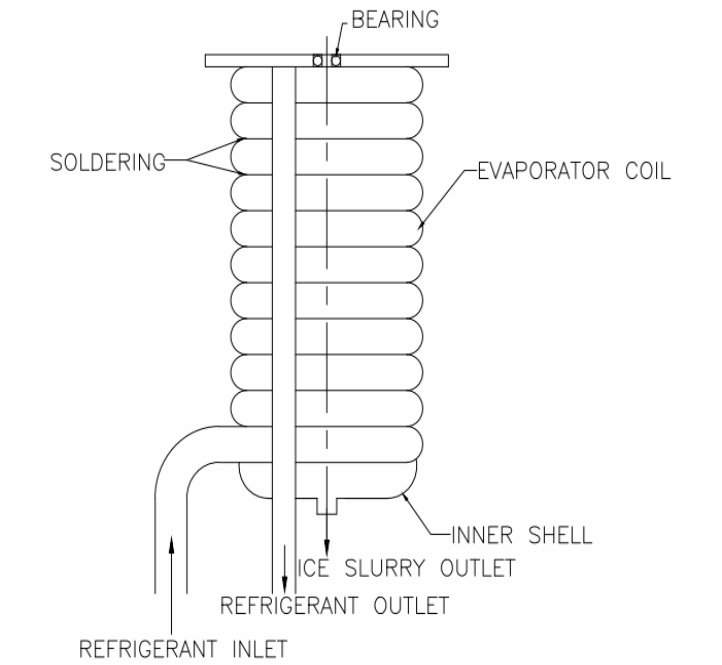

Fig.3.2 Schematic diagram of coil of shell and coil type evaporator

(b) Scraper blade assembly

A blade shaft assembly to be positioned at the centre of the inner shell carries a plurality of blades each of which is spring loaded are in contact with the inner surface of inner shell. Scraper blade assembly of stainless steel (SS 304) is fabricated by welding four number of spring loaded blades at a phase difference of 90 degree angle on the 25 mm diameter central shaft. Each blade is 75 mm long in the axial direction and 18.5 mm wide in the radial direction. Shaft is fitted (Fig.3.3 and Fig. 3.4) in the end plate and bearings to provide smooth rotational speed. The top portion of scraper blade assembly is coupled with electric motor (0.37 kW, 1425 rpm, single phase) via a reducing gear box of ratio 1:60 to provide rotational speed of 24 rpm to the scraper shaft (Figures 3.6 and Figure 3.7).The rotational speed of the scraping mechanism was kept constant in all experimental observations presented herein this research which is the minimum speed with the lowest internal thermal resistance of ice layer formed. Scraper shaft having blades across the heat exchange surface of inner shell removes ice crystals and hence prevents the deposition. This scraping action is required to prevent the formation of an ice layer on the ice generator walls. Turbulence is mechanically induced into the ice

slurry flow by the action of the rotating scarper blades thus greatly increasing the heat transfer rates and facilitating the production of a homogeneous ice slurry mixture.

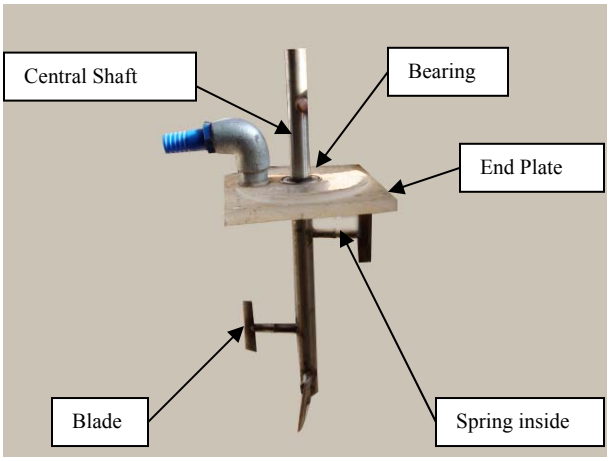

Fig.3.3 Photograph of Scraper blade assembly

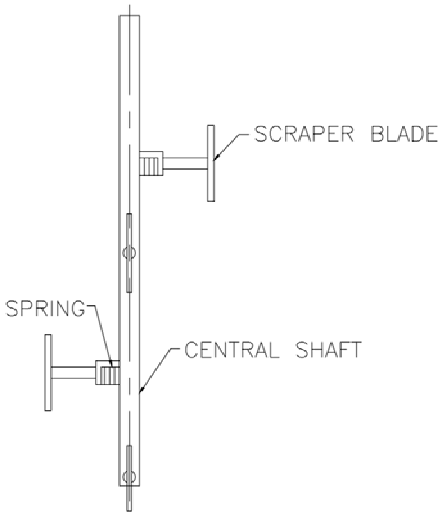

Fig.3.4 Schematic diagram of Scraper blade assembly

(c) Primary refrigeration system

Circuit diagram of the experimental facility is presented in Figure 3.5. It consists of a condensing unit having a compressor, air cooled condenser, thermostatic expansion valve, ice slurry generator. This unit supplies the refrigerant to the coil of the ice slurry generator (referred as evaporator in the refrigeration cycle in Figure 3.5) where evaporating refrigerant at lower pressure withdraws heat from the binary solution which

is finally converted into ice slurry inside the generator. At the exit of the evaporator, a refrigerant vapour having enough superheat is generated from indirect heat exchange process, is recompressed and recondensed at high pressure to complete the refrigeration cycle. An air-cooled, direct-expansion, single-stage mechanical vapor compression refrigeration system with R134a as primary refrigerant is fabricated and assembled for scraped surface ice slurry generator.

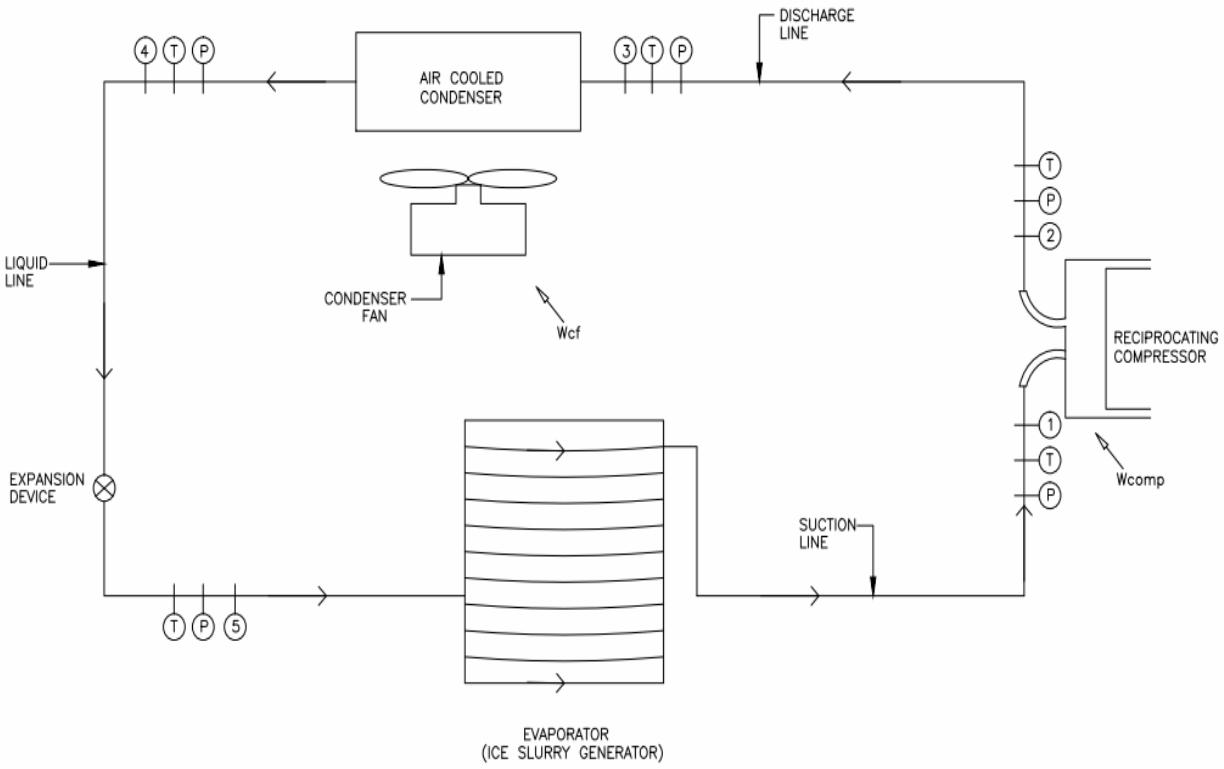

Fig 3.5 Schematic of Direct-expansion, single-stage mechanical vapor compression refrigeration system of scraped surface ice slurry generator (T) = Temperature sensor, (P) = Pressure sensor

(d) Secondary system

The secondary circuit consists of ice slurry storage tank fabricated by bending of stainless steel (SS-304) sheet, and joined by electric arc welding. Polyurethane foam insulation is provided on the outer surface. Ice slurry tank is connected with ice slurry generator through ice slurry circulation pump.

3.1.2 ASSEMBLY OF EXPERIMENTAL SETUP FOR ICE SLURRY GENERATION

A schematic diagram (elevation) of the assembled experimental apparatus is presented in Fig. 3.5. Table 3.1(a) and (b) summarizes the specifications of the present ice slurry generator fabricated for laboratory purpose.

Table 3.1(a): Specifications of primary circuit components of ice slurry generator

S. No.	**Name of the component**	**Specifications(material/size)**
1	Reciprocating Compressor	1/6 horse power (124.34 W), single phase
2	Condenser	Air cooled fin and coil type
3	Capillary tube	0.787 mm (0.031 inch) size
4	Evaporator	Circular shell and coil type of 9.525 mm (3/8 inch) coil
5	Inner shell	150 mm inner diameter (SS 304)

Table 3.1(b): Technical specifications of ice slurry generator

Component	**Specifications**
Tube Material	304-Grade Stainless Steel
Freezing point depressant	Propylene glycol, mono ethylene glycol
Crystal size (mm)	0.2- 0.3
Inner tube diameter (m)	0.15
Tube length (m)	0.30
Heat transfer area (m^2)	0.1414
Scraper blade assembly	SS 304 scraper blades 7.5 cm (L), 1.85 cm (W), 25 mm diameter central shaft (SS 304)
Agitation speed (rpm)	24
Evaporator type	Vertical type arrangement, Circular shell and coil type of 9.525 mm (3/8 inch coil)
Refrigerant type	R134a

The present condensing refrigeration unit (Fig. 3.7) consisting of a compressor [124.34 W (1/6 hp), 1-φ, 230V, 50 Hz], air cooled condenser (fin and coil type 220 ×230 mm, 2 row deep 9.525 mm (3/8 inch) diameter copper tubes, 6 fins per inch, 1300 fan rpm) and capillary tube (5/16 inch size having two 7 feet long passage) and measurement facilities having resistance-temperature detectors -50 ºC to 99 ºC, pressure transmitter 0 to 20 bar and rotameter 0 to 1.0 lpm. Ice slurry tank (300 mm×300 mm ×300 mm size, insulated with 60 mm thick polyurethane foam) is connected with ice slurry generator through a ice slurry circulation pump (1/4 hp). This unit supplies the refrigerant to the coil of the ice slurry generator (referred as evaporator in the refrigeration cycle in Fig.3.6) where evaporating refrigerant at lower pressure withdraws heat from the binary solution which is finally converted into ice slurry inside the generator. At the exit of the evaporator, a refrigerant vapour of enough superheat is generated from this indirect heat exchange process, recompressed and recondensed at high pressure to complete the refrigeration cycle. During the experimentation, ice slurries are made of an aqueous solutions of propylene glycol [PG] and mono ethylene glycol [MEG] having the initial weight concentration of 10%, 20%, and 30%, respectively.

The scraped surface ice slurry generator consists of a circular shell-and-coil type heat exchanger (Figure 3.1), where outer shell side is cooled by an evaporating refrigerant and inside surface is scraped by spring loaded rotating blades (Figure 3.3) to prevent any deposition of ice crystals on the cooled surface. This scraping action prevents the formation of an ice layer on the inner wall of ice generator, which would otherwise introduce an additional thermal resistance and could seriously lower the heat transfer. The continuous accumulation of the ice layer on the ice generator walls would eventually block rotation of the scraper blades and cause freezing up of the ice slurry generator. Depressants (PG and MEG) are added with water to depress the freezing point of the solution to prevent the freeze-up of the ice generator walls and alternatively provide impact on the temperature driving force for heat transfer. Turbulence is mechanically induced into the ice slurry flow by the action of the rotating scarper blades mounted in the centre of the heat exchanger, thus greatly enhance the heat transfer rates and facilitating the production of a homogeneous ice slurry mixture.

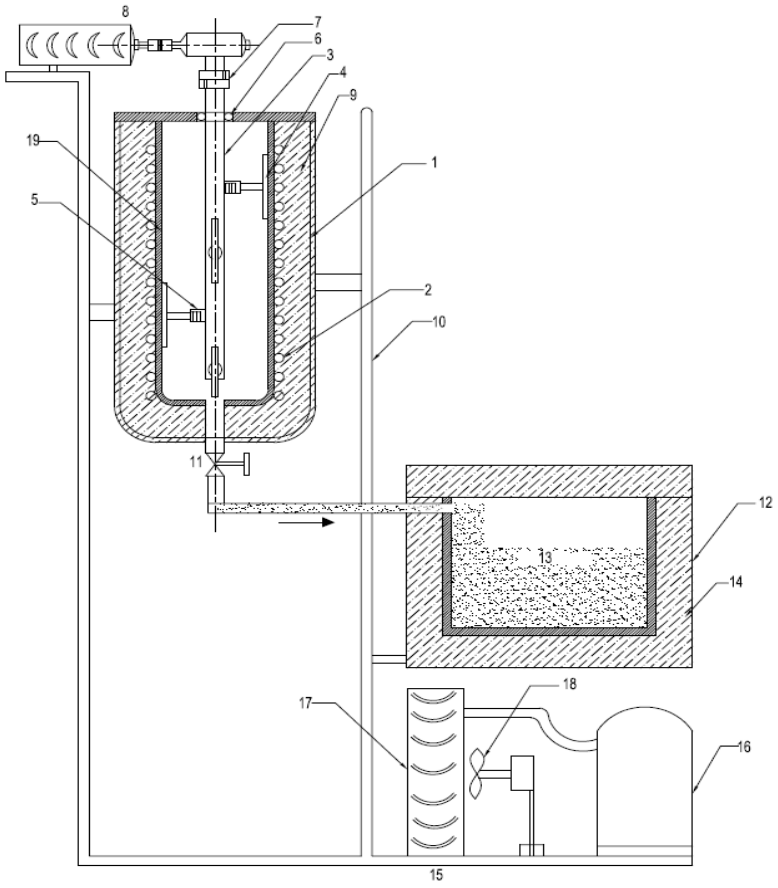

Fig.3.6 Schematic diagram of Ice Slurry System

1 = Ice Slurry Generator
2 = Evaporator Coil
3 = Scraper Shaft
4 = Scraper Blade
5 = Spring
6 = Bearing
7 = Coupling
8 = Motor
9 = Insulation
10 = Frame
11= Valve
12 = Ice Slurry Tank
13 = Ice Slurry
14 = Insulation
15 = Condensing Unit
16 = Compressor
17 = Condenser
18 = Condenser Fan
19 = Inner Shell
20 = Soldering
21 = Refrigerant In
22 = Refrigerant Out
23 = Ice Slurry Out
24 = Ice Slurry Pump
25 = Cooling Load

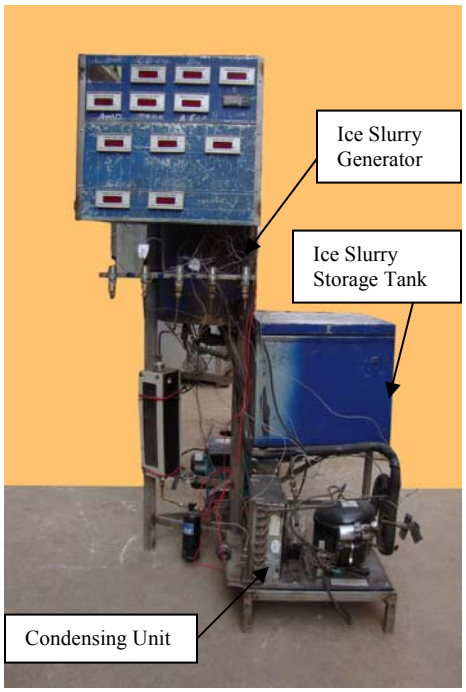

Fig.3.7 Photograph of Ice Slurry System (5 litre capacity)

3.1.3. EXPERIMENTAL DATA COLLECTION

The temperatures at condenser inlet and outlet, compressor suction and discharge, ice slurry tank and ice slurry in the ice slurry generator were measured by resistance temperature detectors. The pressures of primary refrigerant at condenser inlet and outlet, compressor suction and discharge, expansion outlet measured using pressure transmitters with a range of 0 to 20 bar having accuracy of 0.01 bar. Mass flow rate of primary refrigerant was measured using rotameter. Propylene Glycol (PG) and Mono Ethylene Glycol (MEG) were used as additives.

The instruments used for measuring various operating parameters (pressure, temperature and mass flow rates) are shown in Table 3.2. All measuring instruments are calibrated and repeatability of the experiments has been checked.

Table 3.2. Specifications of measuring instruments

Instrumentation	**Type/make/model**	**Range**	**Accuracy**
Resistance-temperature detectors	LTX-3000/D	-50 ºC to 0 ºC to 99 ºC	± 0.01 K
Pressure transmitter	Druck	0 to 20 bar	± 0.01 bar
Rotameter	Eureka	0 to 1.0 lpm	± 0.1 % (of reading)

After starting the power supply, data were collected with an interval of 120 seconds. Table 3.3 (a) and Table 3.3 (b) summarizes the operating parameters at inlet and outlet of various primary refrigerant components collected at the end of the experiments when ice slurry was formed.

Table 3.3(a) Operating parameters of refrigeration system (MEG as Antifreeze in Ice Slurry Generator)

State	Pressure (kPa)			Temperature (°C)		
	10%	20%	30%	10%	20%	30%
1. Compressor suction	100	083	068	-6.9	-8.9	-12.0
2. Compressor discharge	1051	1005	985	46.7	45.7	42.1
3. Condenser inlet	1014	971	946	46.6	44.9	41.6
4. Condenser outlet	1005	961	939	36.3	35.5	35.4
5. After expansion	108	091	077	-7.0	-9.5	-12.1
6. Ice slurry temperature				-3.4	-7.1	-11.9

Table 3.3(b) Operating parameters of refrigeration system (PG as Antifreeze in Ice Slurry Generator)

State	Pressure (kPa)			Temperature (°C)		
	10%	20%	30%	10%	20%	30%
1. Compressor suction	104	082	062	-5.0	-8.7	-11.2
2. Compressor discharge	1045	1006	972	45.9	43.0	41.2
3. Condenser inlet	1010	972	935	45.8	42.6	40.9
4. Condenser outlet	999	962	929	35.7	35.3	35.2
5. After expansion	112	091	071	-6.8	-9.1	-11.5
6. Ice slurry temperature				-2.9	-6.4	-11.0

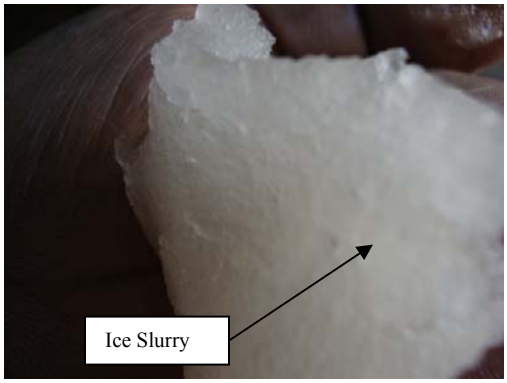

Fig.3.8 Photograph of Ice Slurry

The aqueous solution of antifreezes, Propylene Glycol (PG) and Mono Ethylene Glycol (MEG) with water at weight percentages 10%, 20% and 30% of antifreezes were used in the freezing process. With antifreeze PG 7.4 kg of by weight and 66.6 kg of water by weight, the lowest ice slurry temperatures achieved are -3.1 ^{0}C, -6.4 ^{0}C and -11.0 ^{0}C at 10%, 20% and 30% concentrations respectively, whereas with antifreeze MEG, lowest ice slurry temperatures achieved are -3.4 ^{0}C, -7.3 ^{0}C and -11.9 ^{0}C at 10%, 20% and 30% concentrations respectively (Table 3.3). The photograph of ice slurry is given in Fig.3.8.

3.1.4. RESULTS AND DISCUSSIONS

Historical time curves (recorded temperatures of aqueous solution of antifreezes, refrigerant temperatures at evaporator inlet and outlet, refrigerant temperatures at condenser inlet and outlet, ice slurry temperatures at different concentrations), and freezing temperatures vs. antifreeze mass fraction are plotted. Based on operating data, first law analysis is performed.

(a) Historical time curves

Recorded temperatures of aqueous solution of antifreezes, refrigerant temperatures at evaporator inlet and outlet, refrigerant temperatures at condenser inlet and outlet at different concentrations are plotted (Figures. 3.9 to 3.11 for PG and Figures

3.12 to 3.14 for MEG) with respect to freezing time. From the present experimental ice slurry generation data it can be observed that ice slurry generation process can be divided into three stages- cool down or chilling period, nucleation or unstable ice slurry generation period and stable ice generation period. The first stage (cool down period) starts t_0 to t_1, where t_0 is the starting time of the experiment and t_1 is the time at the end of the chilling period which is the on-set of the super-cooling phenomenon. During the chilling period volumetric ice concentration is zero. As observed in Figures 3.9 to 3.11, the freezing temperature reduces with increase in antifreeze mass fraction for PG and MEG solution initially chilled continuously without phase change in stage 1. First phase time duration is 1500, 1600 and 2000 seconds respectively for 10%, 20% and 30% concentration of PG. Similar trend was observed for MEG (Figures 3.12 to 3.14) but first phase time duration was relatively higher as compared to PG. During this stage the average evaporator temperature decreases sharply which causes increase in the refrigeration capacity and compressor work. Therefore, the condenser inlet temperature increases due to higher heat rejection quantity. The second stage (nucleation period) starts from t_1 to t_2, where the ice seeds after the super cooling phenomenon is observed and the volumetric ice concentration increases till its maximum value at the end of this period (at t_2). In stage 2, nucleation of ice particles occurs and it is characterized by 0.5 to 1^0C jump in temperature of the process fluid due to the release of the fusion heat of ice. Finally the third stage (ice slurry generation period) starts from t_2 to the end of the experiment, at t_f. During this stage the ice concentration is maintained constant at its maximum value. During stage 3 the heat transfer is affected by the release of the latent heat of water freezing.

Freezing temperatures vs. antifreeze mass fraction is shown in Fig. 3.15. Here, freezing temperature is inversely proportional to antifreeze mass fraction. When water freezes out after the temperature of the liquid mixture has passed below the freezing point, the concentration of the additive increases in the liquid-phase. The increased additive concentration implies that the freezing point of the remaining liquid-phase is further lowered and in order to freeze out more ice the temperature of the mixture has to be further lowered below the current freezing point of the liquid. The result is that the

fluid has a freezing range rather than a definitive freezing point. Thus by plotting the freezing point as a function of the additive concentration, one obtains a freezing point curve as a function of the additive mass concentration of different freezing point depressants (Figure 3.15). The lowering of the temperature of the ice slurry is independent of the effect of the latent heat from the phase change, but dependent on the sensible heat of the mixture. Since it is the advantage of the latent heat in ice slurry that is desired, one desires a liquid mixture where the latent heat dominates. To minimize the influence of the sensible heat, a fluid with a relatively low first derivative of the freezing point curve (flat freezing point curve) is to be preferred.

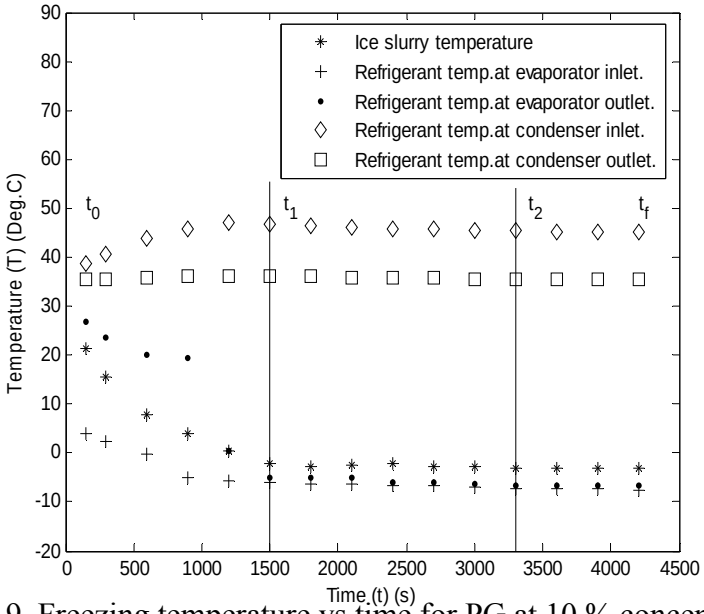

Fig.3.9. Freezing temperature vs time for PG at 10 % concentration

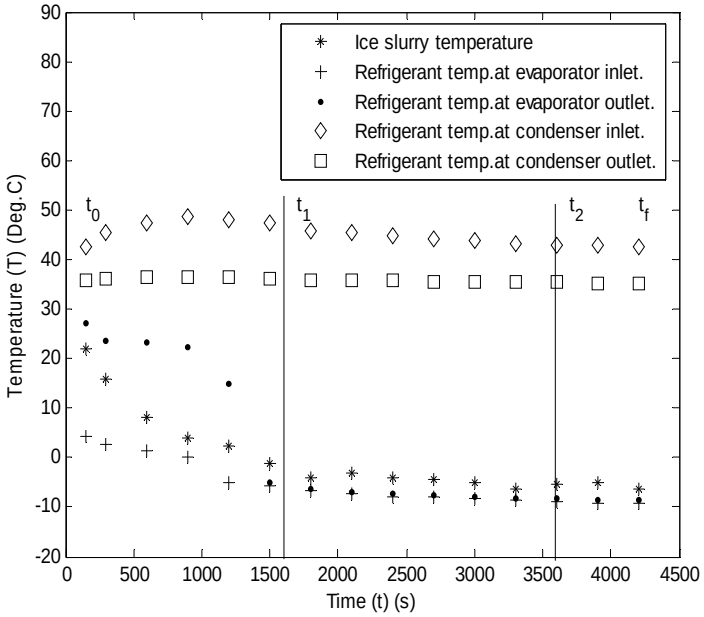

Fig.3.10. Freezing temperature vs time for PG at 20 % concentration

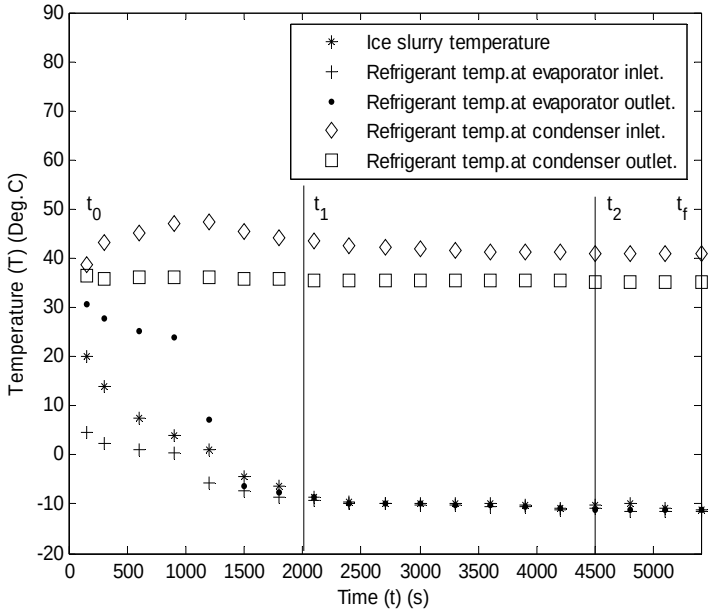

Fig.3.11. Freezing temperature vs time for PG at 30 % concentration

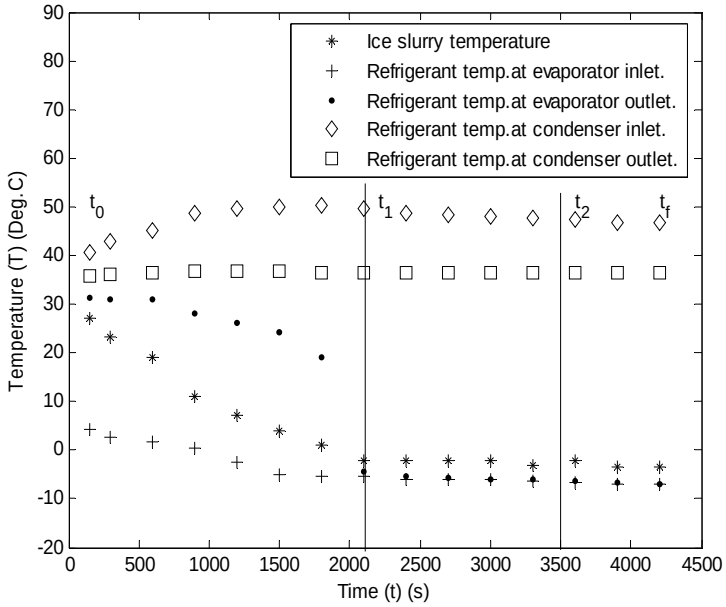

Fig.3.12. Freezing temperature vs time for MEG at 10 % concentration

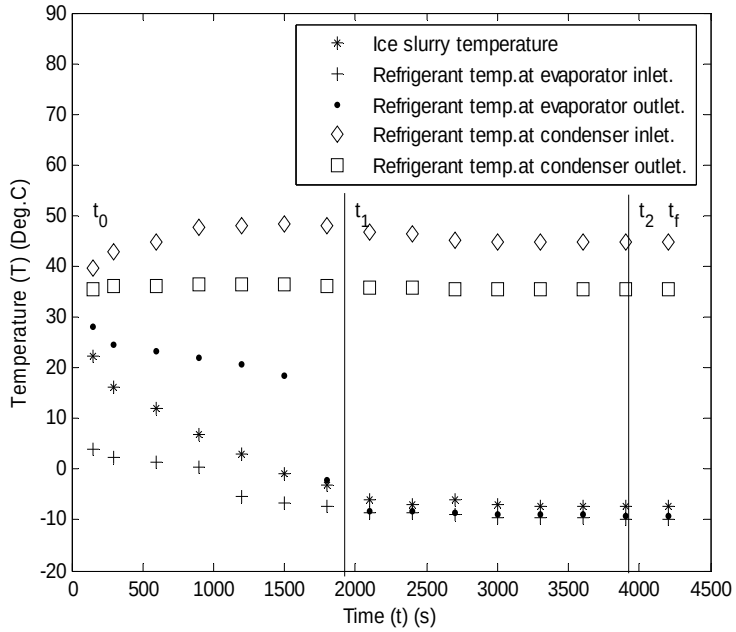

Fig.3.13. Freezing temperature vs time for MEG at 20 % concentration

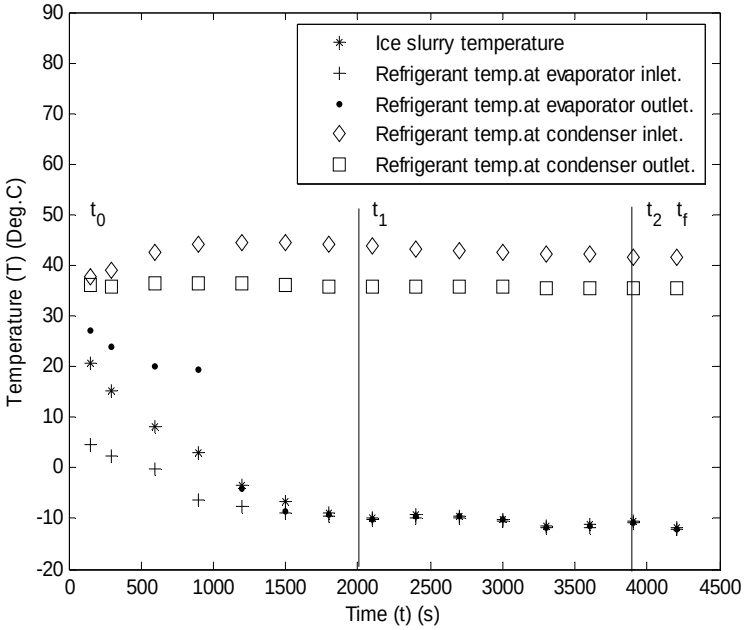

Fig.3.14. Freezing temperature vs time for MEG at 30 % concentration

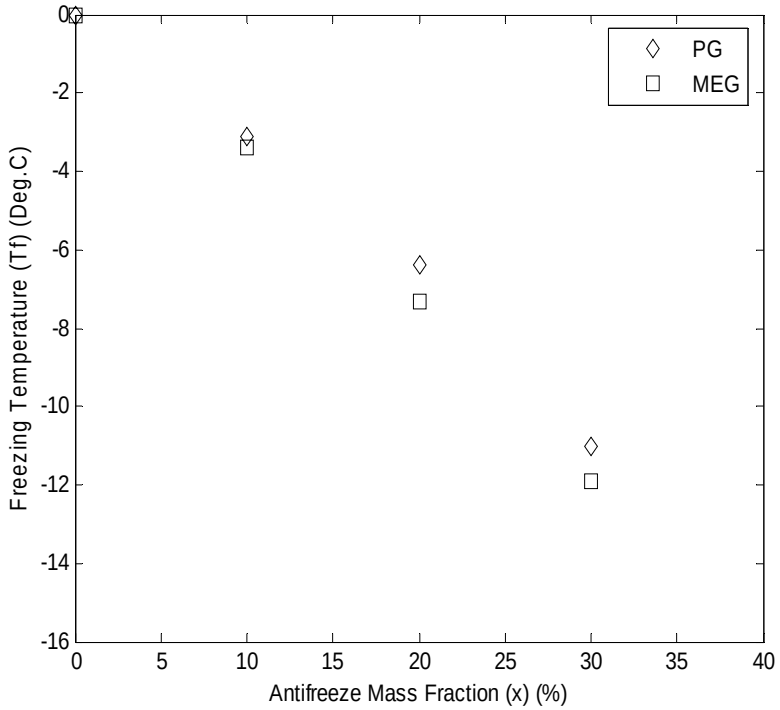

Fig.3.15. Freezing curve of water-PG and water- MEG mixture

(b) First law analysis

Using the experimental data given in Table 3.3(a) and Table 3.3(b) thermodynamic heat and work calculations of Ice Slurry Generation System is shown in Table 3.4. For different concentrations of additives PG and MEG the COP of the system is between 3.68 to 4.18. Sample calculation for PG is shown in appendix-I.

Table 3.4 Thermodynamic heat and work calculations of Ice Slurry Generation System

	Concentration of PG			Concentration of MEG		
	10%	20%	30%	10%	20%	30%
Refrigerating Effect, $N= h_1 - h_5$ (W)	242.52	245.97	248.85	236.47	236.09	234.41
Compressor Work, $W= h_2 - h_1$ (W)	58.01	60.09	61.65	61.40	63.13	63.70
Coefficient of Performance (COP=N/W)	4.18	4.09	4.03	3.85	3.74	3.68
Heat Rejected in Condenser, $Qc=h_2-h_4$ (W)	300.54	306.06	310.50	297.88	299.23	298.11

Experimental uncertainties:

Uncertainty analysis of thermodynamic heat and work calculations of Ice Slurry Generation System is shown in Table 3.5. (for details refer APPENDIX-II)

Table 3.5 Uncertainty analysis of thermodynamic heat and work calculations of Ice Slurry Generation System

Operation Parameters	Uncertainty (Concentration of PG)			Uncertainty (Concentration of MEG)		
	10%	20%	30%	10%	20%	30%
Refrigerating Effect, (N)	±0.000106	±0.000129	±0.000112	±0.0000714	±0.0001590	±0.0000787
Compressor Work, (W)	±0.006083	±0.005835	±0.005896	±0.006287	±0.006551	±0.006225
Coefficient of Performance (COP)	±0.000449	±0.000465	±0.000455	±0.000432	±0.000415	±0.000431
Heat Rejected in Condenser, (Qc)	±0.039440	±0.039100	±0.038880	±0.039330	±0.039690	±0.038940

3.2. DEVELOPMENT OF SCRAPED SURFACE ICE SLURRY GENERATOR OF 74 LITRE CAPACITY FOR INDUSTRIAL APPLICATIONS

Based on the encouraging results of five litre capacity ice slurry generator, it was decided to fabricate a bigger size version for commercial applications. A scraped surface ice slurry generator of 74 litre capacity has been designed, developed and fabricated successfully through commonly used cost effective manufacturing processes employed by small and medium scale industries. Experimental data related to ice slurry production using 10%, 20%, 30% and 40% concentrations of antifreezes (PG, MEG and DEG) were collected. R410A (refrigerant blend having zero ODP) as primary refrigerant in the primary refrigeration circuit of scraped surface ice slurry generator was used.

3.2.1 DETAILS OF COMPONENTS

The components of ice slurry generator consist of circular shell and tube heat exchanger, scraper assembly, primary refrigeration system, secondary system and instrumentation. The details are discussed below:

(a) Circular shell and tube heat exchanger

A stainless steel (SS-304) sheet of 3 mm thick, 300 mm wide and 1050 mm long sheet was bend in circular shape with the help of bending machine to form inner shell. Ends of sheet were joined by electric arc welding (Fig.3.16 and Fig. 3.17). Inner surface of the inner shell was finished by grinding machine. The total volume of the inner shell is 74 litre. Refrigerant circuit consists of a spiral shape coil (1.58 cm diameter with 50 number of turns) soldered around the outer surface of inner shell to achieve maximum contact. This copper coil having three inlets and three outlets joined by common headers. The total 48 meter length of copper tube was consumed. Polyurethane foam insulation of thickness 60 mm was provided around the copper tube coil and inserted in the outer shell. The two concentric shells are connected by welding top and bottom plates. This type of evaporator ensures proper turbulence for the refrigerant flow. Heat from the binary mixture is removed by evaporating refrigerant flowing through spiral shape coil.

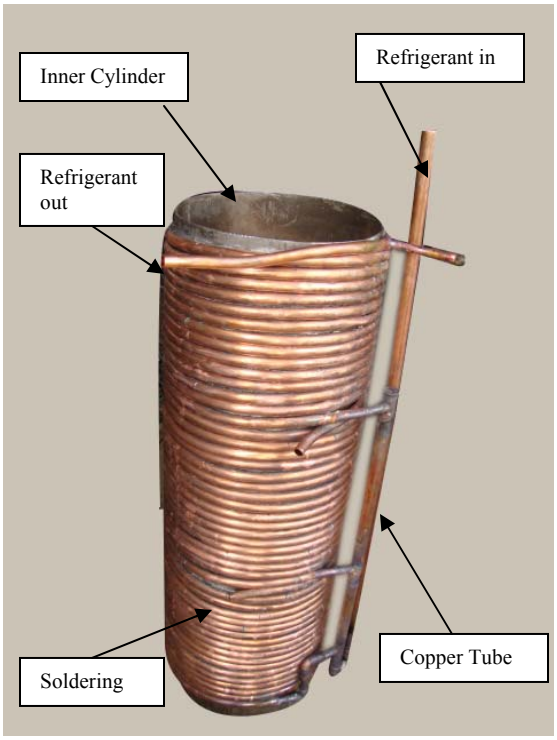

Fig.3.16 Photograph of coil of shell and coil type evaporator

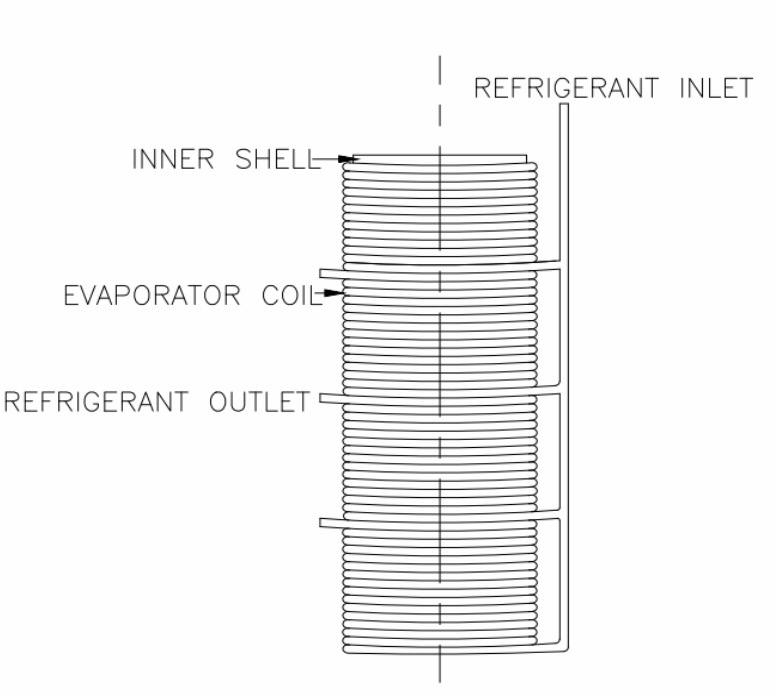

Fig.3.17 Schematic diagram of coil of shell and coil type evaporator

(b) Scraper blade assembly

Scraper blade assembly of stainless steel (SS 304) is fabricated by welding six number of spring loaded blades 152.4 mm long in the axial direction and 25.4 mm wide in the radial direction of a 32 mm diameter central shaft (Fig.3.18 and Fig. 3.19). Shaft is fitted in the end plate and ball bearing (32 mm inside diameter) to provide smooth rotational speed. The scraper blade assembly is coupled to electric motor (0.37 kW, 1428 rpm) via a reducing gear box of ratio 1:15 to provide rotational speed of 75 rpm to the scraper shaft. The rotational speed of the scraping mechanism was kept constant in all experimental observations which is the minimum speed with the lowest internal thermal resistance of ice layer formed. Crystals are remove by scraper shaft blades across the heat exchange surface and inhibit the deposition of ice crystals. This scraping action is required to prevent the formation of an ice layer on the ice generator walls.

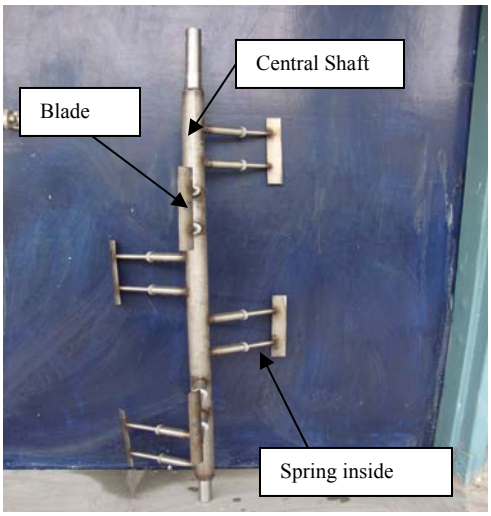

Fig.3.18 Photograph of Scraper blade assembly

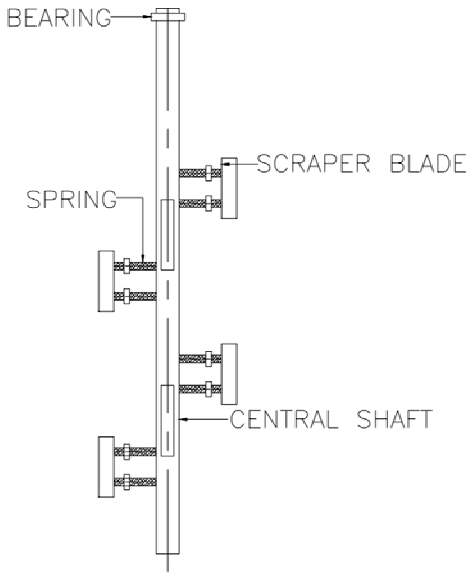

Fig.3.19 Schematic diagram of Scraper blade assembly

(c) Primary refrigeration system

An air-cooled, direct-expansion, single-stage mechanical vapor compression refrigeration system with R410 A as primary refrigerant is used in the primary refrigeration circuit. It consists of a condensing unit having a compressor, air cooled condenser, thermostatic expansion valve and ice slurry generator. This unit supplies the refrigerant to the coil of the ice slurry generator (referred as evaporator in the refrigeration cycle in Figure 3.5) where evaporating refrigerant at lower pressure withdraws heat from the binary solution which is finally converted into ice slurry inside the generator.

(d) Secondary system

The secondary circuit consists of ice slurry storage tank, ice slurry circulation pump, valves and fittings. Ice slurry storage tank is made by bending SS-304 sheet, ends of sheet are joined by welding, and polyurethane foam insulation of 60 mm thickness is

provided on the outer surface, Ice slurry tank is connected with ice slurry generator through ice slurry circulation pump.

Table3.6(a) and (b) summarizes the specifications of the present ice slurry generator manufactured.

Table 3.6(a): Specifications primary and secondary circuit components of ice slurry generator

S. No.	**Name of the component**	**Specifications(material/size)**
1	Compressor	5TR (Model TF265) single phase, 230V, 50 Hz
2	Condenser	Air cooled fin and coil type, 53.34 cm× 48.26 cm(21 inch ×19 inch), 3 row deep, 9.525 mm (3/8 inch) diameter copper tubes, 10 fins per inch, fan 1380 rpm
3	Expansion valve	Thermostatic expansion valve with five way distribution
4	Evaporator	Circular shell and coil type of 15.875 mm (5/8 inch) diameter tube, 50 number of turns
5	Ice slurry generator	74 litre capacity, scraped surface type

Table 3.6(b): Technical specifications of ice slurry generator

Specifications	**The present design**
Ice slurry side	
Tube Material	304-Grade Stainless Steel
Evaporator type arrangement	Vertical
Freezing point depressant	Propylene glycol, mono ethylene glycol, di ethylene glycol
Crystal size (mm)	0.15- 0.20
Inner tube diameter (m)	0.30
Tube length (m)	1.050
Heat transfer area (m^2)	0.9896
Agitation mechanism	SS 304 scraper blades 152.4 mm (L), 25.4 mm (W)
Agitation speed (rpm)	75

Refrigerant side	
Evaporator type	Circular shell and coil type of 15.875 mm (5/8 inch) diameter tube, 50 number of turns tube
Refrigerant type	R410 A
Ice slurry tank	500 mm×500 mm× 500 mm size, insulated with 60 mm thick polyurethane foam
Antifreeze solution tank	500 mm×500 mm× 500 mm size, insulated with 60 mm thick polyurethane foam

3.2.2 ASSEMBLY OF EXPERIMENTAL SETUP FOR ICE SLURRY GENERATION

A schematic diagram of the experimental apparatus is presented in Fig. 3.5. The present condensing refrigeration unit consisting of a compressor (5TR, 1-φ, 230V, 50 Hz), air cooled condenser (fin and coil type 533 ×483 mm, 3 row deep 3/8 inch diameter copper tubes, 10 fins per inch, fan 1380 rpm) and thermostatic expansion valve with five way distribution and measurement facilities. Ice slurry tank (500 mm×500 mm ×500 mm size, insulated with 60 mm thick polyurethane foam) is connected with ice slurry generator through a ice slurry circulation pump (0.6 kW). This unit supplies the refrigerant to the coil of the ice slurry generator (referred as evaporator in the refrigeration cycle in Fig.3.20 and Fig.3.21) where evaporating refrigerant at lower pressure withdraws heat from the binary solution which is finally converted into ice slurry inside the generator. In indirect heat exchange process at the exit of the evaporator, a refrigerant vapour of enough superheat is generated, recompressed and recondensed at high pressure to complete the refrigeration cycle. During the experimentation, ice slurries are made of an aqueous solutions of propylene glycol [PG], mono ethylene glycol [MEG] and di-ethylene glycol [DEG] having the initial weight concentration of 10%, 20%, 30% and 40%, respectively.

Outer shell side of scraped surface ice slurry generator is cooled by an evaporating refrigerant and inside surface is scraped by spring loaded rotating blades (Figure 3.18) to prevent any deposition of ice crystals on the cooled surface. To depress

the freezing point of the solution depressants are added with water to prevent the freeze-up of the ice generator walls and alternatively provide impact on the temperature driving force for heat transfer. To enhance the heat transfer rates and facilitating the production of a homogeneous ice slurry mixture turbulence is mechanically induced into the ice slurry flow by the action of the rotating scarper blades mounted in the centre of the heat exchanger,

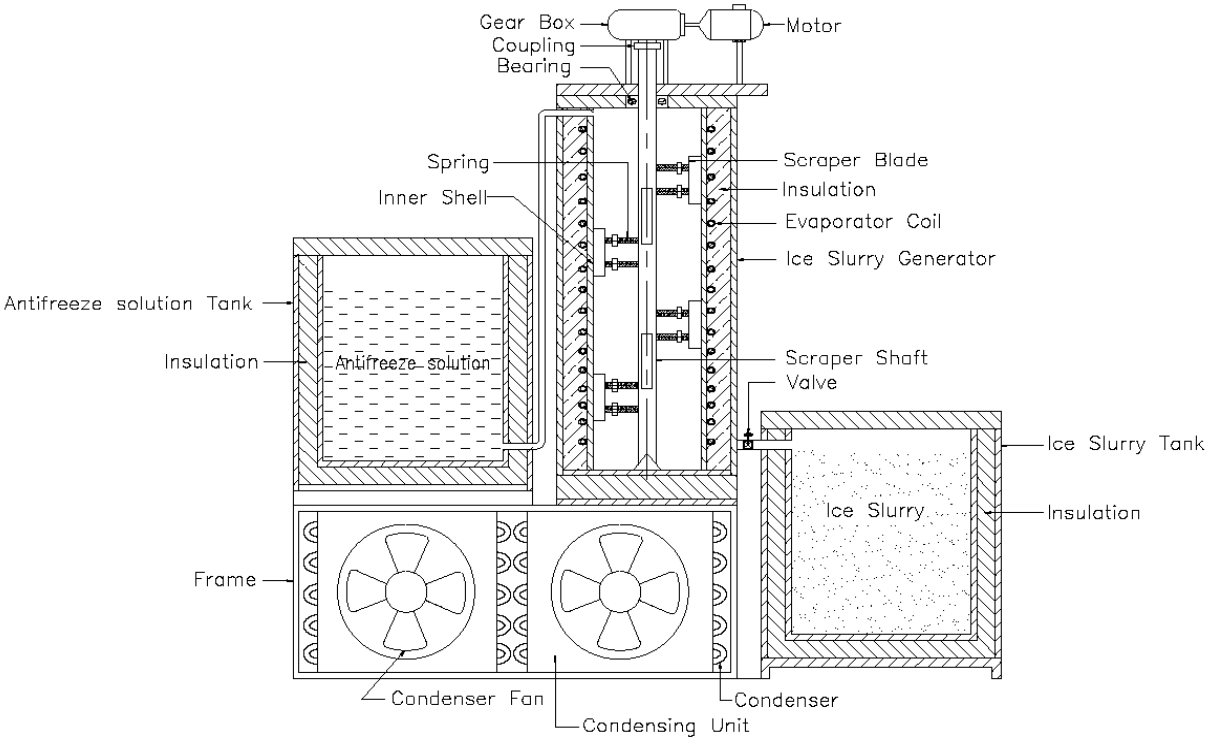

Fig. 3.20 Schematic diagram of Ice Slurry System

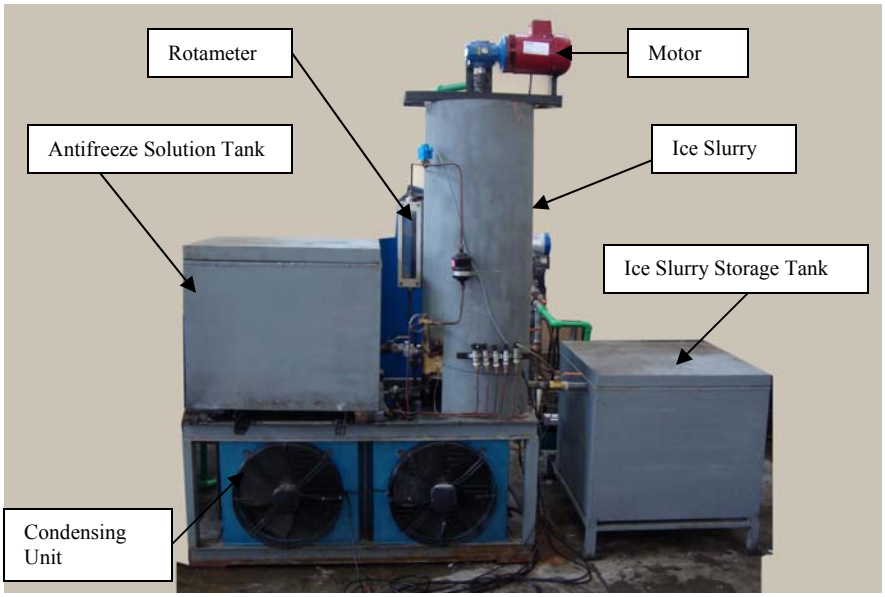

Fig.3 21 Photograph of Ice Slurry System (74 litre capacity)

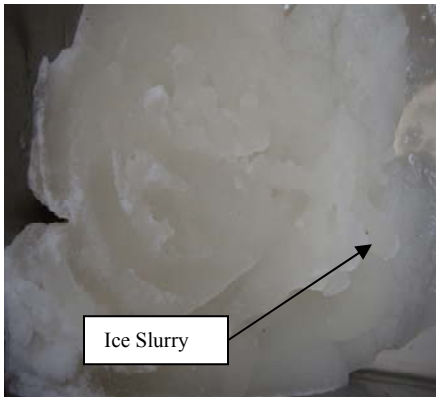

Fig.3.22 Photograph of Ice Slurry

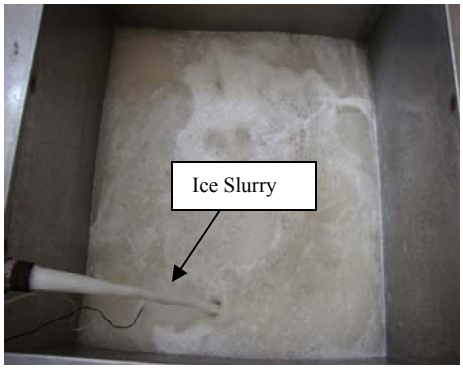

Fig.3.23 Photograph of Ice Slurry flowing in tank

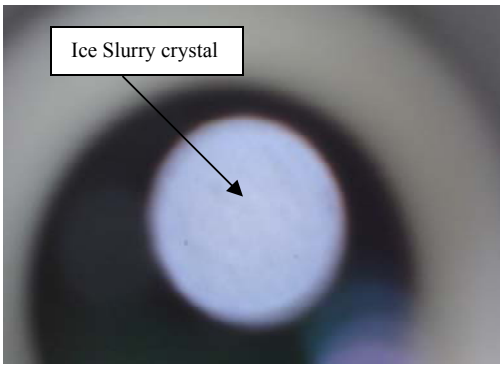

Fig.3.24 Photograph of crystal of Ice Slurry

3.2.3. EXPERIMENTAL DATA COLLECTION

Propylene Glycol (PG), Mono Ethylene Glycol (MEG) and Di Ethylene Glycol (DEG) were used as additives. Data logger DT80 of 16 terminal points (Table 5.1) with an accuracy of ± 0.01 % and response time of 1 sec is used. Sample of PG antifreeze 10% by weight is mixed with 90% by weight of water in antifreeze solution tank and then pumped to the ice slurry generator and the compressor was started. The temperatures at condenser inlet and outlet, compressor suction and discharge, ice slurry tank and ice slurry in the ice slurry generator were measured by resistance-temperature detectors (range -50 ºC to 99 ºC, accuracy ± 0.01).The pressures of primary refrigerant at condenser inlet and outlet, compressor suction and discharge, expansion outlet were measured using pressure transmitters with a range of 0 to 20 bar having accuracy of ± 0.01 bar. Mass flow rate of primary refrigerant was measured using rotameter. Data are stored at a frequency of 30 seconds and the criteria for steady state condition is taken when variation of data is independent of time. The same procedure was repeated for 20%, 30% and 40% of PG by weight. Similarly the whole procedure was repeated for MEG and DEG. After mixing a sample of ice slurry was taken from ice slurry generator and ice concentration was measured for 10%, 20%, 30% and 40% by weight of antifreezes PG, MEG and DEG.

Table 3.7(a), 3.7(b) and 3.7(c) summarizes the operating parameters at inlet and outlet of various primary refrigerant components and effect of depressant percentage

on ice slurry temperatures. With increase in depressant percentage ice slurry temperature decreases.

Table 3.7(a) Operating parameters of Refrigeration System (PG as Antifreeze in Ice Slurry Generator)

State	Pressure (kPa)				Temperature (°C)			
	10%	20%	30%	40%	10%	20%	30%	40%
1. Compressor suction	4	17	12	2	7.8	7.5	5.9	4.8
2. Compressor discharge	886	930	923	918	78.3	83.5	81.5	80.3
3. Condenser inlet	876	925	913	913	57.6	64.4	61.5	59.9
4. Condenser outlet	868	917	902	903	18.5	22.4	21.7	21.6
5. After expansion	7	19	14	4	-34.9	-32.8	-28.3	-32.6
6. Ice slurry temperature					-5.7	-10.2	-15.5	-20.7

Table 3.7(b) Operating parameters of Refrigeration System (MEG as Antifreeze in Ice Slurry Generator)

State	Pressure (kPa)				Temperature (°C)			
	10%	20%	30%	40%	10%	20%	30%	40%
1. Compressor suction	19	21	9	2	8.9	8.3	4.5	5.1
2. Compressor discharge	947	962	935	949	86.3	86.4	81.6	82.9
3. Condenser inlet	937	954	930	942	67.1	67.5	62.3	60.6
4. Condenser outlet	927	945	915	933	23.6	25.0	22.8	24.2
5. After expansion	21	24	12	4	-22.6	-24.7	-26.4	-35.6
6. Ice slurry temperature					-6.3	-12.6	-19.0	-25.6

Table 3.7(c) Operating parameters of Refrigeration System (DEG as Antifreeze in Ice Slurry Generator)

State	Pressure (kPa)				Temperature (°C)			
	10%	20%	30%	40%	10%	20%	30%	40%
1. Compressor suction	24	34	31	19	10.9	9.4	8.9	6.1
2. Compressor discharge	981	1010	1020	1006	90.5	93.0	93.5	90.1
3. Condenser inlet	979	1008	1018	996	69.1	70.9	71.3	65.4
4. Condenser outlet	964	990	1006	986	26.9	29.1	30.2	28.9
5. After expansion	26	36	34	21	-16.1	-14.5	-17.1	-22.4
6. Ice slurry temperature					-5.1	-10.0	-14.6	-19.9

3.2.4. EXPERIMENTAL RESULTS

The lowest ice slurry temperatures achieved are -5.7 ^{0}C, -10.2 ^{0}C, -15.5 ^{0}C and -20.7 ^{0}C for PG, -6.3 ^{0}C, -12.6 ^{0}C, -19.0 ^{0}C and -25.6 ^{0}C for MEG and -5.1 ^{0}C, -10.0 ^{0}C, -14.6 ^{0}C and -19.9 ^{0}C for DEG at 10%, 20%, 30% and 40% concentrations respectively. A summary of these temperatures are given in Table 3.8.

Freezing temperatures vs. antifreeze mass fraction is shown in Figure 3.25. Here, freezing temperature is inversely proportional to antifreeze mass fraction. When water freezes out after the temperature of the liquid mixture has passed below the freezing point, the concentration of the additive increases in the liquid-phase. The increased additive concentration implies that the freezing point of the remaining liquid-phase is further lowered and in order to freeze out more ice the temperature of the mixture has to be further lowered below the current freezing point of the liquid. The result is that the fluid has a freezing range rather than a definitive freezing point. Thus by plotting the freezing point as a function of the additive concentration, one obtains a freezing point curve as a function of the additive mass concentration of different freezing point depressants (Figure 3.25). The lowering of the temperature of the ice slurry is

independent of the effect of the latent heat from the phase change, but dependent on the sensible heat of the mixture. Since it is the advantage of the latent heat in ice slurry that is desired, one desires a liquid mixture where the latent heat dominates. To minimize the influence of the sensible heat, a fluid with a relatively low first derivative of the freezing point curve (flat freezing point curve) is to be preferred.

Table 3.8 Minimum ice slurry temperature at various concentrations of PG, MEG and DEG

Antifreeze	Minimum ice slurry temperature achieved (^{0}C)			
	10%	20%	30%	40%
PG	-5.7	-10.2	-15.5	-20.7
MEG	-6.3	-12.6	-19.0	-25.6
DEG	-5.1	-10.0	-14.6	-19.9

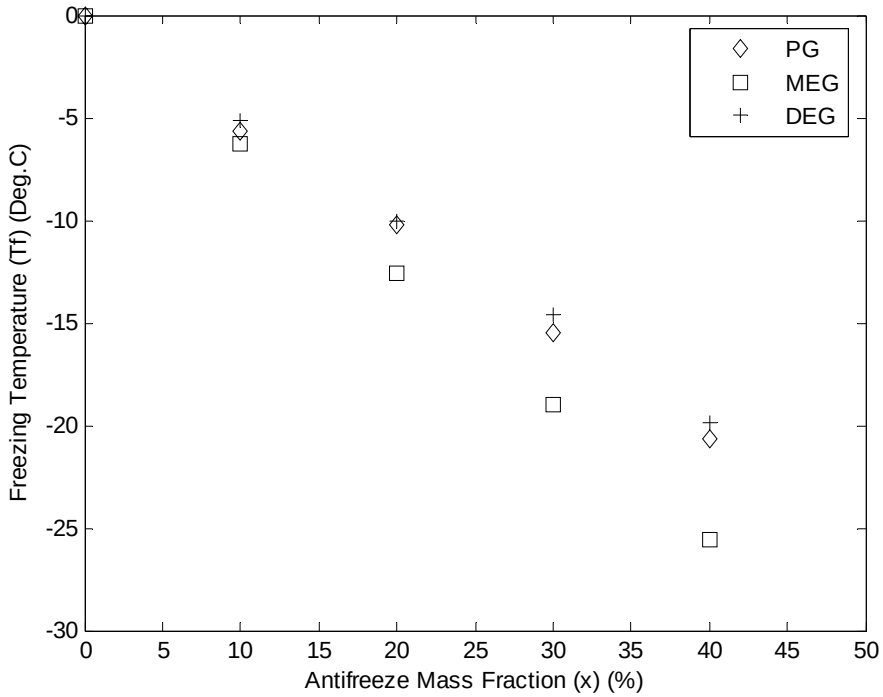

Fig.3.25. Freezing curve of water-PG, water- MEG and water- DEG mixture

Recorded temperatures of aqueous solution of antifreezes, refrigerant temperatures at evaporator inlet and outlet, refrigerant temperatures at condenser inlet

and outlet at different concentrations are plotted for better understanding of the system (Figures. 3.26 to 3.29 for PG, Figures 3.30 to 3.33 for MEG and Figures 3.34 to 3.37 for DEG) with respect to freezing time required for ice slurry formation.

From the present experimental ice slurry generation data it can be observed that ice slurry generation process can be divided into three stages- cool down or chilling period, nucleation or unstable ice slurry generation period and stable ice slurry generation period. The first stage (cool down period) starts t_0 to t_1, where t_0 is the starting time of the experiment and t_1 is the time at the end of the chilling period which is the on-set of the super-cooling phenomenon. During the chilling period volumetric ice concentration is zero. As observed in Figures 3.26 to 3.29, the freezing temperature reduces with increase in antifreeze mass fraction for PG and MEG solution initially chilled continuously without phase change in stage 1. First phase time duration is 64, 69, 87 and 90 minutes respectively for 10%, 20%, 30%and 40% concentration of PG. Similar trends were observed for MEG (Figures 3.30 to 3.33) and DEG (Figures 3.34 to 3.37) but first phase time duration was relatively higher as compared to PG. During this stage the average evaporator temperature decreases sharply which causes increase in the refrigeration capacity and compressor work. Therefore, the condenser inlet temperature increases due to higher heat rejection quantity. The second stage (nucleation period) starts from t_1 to t_2, where the ice seeds after the super cooling phenomenon is observed and the volumetric ice concentration increases till its maximum value at the end of this period (at t_2). In stage 2, nucleation of ice particles occurs and it is characterized by 0.5 to 1^0C sudden increase in temperature of the process fluid due to the release of the fusion heat of ice. Finally the third stage (ice slurry generation period) starts from t_2 to the end of the experiment, at t_f. During this stage the ice concentration is maintained constant at its maximum value. During stage 3 the heat transfer is affected by the release of the latent heat of water freezing.

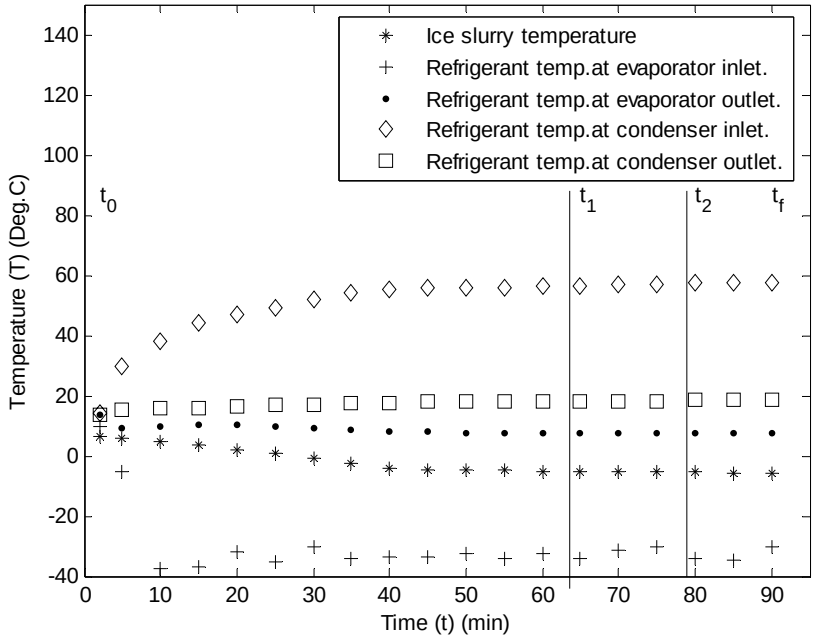

Fig.3.26. Freezing temperature vs time for PG at 10 % concentration

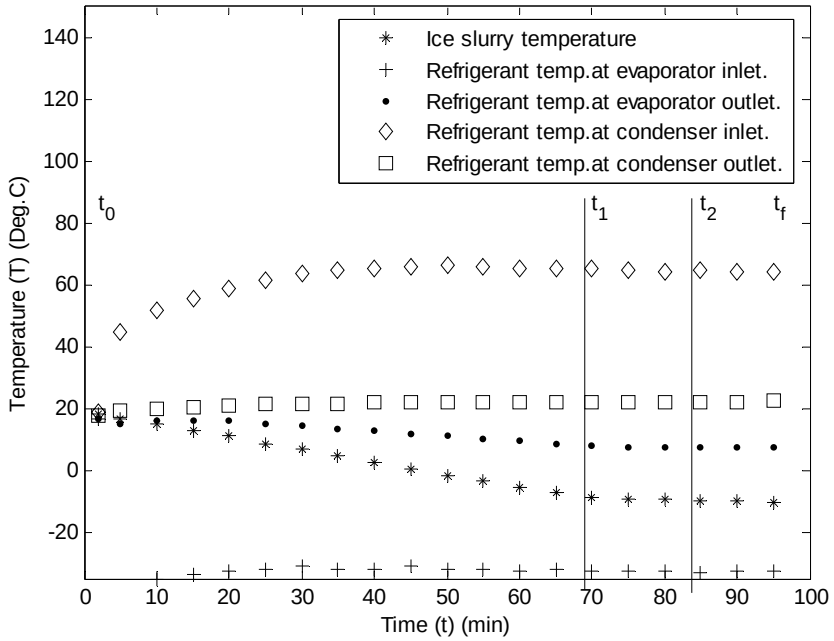

Fig.3.27. Freezing temperature vs time for PG at 20 % concentration

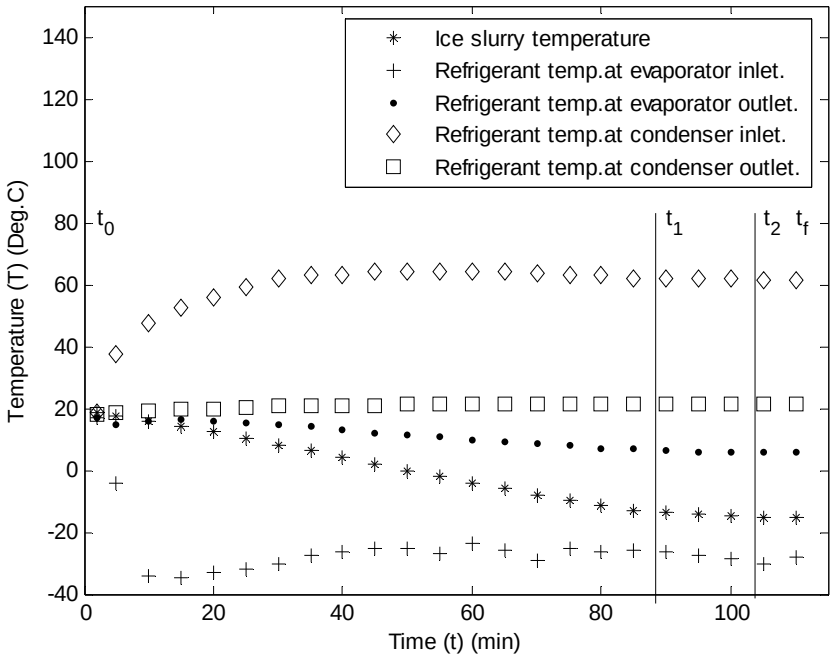

Fig.3.28. Freezing temperature vs time for PG at 30 % concentration

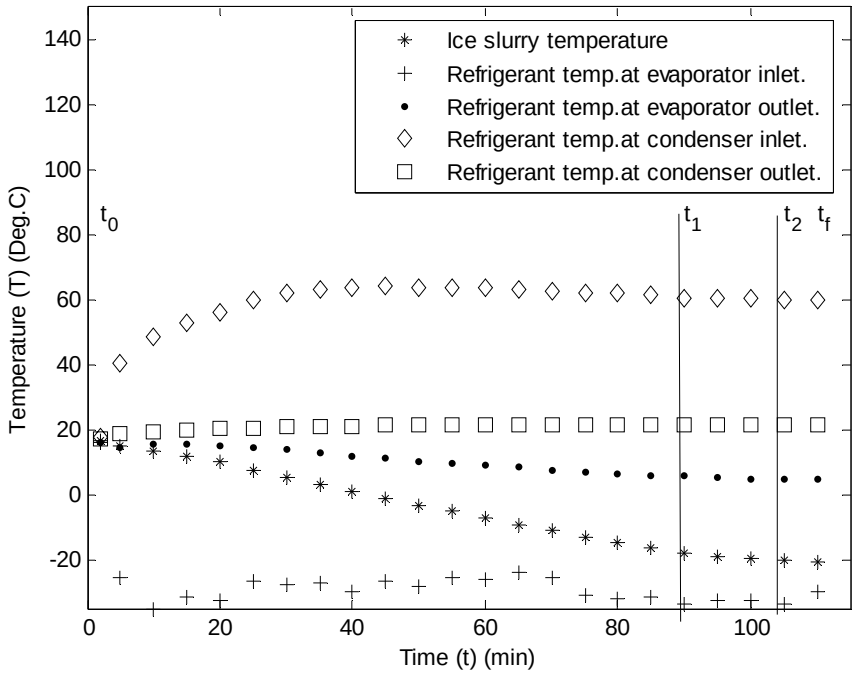

Fig.3.29. Freezing temperature vs time for PG at 40 % concentration

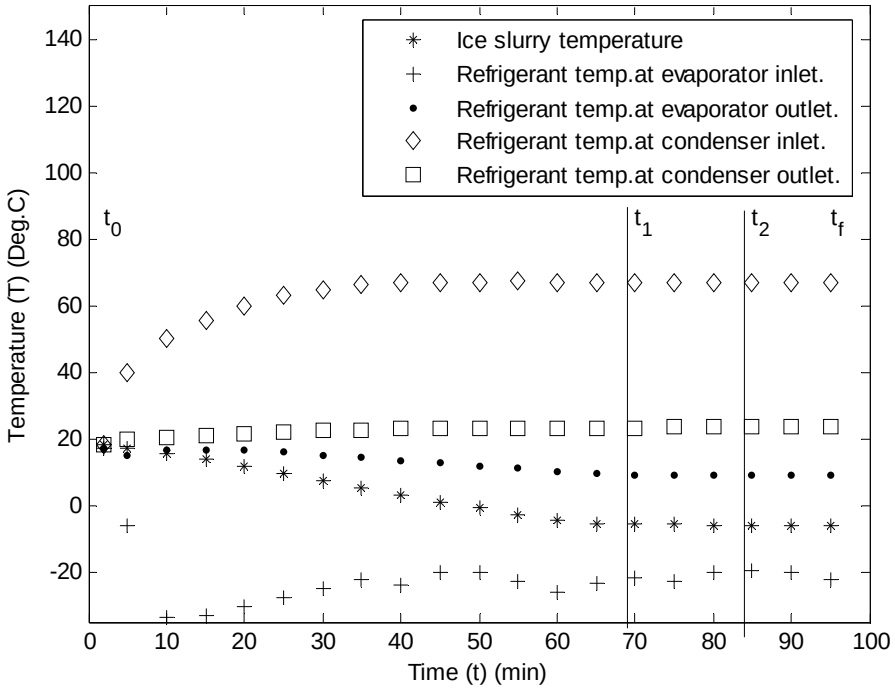

Fig.3.30. Freezing temperature vs time for MEG at 10 % concentration

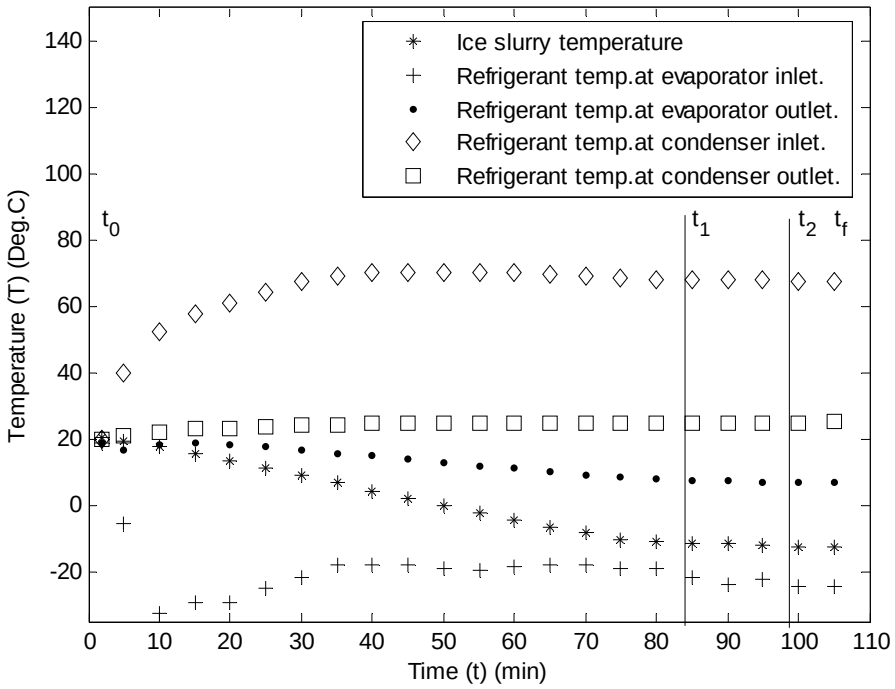

Fig.3.31. Freezing temperature vs time for MEG at 20 % concentration

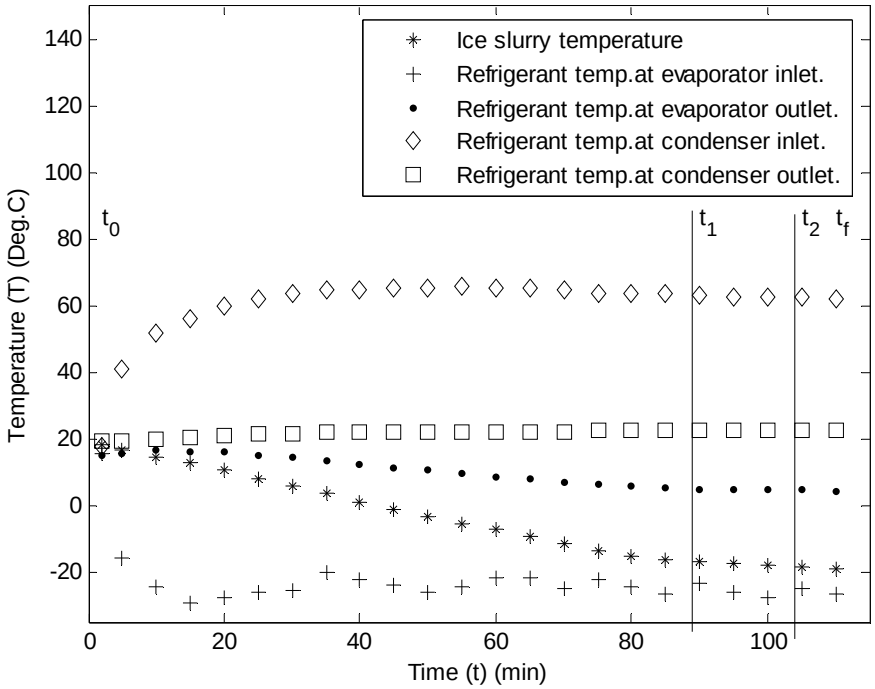

Fig.3.32. Freezing temperature vs time for MEG at 30 % concentration

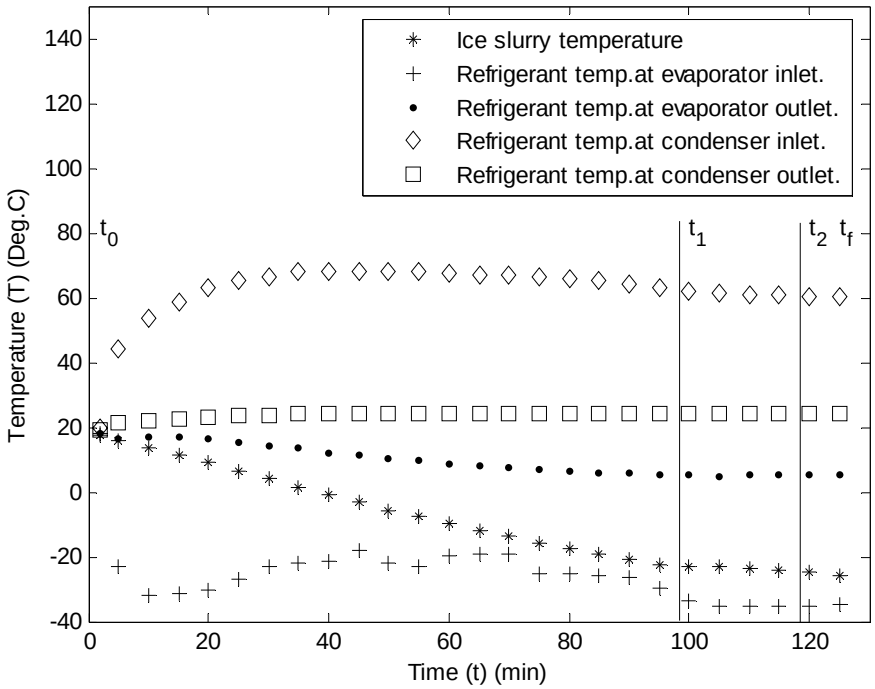

Fig.3.33. Freezing temperature vs time for MEG at 40 % concentration

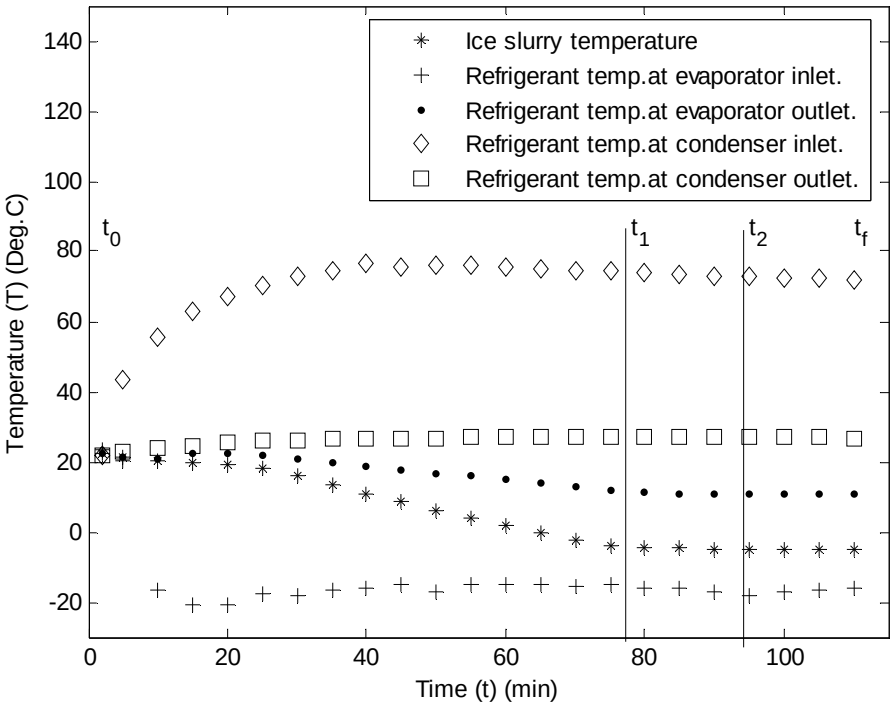

Fig.3.34. Freezing temperature vs time for DEG at 10 % concentration

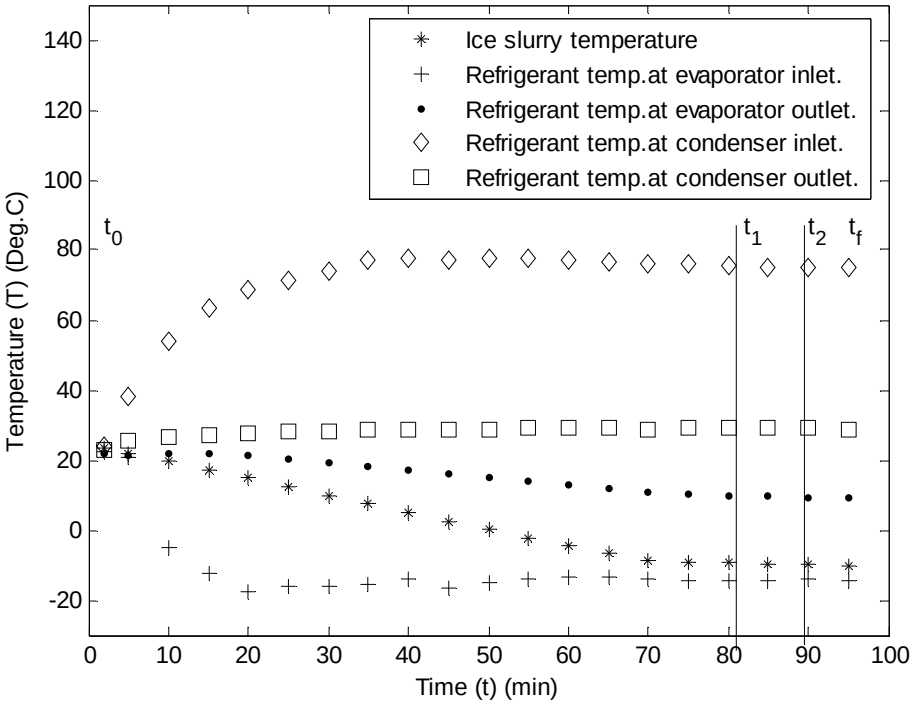

Fig.3.35. Freezing temperature vs time for DEG at 20 % concentration

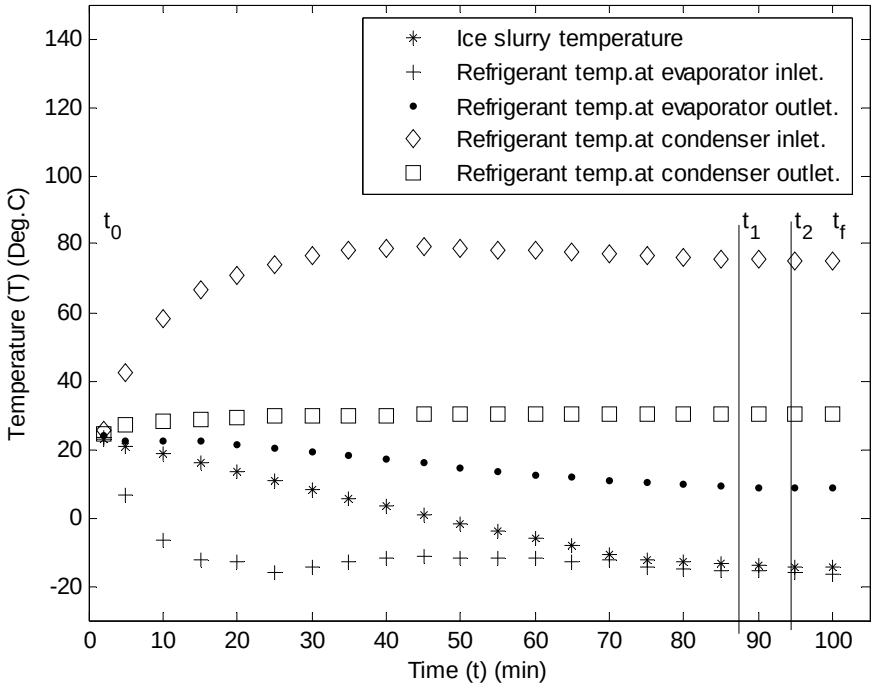

Fig.3.36. Freezing temperature vs time for DEG at 30 % concentration

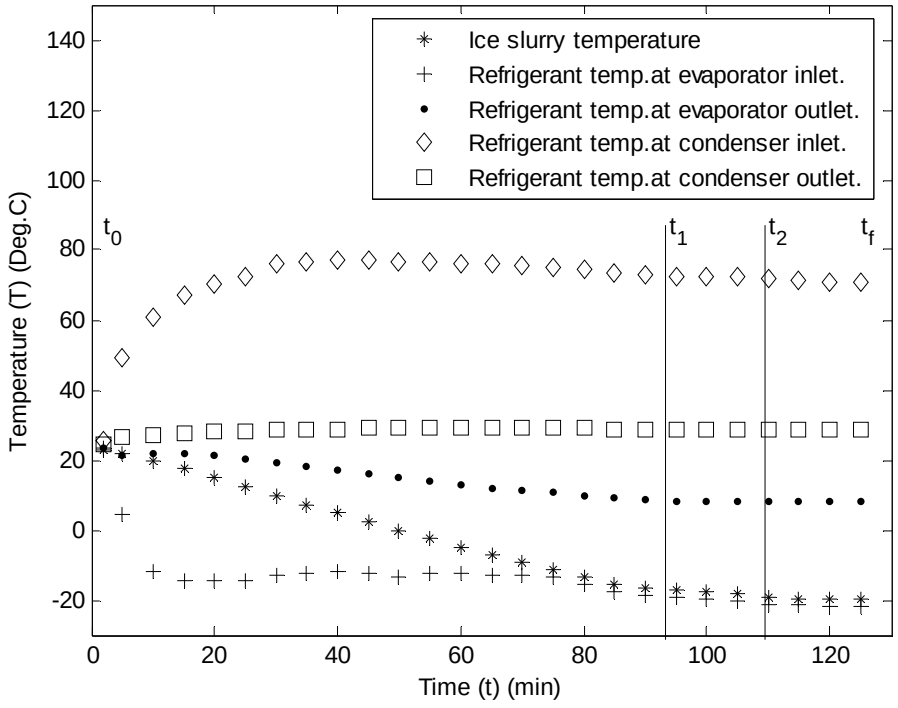

Fig.3.37. Freezing temperature vs time for DEG at 40 % concentration

The measured volumetric ice concentration vs. time for 10%, 20%, 30% and 40% concentrations of PG, MEG and DEG are shown in Figures 3.38 to 3.40. The measured volumetric ice concentration increases with increase in concentrations. Here, the time required for 50% measured volumetric ice concentration increases with increase in concentrations of PG, MEG and DEG.

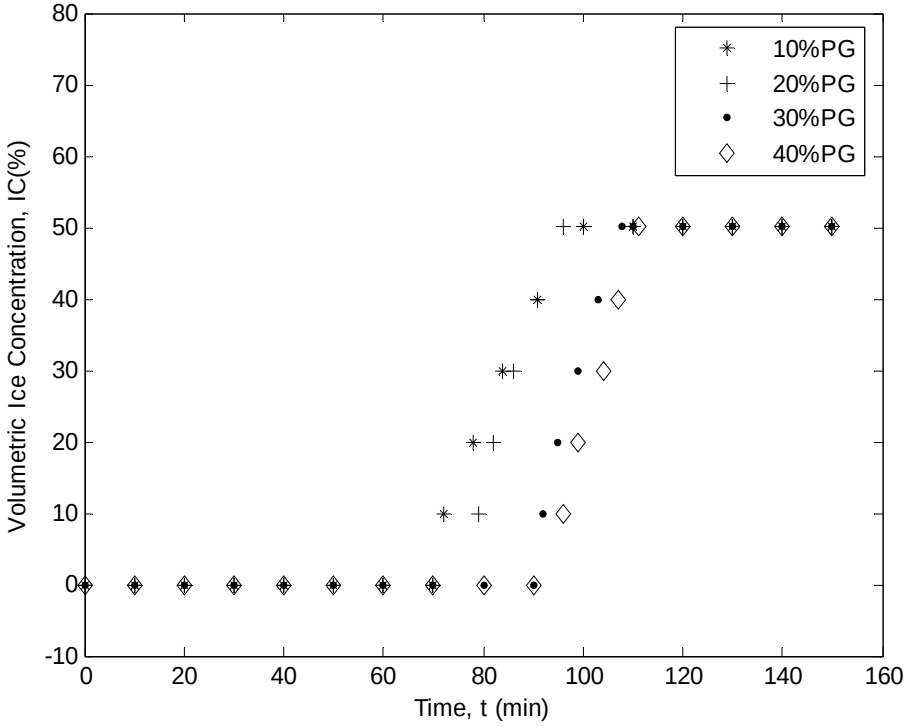

Fig.3.38. Volumetric ice concentration vs time for PG

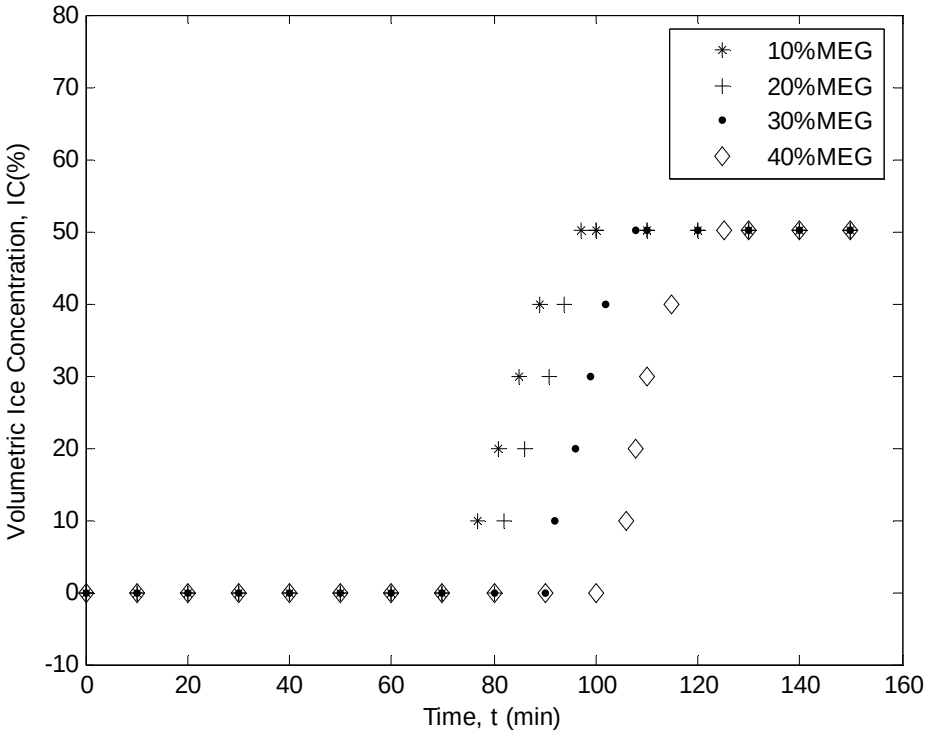

Fig.3.39. Volumetric ice concentration vs time for MEG

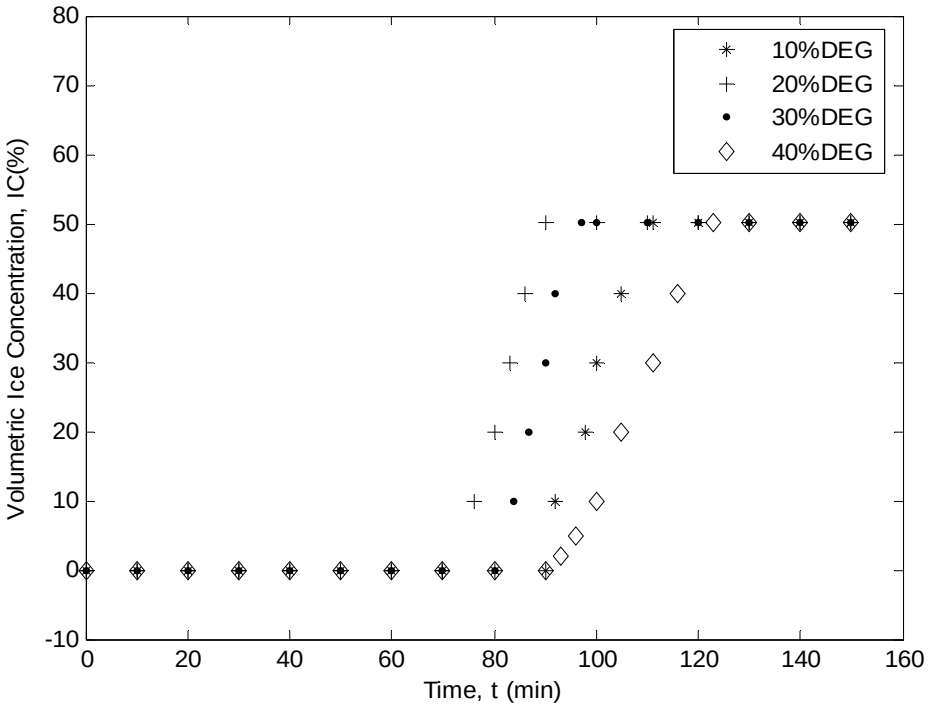

Fig.3.40. Volumetric ice concentration vs time for DEG

3.2.5. CALCULATION OF THERMOPHYSICAL PROPERTY DATA OF ICE SLURRY

Table 3.9.(a) and 3.9. (b) Summarizes the calculated thermophysical Properties of Ice Slurry at 10%, 20%, 30% and 40% concentrations of PG and MEG respectively and 10% ice fraction (Equations 4.39 to 4.45). With increase in concentrations of PG and MEG, density, dynamic viscosity and Prandtl number increases whereas specific heat and thermal conductivity decreases with increase in concentrations. As compare to water, PG and MEG solutions having higher density, higher dynamic viscosity, higher thermal conductivity and higher Prandtl number whereas lower specific heat.

Table 3.9 also shows the comparison of thermo-physical properties of ice slurry with respect to the water. Density of ice slurry slightly increases with increase in depressant concentration. Due to two phase mixture present in the ice slurry, the change in dynamic viscosity with increase of concentration of depressant are significant. Presence of ice particles causes 6 to 8 times increase in dynamic viscosity. The thermal conductivity of ice slurry initially increases upto 10% concentration of depressant and then decreases with further addition of depressant concentration. Specific heat of ice slurry reduces due to weighted average properties of mixture constituents. There is significant increase in magnitude of Prandtl number due the increase in dynamic viscosity.

Table 3.9(a) Calculated thermophysical properties of ice slurry at various concentrations of PG

Thermophysical Properties	Concentration of PG				
	0%	10%	20%	30%	40%
Temperature (^{0}C)	4.0	-5.7	-10.2	-15.5	-20.7
Density (Kg/ m^3)	990.54	996.45	1001.9	1007.5	1013.1
Dynamic viscosity (Kg/m-s)	0.0013	0.0029	0.0043	0.0066	0.0099
Thermal conductivity (W/m-K)	0.5881	0.6605	0.6402	0.6183	0.5951
Specific heat (J/Kg-K)	4196.00	4140.40	4077.40	4010.60	3939.50
Prandtl number	9.09	17.91	27.26	42.73	65.78

Table 3.9(b) Calculated thermophysical properties of ice slurry at various concentrations of MEG

Thermophysical Properties	Concentration of MEG				
	0%	10%	20%	30%	40%
Temperature (^{0}C)	4.0	-6.3	-12.6	-19.0	-25.6
Density (Kg/ m^3)	990.54	996.46	1002.00	1007.5	1013.1
Dynamic viscosity (Kg/m-s)	0.0013	0.0029	0.0047	0.0076	0.0121
Thermal conductivity (W/m-K)	0.5881	0.6601	0.6384	0.6151	0.5896
Specific heat (J/Kg-K)	4196.00	4140.60	4077.60	4009.50	3935.90
Prandtl number	9.09	18.21	29.79	49.34	76.49

3.2.6. FIRST LAW ANALYSIS

Using the experimental data given in Table 3.6(a), Table 3.6(b) and Table 3.6(c) thermodynamic heat and work calculations of Ice Slurry Generation System is shown in Table 3.10.(a), (b) and (c). For different concentrations of additives PG, MEG and DEG, the COP of the system is between 2.92 to 3.33 for PG, 2.75 to 2.88 for MEG and 2.30 to 2.55 for DEG.

Table 3.10(a) Thermodynamic heat and work calculations of Ice Slurry Generation System at various concentrations of PG (Sample calculation in given in APPENDIX-I)

	Concentration of PG			
	10%	20%	30%	40%
Refrigerating Effect, $N= m_r (h_1 - h_5)$ (W)	3822.70	3653.50	3673.40	3663.70
Compressor Work, $W= m_r (h_2 - h_1)$ (W)	1148.00	1231.30	1241.50	1251.00
Coefficient of Performance (COP=N/W)	3.33	2.97	2.95	2.92
Heat Rejected in Condenser, $Qc= m_r (h_2 - h_4)$ (W)	4970.70	4884.80	4914.90	4914.70

Table 3.10(b) Thermodynamic heat and work calculations of Ice Slurry Generation System at various concentrations of MEG

	Concentration of MEG			
	10%	20%	30%	40%
Refrigerating Effect, $N= h_1 - h_5$ (W)	3564.70	3526.70	3561.00	3533.00
Compressor Work, $W= h_2 - h_1$ (W)	1237.30	1253.50	1277.80	1282.10
Coefficient of Performance (COP=N/W)	2.88	2.81	2.78	2.75
Heat Rejected in Condenser, $Qc=h_2-h_4$ (W)	4802.00	4780.10	4838.80	4815.10

Table 3.10(c) Thermodynamic heat and work calculations of Ice Slurry Generation System at various concentrations of DEG

	Concentration of DEG			
	10%	20%	30%	40%
Refrigerating Effect, $N= h_1 - h_5$ (W)	3179.70	3135.20	3098.00	3141.70
Compressor Work, $W= h_2 - h_1$ (W)	1247.70	1320.00	1339.60	1361.90
Coefficient of Performance (COP=N/W)	2.55	2.37	2.31	2.30
Heat Rejected in Condenser, $Qc=h_2-h_4$ (W)	4427.40	4455.20	4437.50	4503.60

Experimental uncertainties:

Uncertainty analysis of thermodynamic heat and work calculations of Ice Slurry Generation System is shown in Table 3.11. (a), (b) and (c) (for details refer APPENDIX-II).

Table 3.11(a) Uncertainty analysis of thermodynamic heat and work calculations of Ice Slurry Generation System at various concentrations of PG

Operation Parameters	Uncertainty (Concentration of PG)			
	10%	20%	30%	40%
Refrigerating Effect, (N)	±0.003241	±0.003213	±0.002687	±0.002913
Compressor Work, (W)	±0.005003	±0.005754	±0.005590	±0.005551
Coefficient of Performance (COP)	±0.000339	±0.000293	±0.000282	±0.000291
Heat Rejected in Condenser, (Qc)	±0.005964	±0.006393	±0.006141	±0.006049

Table 3.11(b) Uncertainty analysis of thermodynamic heat and work calculations of Ice Slurry Generation System at various concentrations of MEG

Operation Parameters	Uncertainty (Concentration of MEG)			
	10%	20%	30%	40%
Refrigerating Effect, (N)	±0.002558	±0.002718	±0.002455	±0.003236
Compressor Work, (W)	±0.005947	±0.006083	±0.005753	±0.005893
Coefficient of Performance (COP)	±0.000263	±0.000264	±0.000267	±0.000285
Heat Rejected in Condenser, (Qc)	±0.006592	±0.006568	±0.006112	±0.006210

Table 3.11(c) Uncertainty analysis of thermodynamic heat and work calculations of Ice Slurry Generation System at various concentrations of DEG

Operation Parameters	Uncertainty (Concentration of DEG)			
	10%	20%	30%	40%
Refrigerating Effect, (N)	±0.002277	±0.002063	±0.002266	±0.002409
Compressor Work, (W)	±0.006361	±0.006878	±0.007048	±0.006794
Coefficient of Performance (COP)	±0.000242	±0.000221	±0.000221	±0.000229
Heat Rejected in Condenser, (Qc)	±0.006896	±0.007074	±0.007116	±0.006750

3.3. ECONOMICS OF ICE SLURRY GENERATOR (74 LITRE CAPACITY)

The economic details of present ice slurry generator of 74 Litre capacity are given below:

1. Inner cylinder: SS, inner dia =0.30m, tube length = 1.050 m = Rs. 14000-00
2. Insulation = 60 mm thick polyurethane foam = Rs 4500-00
3. Outer shell: MS = Rs 6500-00
4. Evaporator Coil: Circular shell and coil type of 5/8 inch diameter copper tube, 50 number of turns = Rs 4500-00
5. Compressor :5TR (Model TF265) single phase, 230V, 50 Hz = Rs. 56000-00
6. Compressor motor: 5 hp = Rs. 18000-00
7. Pulley-Belt Driver Set = Rs 9500-00
8. Condenser: Air cooled fin and coil type, 21 inch ×19 inch, 3 row deep, 3/8 inch diameter copper tubes, 10 fins per inch, fan 1380 rpm = Rs. 12500-00
9. Condenser fan 1380 rpm = Rs 6400-00
10. Thermostatic expansion valve with five way distribution = Rs 2000-00
11. Accumulator = Rs 1200-00
12. Liquid Receiver = Rs 4500-00
13. Solenoid Valve = Rs 2200-00
14. Drier = Rs 800-00
15. Scraper /Agitation mechanism: SS 304 scraper blades 152.4 mm (L), 25.4 mm (W) = Rs 4500-00

16. Gear and Scraper motor = Rs. 18500-00
17. Refrigerant Piping = Rs. 21000-00
18. Electrical Panel = Rs. 20500-00
19. Refrigerant = R410 A = Rs 5000-00
20. Freezing point depressant: Propylene glycol, mono ethylene glycol, di ethylene glycol = Rs. 38000-00
21. Base Frame = Rs. 10000-00
22. Manufacturing Charges (welding, soldering, bending, grinding, insulating) for assembly = Rs. 25000-00

Total **= Rs. 285150-00**

= Rs. 285150-00 / 74

= Rs. 3853 per TR

The price of 74 litre capacity scraped surface ice slurry generator per TR comes out to be Rs.3858. For very large capacity scraped surface ice slurry generator the price per TR will increase due to manufacturing processes and materials

CHAPTER-IV
MATHEMATICAL FORMULATION FOR PLATE HEAT EXCHANGER USING ICE SLURRIES

This chapter presents the development of various thermohydraulic equations needed for numerical simulation for two cases, viz., water to water, and water to slurry heat transfer in a plate heat exchanger.

4.1. TERMINOLOGY OF PLATE HEAT EXCHANGER

Plate heat exchangers have a number of applications in the refrigeration and air-conditioning, pharmaceutical, petrochemical, chemical, power, industrial dairy, and food & beverage industry. Plate heat exchangers (PHE's) have a high heat transfer rate and low pressure drop compared to other types of heat exchangers due to their large surface area. These are composed of a number of thin metal plates compressed together into a 'plate pack' (Fig.4.1) by two pressure plates (head and follower). Within a plate heat exchanger, the fluid paths alternate between plates allowing the two fluids to interact, but not mix, several times in a small area. Each plate is corrugated to increase the surface area and maximize heat transfer.

The terminology [95] of plate heat exchanger (Fig.4.2) is given as:

Mean channel gap (passage width) is represented by, $b_1 = p - \delta$ (4.1)

Where p = channel pitch

and δ = plate thickness

The channel pitch can be determined as

$$p = \frac{compressed\ length}{(number\ of\ \ plates - 1)} \tag{4.2}$$

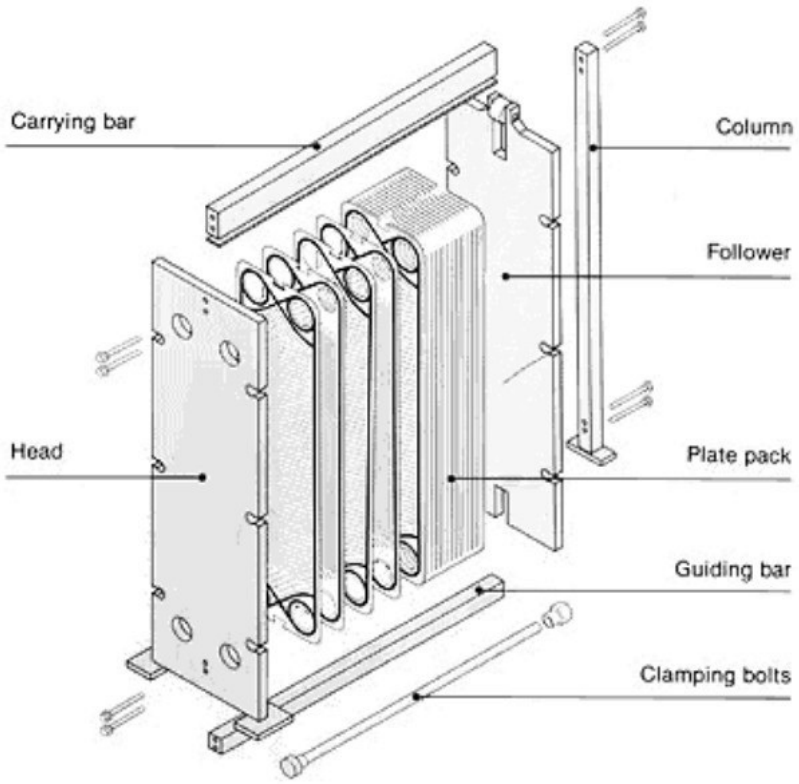

Fig.4.1. A schematic drawing of a chevron- type PHE showing various components

The channel free flow area can be given by

$$A_{free\ flow} = b.w \tag{4.3}$$

Where w is the effective plate width measured between the inner edges of the gaskets on the two sides.

θ = Corrugation angle

d_p = Port diameter

D_e = Equivalent diameter

The plate heat exchanger area can be related to the actual developed area of the plate or on the projected length. For each system a heat transfer coefficient defined on the basis of that particular area. To use the projected area we need to define the ratio ϕ between the developed to the projected length as

$$\phi = \frac{developed\ length}{projected\ length} \tag{4.4}$$

The value of ϕ varies from 1.10 to 1.25. Often an average value of 1.17 is used.

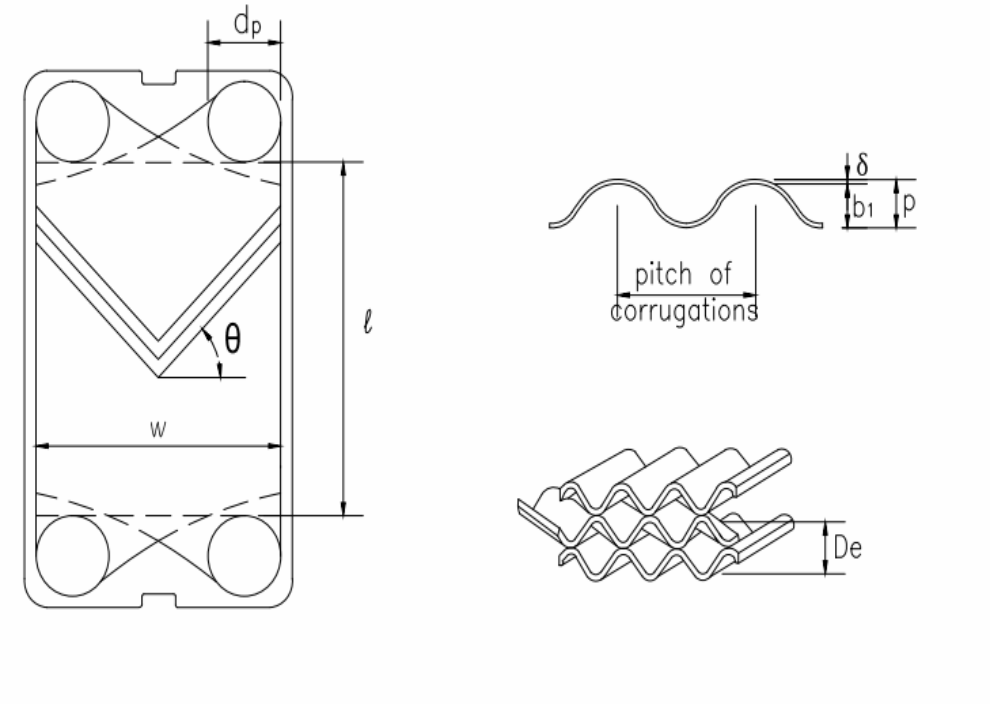

Fig.4.2. A schematic drawing of a chevron- type PHE

The flow hydraulic diameter (also known as equivalent diameter), D_e can be calculated as

$$D_e = 4\frac{channel\ free\ flow area\ for\ fluid}{wetted\ perimeter\ for the\ fluid} \tag{4.5}$$

Now the derivation for D_e depends on the convention used, i.e. whether the projected or developed area is taken as basis. If developed area is used,

$$Wetted\ perimeter\ for the\ fluid = 2.(b + \phi w) \tag{4.6}$$

Substitution of (4.6) and (4.3) to (4.5) gives

$$D_e = \frac{4.bw}{2(b + \phi w)} \tag{4.7}$$

Now for PHE , $b << w$ thus the b in denominator can be neglected, giving

$$D_e = 2.b/\phi \tag{4.8}$$

If instead of developed area, the projected area is considered then the equivalent diameter reduces to

$$D_e = 2.b \tag{4.9}$$

Because of simplicity the projected area is preferred. This allows the heat exchanger area of the plate to be defined simply as

$$A_p = lw \tag{4.10}$$

Where l = Projected plate length

Mean velocity of the fluid in the channel, u can be determined as

$$u = \frac{total\ volume\ flow\ rate\ of\ the\ fluid\ under\ consideration}{free\ flow\ area\ of\ channel \times no.of\ channels\ to\ which\ the\ fluid\ is\ distributed} \tag{4.11}$$

4.2. PLATE HEAT EXCHANGER FORMULATION

Thermo-hydraulic modeling of plate heat exchanger for chilled water vs hot water and ice slurry vs hot water is described below:

4.2.1. CHILLED WATER VS HOT WATER

Thermo-hydraulic modeling [47] represents the relationship between the stream heat transfer coefficient, pressure drop and exchanger area. The present model provides the possibility to predict heat transfer based on the allowable pressure drop and vice versa. Ice slurry to hot water correlations are given in reference [4]. The geometrical details of the PHE used in the present study are shown in Fig.4.2.

The equation for fanning friction factor [47] is given by

$$\frac{1}{\sqrt{f}} = \frac{\cos\theta}{\sqrt{0.045\tan\theta + 0.09\sin\theta + f_0/\cos\theta}} + \frac{1-\cos\theta}{\sqrt{3.8 f_1}} \tag{4.12}$$

Where $f_0 = 16/\mathrm{Re}$ for $\mathrm{Re} < 2000$ and $f_0 = (1.56\ln \mathrm{Re} - 3.0)^{-2}$ for $\mathrm{Re} \geq 2000$ and

$f_1 = (149/\mathrm{Re}) + 0.9625$ for $\mathrm{Re} < 2000$ and $f_1 = 9.75/\mathrm{Re}^{0.289}$ for $\mathrm{Re} \geq 2000$.

Re = Reynolds number

The correlation for the heat transfer coefficient is given by

$$Nu = 0.205\,\mathrm{Pr}^{1/3}(\mu_m/\mu_w)^{1/6}(f\,\mathrm{Re}^2\sin 2\theta)^{0.374} \tag{4.13}$$

Nu = Nusselt number

Pr = Prandtl Number

However, these correlations are not in the conventional forms required by Equations. (4.14) and (4.17) (given below). In order to make the calculation simple, Martin's correlations are converted to the forms of Equations. (4.14) and (4.17) through curve-fit formulas for any specific corrugation angle (θ).

The film heat transfer coefficient is given in the following form

$$Nu = a\,\mathrm{Re}^b\,\mathrm{Pr}^{0.33}(\mu/\mu_w)^{0.17} \tag{4.14}$$

a = Constant

b = Constant

This can be re-arranged to

$$h = k_1 u^b \tag{4.15}$$

Where

$$k_1 = a(\lambda/D_e)(D_e/\nu)^b\,\mathrm{Pr}^{0.33}(\mu/\mu_w)^{0.17} \tag{4.16}$$

λ = Thermal conductivity of PHE material

The Fanning friction factor is often given in the following form

$$f = c\,\mathrm{Re}^d \tag{4.17}$$

c = Constant

d = Constant

And the pressure drop is calculated across inlet and outlet as

$$\Delta P = 2f(nl/D_e)\rho u^2 \tag{4.18}$$

From equations. (4.17) and (4.18), one finds

$$\Delta P = k_2(nl)u^{2+d} \tag{4.19}$$

Where

$$k_2 = 2c(D_e / \nu)^d (\rho / D_e) \tag{4.20}$$

The stream velocity is calculated by

$$u = m_p / (\rho S) \tag{4.21}$$

Mass flow rate per passage is calculated by

$$m_p = 2M / (N+1) \tag{4.22}$$

Cross sectional area of passage is calculated by

$$S = b_1 / w \tag{4.23}$$

The surface area of the heat exchanger is calculated by

$$A = (mw).(nl) \tag{4.24}$$

Therefore, the following equation can be derived

$$nl = k_3 Au \tag{4.25}$$

Where

$$k_3 = D_e / (2V) \tag{4.26}$$

Substituting the exchanger pass length in Equation (4.19) by Equation (4.25), the pressure drop can be calculated as

$$\Delta P = k_2 k_3 A u^{3+d} \tag{4.27}$$

By combining Equations (4.15) and (4.27), the thermo-hydraulic model can finally be obtained as

$$\Delta P = \left(\frac{k_2 k_3}{k_1^{((3+d)/b)}} \right) A h^{((3+d)/b)} = \sigma A h^{((3+d)/b)} \tag{4.28}$$

The values of k_1, k_2 and k_3 are dependent on the stream physical properties, the stream volumetric flow rate (V), the equivalent diameter (D_e) and the plate pattern.

Mass velocity inside the port is calculated by

$$G_p = \left(\frac{M}{(\pi / 4) d_p^{\,2}} \right) \tag{4.29}$$

Port pressure drop is calculated by

$$\Delta P_{port} = 1.4\left(\frac{G_p^{\ 2}}{2\rho}\right)n \tag{4.30}$$

Pressure drop due to elevation is calculated by

$$\Delta P_{elev} = \rho g l \tag{4.31}$$

Therefore the total pressure drop is given by

$$\Delta P_{total} = \Delta P + \Delta P_{port} + \Delta P_{elev} \tag{4.32}$$

For stream 1 (the reference stream), heat transfer coefficient can be calculated from the thermal-hydraulic model

$$h_1 = (\Delta P_1 / \sigma_1 A)^{(b/(3+d))} = f_1(A) \tag{4.33}$$

The heat transfer coefficient h_2 of stream 2 is calculated in the similar manner. The overall heat transfer coefficient of PHEs is given by

$$U = \left(\frac{1}{h_1} + \frac{1}{h_2} + \frac{\delta}{\lambda} + R_{f1} + R_{f2}\right)^{-1} \tag{4.34}$$

Where, δ = plate thickness

λ = thermal conductivity of PHE material

R_f = fouling factor

Predicted cooling duty is calculated by

$$Q_{pr} = U.A.LMTD \tag{4.34a}$$

4.2.2. ICE SLURRY VS HOT WATER

Thermo-hydraulic modeling for ice slurry vs hot water is described below:

Correlation for pressure drop in plate heat exchanger is given by equation (4.35) All fluid properties used in the following correlations are based on average ice slurry properties between the inlet and outlet conditions [4]. For ice slurry pressure drop (ΔP) is calculated by equation (4.35).Using this value of pressure drop, heat transfer coefficient h_1 is calculated similar to the procedure followed above.

$$\Delta P = \frac{f(\mathrm{Re}).1000}{\rho}.M^2.\phi_{ice} \tag{4.35}$$

Where M = Channel mass flow rate (kg/s)

ρ = Fluid density (kg/m^3)

ϕ_{ice} = Two-phase correction factor

$$\phi_{ice} = \left(\frac{\mu_{wall}}{\mu_{bulk}}\right)^{\left(\frac{1.2}{\sqrt{\mathrm{Re}+6}}\right)} \tag{4.36}$$

$$f(\mathrm{Re}) = e^{\left[y+\frac{z}{\mathrm{Re}^{1.5}}\right]} \tag{4.37}$$

Re =Reynolds number

$$\mathrm{Re} = \frac{M^2}{w.\mu_{bulk}} \tag{4.38}$$

w = Channel width (m)

μ_{bulk} = Ice slurry viscosity (Pa-s)

The empirical values [4] for the constants y and z obtained from experimental data are given in Table 4.1. A, B and C are three plate heat exchangers of different physical dimensions 462 mm× 70 mm× 35 mm, 283 mm× 113 mm×35 mm, 183 ×mm ×70mm × 70mm respectively and area.

Table 4.1. Empirical values to correlate pressure drop results [4]

	(C)	(B)	(A)
y	17	16	17.6
z	110	221	181

4.2.3. FORMULATION FOR THERMOPHYSICAL PROPERTIES OF ICE SLURRY

4.2.3.1. Mass fraction of ice

The mass fraction [4] of ice or ice concentration, c_I, can be calculated from:

$$c_I = m_I /(m_I + m_S) = (c_S - c_0)/c_S \tag{4.39}$$

Where, m_I is the mass of ice, m_S is the mass of the concentrated aqueous solution, c_S is the concentration of the concentrated aqueous solution and c_0 is the initial concentration of depressant.

4.2.3.2. Density and volumetric ice fraction

The density of ice slurries at equilibrium, ρ_{IS}, may be estimated [4] with a mixing equation where ρ_S is the density of the concentrated aqueous solution.

$$\rho_{IS} = 1/[(c_I/\rho_I) + (1 - c_I)/\rho_S] \tag{4.40}$$

Where ρ_I is the density of ice.

Volume fraction of ice slurries c_{Iv} is given by:

$$c_{Iv} = c_I /((c_I + (1 - c_I)\rho_I/\rho_S) \tag{4.41}$$

4.2.3.3. Viscosity of ice slurries in equilibrium

Viscosity of ice slurries for low or moderate ice concentrations is given by [4]:

$$\mu_{IS} = \mu_S (1 + 2.5\, c_{Iv} + 10.05\, c_{Iv}^{\ 2} + 0.00273\, e^{16.6 c Iv}) \tag{4.42}$$

Where c_{Iv} is the volumetric ice fraction and μ_S is the viscosity of the concentrated aqueous solution.

4.2.3.4. Thermal conductivity of ice slurry

Thermal conductivity k_{IS} of ice slurries is given by [4]:

$$k_{IS} = k_S (1 + 2\, c_{Iv} y) / (1 - c_{Iv} y) \tag{4.43}$$

Where

$$y = (1 - k_S / k_I) / (2.k_S / k_I + 1) \tag{4.44}$$

Where k_S is the thermal conductivity the concentrated aqueous solution.

4.2.3.5. Mean specific heat of ice slurry

Mean specific heat of ice slurry [4] can be expressed as:

$$c_{pIS} = ((c_S / 100)\, c_{pI}) + (1 - c_S / 100).c_{pS} \tag{4.45}$$

Where c_{pI} is the specific heat of ice and c_{pS} is the specific heat of concentrated aqueous solution.

4.3. SOLUTION METHODOLOGY

The steps involved in thermohydraulic modeling [47] are followed for calculation of pressure drop and heat transfer by developing a computer program in Matlab. The geometrical and operating input parameters are supplied at the beginning for stream 1. After calculating the fanning factor (f) from equation (4.12), the coefficients c and d of equation (4.17) are calculated by curve fitting. In a similar manner after calculating Nusselt number, coefficients (a and b) are calculated using equations (4.14) to (4.16). By using these coefficients, pressure drop (ΔP) for stream 1 is calculated by equation (4.28).Using this value of pressure drop, heat transfer coefficient h_1 for reference stream 1 is calculated by equation (4.33).

The complete procedure is repeated to calculate heat transfer coefficient h_2 for stream 2. The overall heat transfer coefficient of the plate heat exchanger is calculated

using equation (4.34). In the above procedure the stream for which the pressure drop is higher is selected as reference stream.

For ice slurry pressure drop (ΔP) is calculated by equation (4.35).Using this value of pressure drop, heat transfer coefficient h_1 is calculated as above by supplying thermophysical properties of ice slurry and finally the overall heat transfer coefficient is calculated. Thermophysical properties of ice slurry are calculated with the help of equations (4.39) to (4.45).

CHAPTER-V
EXPERIMENTAL STUDIES OF ICE SLURRIES IN PLATE HEAT EXCHANGER

Chapter 5 describes the details of the development and fabrication of PHE test rig for experimental studies. The experimental facility, consisting mainly of two independent circuits: the ice slurry formation circuit (described in Chapter 3) and the ice flow circuit. The ice flow circuit was designed and constructed to enable pressure drop and heat transfer measurements at the inlet and outlet of plate heat exchanger.

5.1. DESCRIPTION OF EXPERIMENTAL SETUP FOR PHE

Fig. 5.1 shows a schematic diagram of the experimental facility, consisting mainly of two independent circuits. The ice slurry formation circuit and the ice flow circuit.

5.1.1 THE ICE SLURRY FORMATION CIRCUIT

The ice slurry formation circuit mainly consists of scraped surface ice slurry generator of 74 litre capacity (Fig.5.1). The details of ice slurry formation is discussed in Chapter 3. This system produces fine ice crystals with diameters in the range between 0.15 and 0.20 mm.

5.1.2 ICE SLURRY FLOW CIRCUIT

The ice slurry flow circuit consists of ice slurry generator (1), condensing unit (9), ice slurry pump (2), ice slurry storage tank(4), agitator (8), plate heat exchanger (22), mass flow meters (14 & 19), thermocouple (20), pressure transducers (21), data acquisition system (10) and sampling points (17) etc. The details of these components are described below:

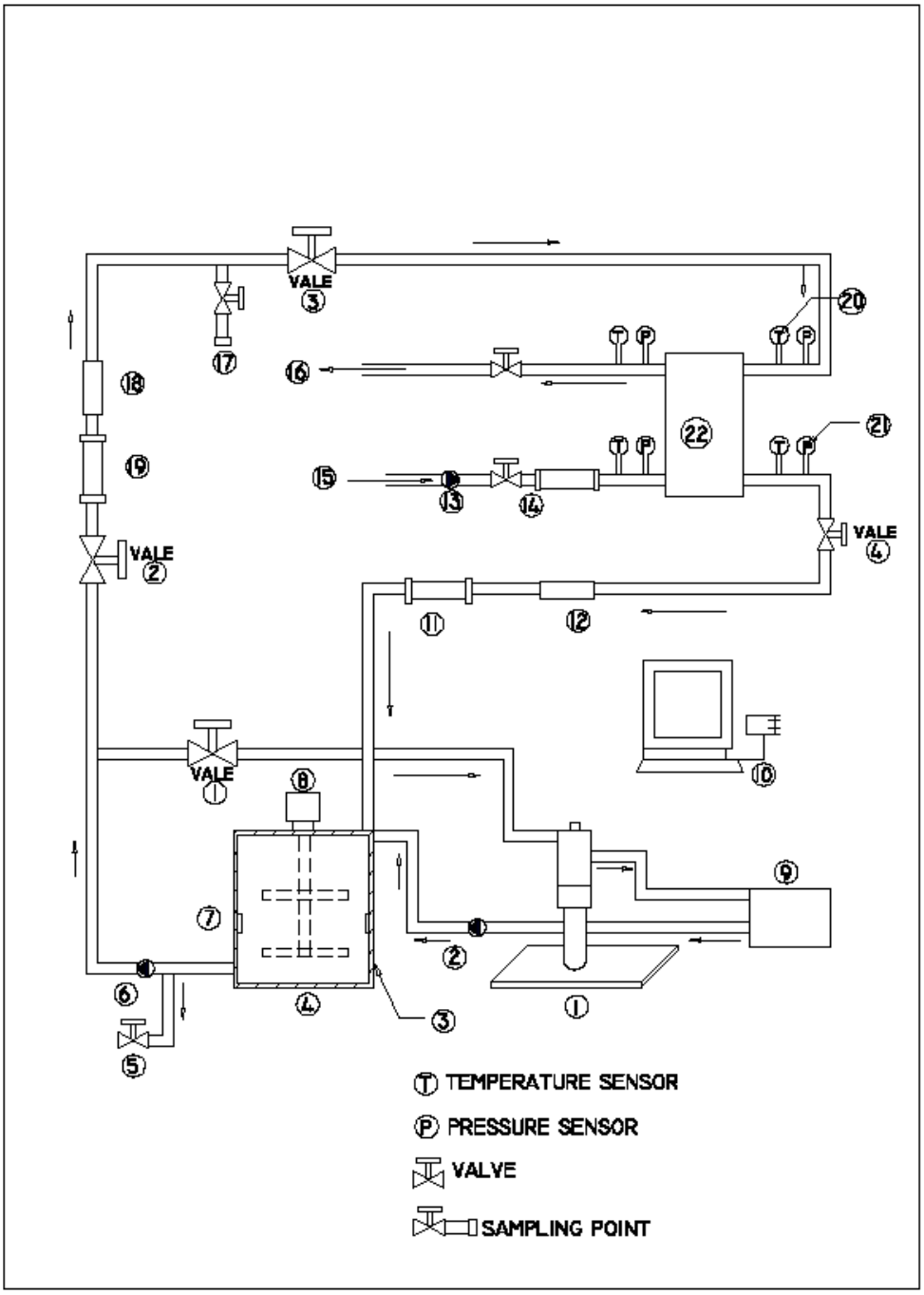

Fig.5.1. Schematic diagram of the experimental facility (1 = Ice Slurry Generator, 2 = Pump, 3 = Insulation, 4 = Ice Slurry Storage Tank, 5 = Drainage, 6 = Pump, 7 = Thermocouple, 8 = Agitator, 9 = Condensing Unit, 10 = Data Acquisition System, 11 = Mass Flow Meter, 12 = Transparent Viewing Section, 13 = Pump, 14 = Mass Flow Meter, 15 = Water in, 16 = Water out, 17 = Sampling Point, 18 = Transparent Viewing Section, 19 = Mass Flow Meter, 20 = Thermocouple, 21 = Pressure Transducer, 22 = Plate Heat Exchanger)

(a) Plate heat exchanger

The gasketted-plate heat exchanger has 24 plates with 11 channels on each side (see Fig. 5.2 and Fig.5.3). Each plate size is 480 mm in height and 150 mm wide. The hydraulic diameter is 4 mm. The entire pipe work is well insulated using polyurethane foam.

Geometrical parameters

Number of plates (N) = 24

Equivalent diameter (D_e) = $0.004\,m$

Port diameter (d_p) = $0.032\,m$

Pass number (n) = 1

Projected plate length (l) = $0.410\,m$

Path number of chilled water (m_1) =11

Path number of hot water (m_2) =11

Plate width (w) = $0.150\,m$

Corrugation angle (θ) = $60°$

Plate thickness (δ) = $0.0005\,m$

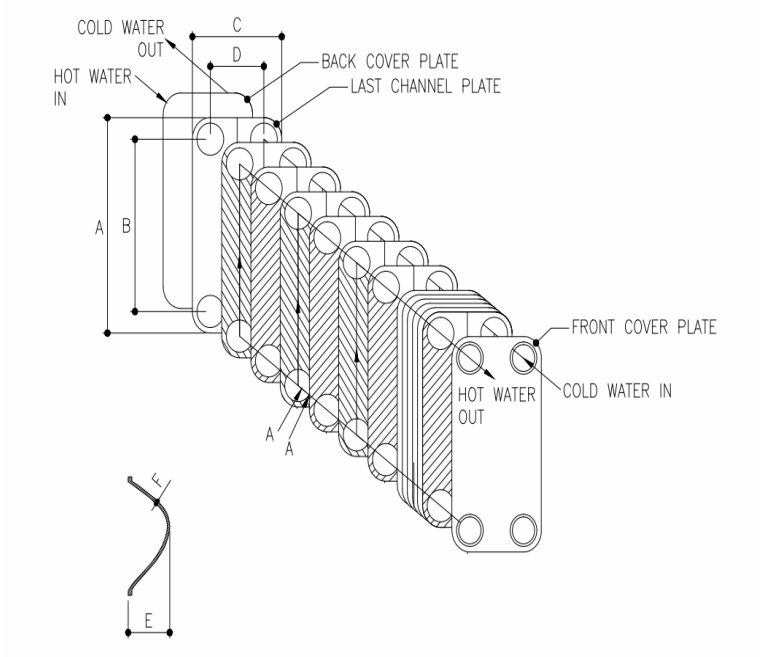

A = 0.480 m D = 0.075 m
B = 0.410 m E = 2.4 mm
C = 0.150 m F = 0.4 mm

Fig.5.2. Dimensions of plate heat exchanger

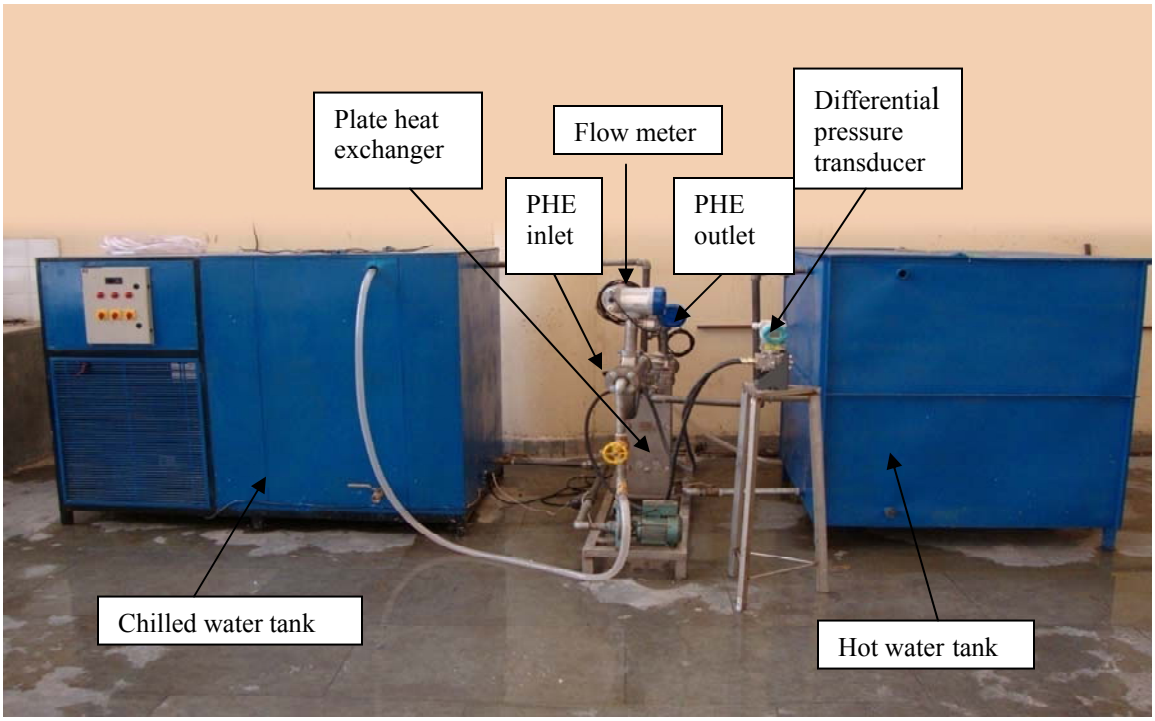

Fig.5.3 Photograph of the experimental facility

(b) Condensing unit

Condensing unit of 1.5 TR capacity (Fig.5.4) consists of sealed compressor (1.5 TR), air-cooled condenser, capillary tube and evaporator coil consist of 9.525 mm (3/8 inch) diameter copper tube (Fig.5.5), used to produce chilled water which is supplied to PHE through chilled water inlet (15as shown in Fig 5.1).

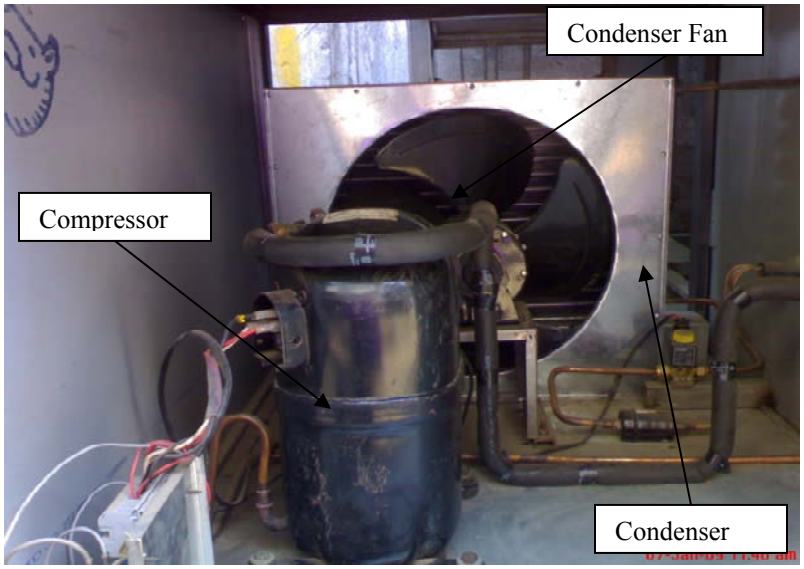

Fig.5.4 Photograph of condensing unit

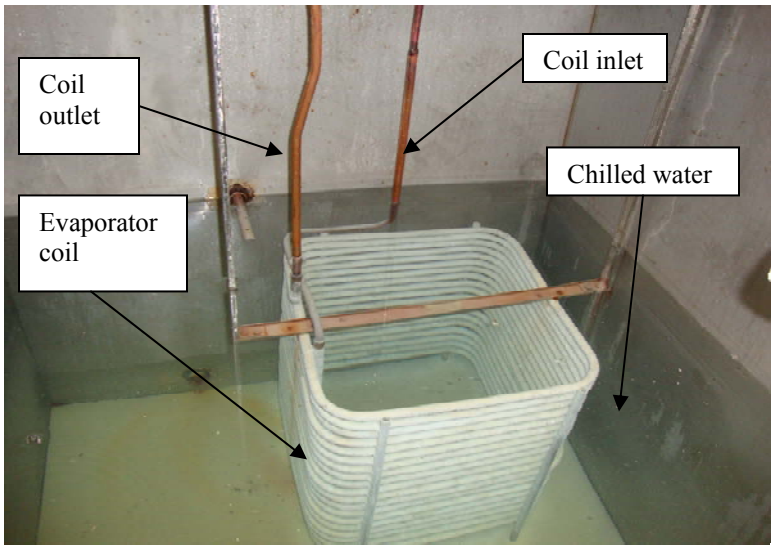

Fig.5.5 Photograph of evaporator of chilled water system

(c) Circulating Ice slurry / Chilled water pumps

Ice slurry pump (centrifugal) of 0.6 kW capacity (Fig.5.7) is used for circulation of ice slurry to the plate heat exchanger. Chilled water is circulated by a centrifugal water pump of 0.37 kW capacity (Fig.5.6).

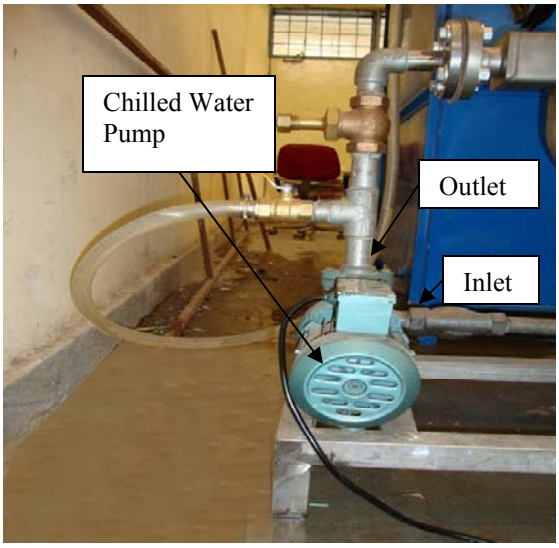

Fig.5.6 Photograph of Chilled Water Pump

Fig.5.7 Photograph of Ice slurry pump

(d) Instrumentation

The various instrumentation used for measurements are shown in Table 5.1.

Table 5.1 Specifications of measuring instruments

Instrumentation	Type/make/model	Range	Accuracy
Mass flow meter	OPTIMASS 8300C S25	0 to 5000 kg/h	± 0.1 % (of reading)
Differential pressure transmitter	SIEMENS	0 to 1000 mbar	± 0.01 bar
Pressure transmitter	Druck	0 to 20 bar	± 0.01 bar
Resistance-temperature detectors	LTX-3000/D	-50 ºC to 0 ºC to 99 ºC	± 0.01 K
Data logger (Data Acquisition System)	DT80-2	16 terminal points (10) as shown in Fig 5.1.	± 0.01 %

Mass flowmeter works on the principle that is if a moving mass is subjected to an oscillation perpendicular to its direction of movement, coriolis forces occur depending on the mass flow. A mass flowmeter has oscillating measuring tubes to precisely achieve this effect. The differential pressure transmitter is based on the principle of separating diaphragms of the differential pressure transmitter deflected by the existing pressures. The filling oil transmits this pressure to a semiconductor measuring bridge, and the differential pressure dependent output signal of which is measured and further processed'.

As mentioned above, the plate heat exchanger was tested for water to water flow, and ice slurry to water flow. The hot (primary) fluid in the heat exchanger was tape water. Chilled water and ice slurry were used as secondary fluid. The secondary fluid flow rate was measured upstream of the heat exchanger using a mass flow meter (Fig.5.8) while the mains water flow rate was measured using a mass flow meter just before the inlet to the heat exchanger. Data are collected at a frequency of 30 seconds and the criteria for steady state condition is based on when the observed value is independent of time. The temperatures for both the flowing fluids were measured at the inlet and the

outlet of the heat exchanger using mineral insulated (type-T) thermocouples (Fig.5.1). Two additional thermocouples were used to monitor the temperature of the mixture in the storage tank. Pressure drop in the heat exchanger was measured using pre-calibrated differential pressure transducer [Fig.5.9 and Table 5.1]. All the eight temperatures, six pressure and two flow rate sensors were connected to a PC based data acquisition system. The temperatures at condenser inlet and outlet, compressor suction and discharge, ice slurry tank and ice slurry in the ice slurry generator were measured by resistance-temperature detectors with a range of -50 ºC to 0 ºC to 99 ºC with the accuracy of ± 0.01 K. All measuring instruments are calibrated and repeatability of the experiments has been checked.

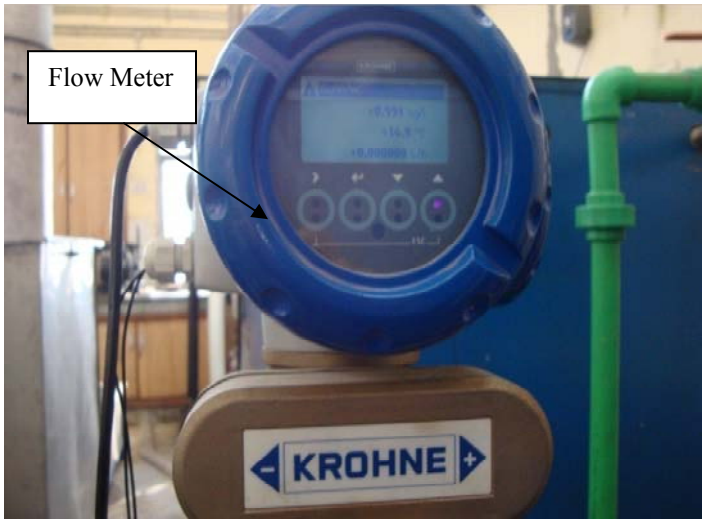

Fig.5.8 Photograph of Flow Meter

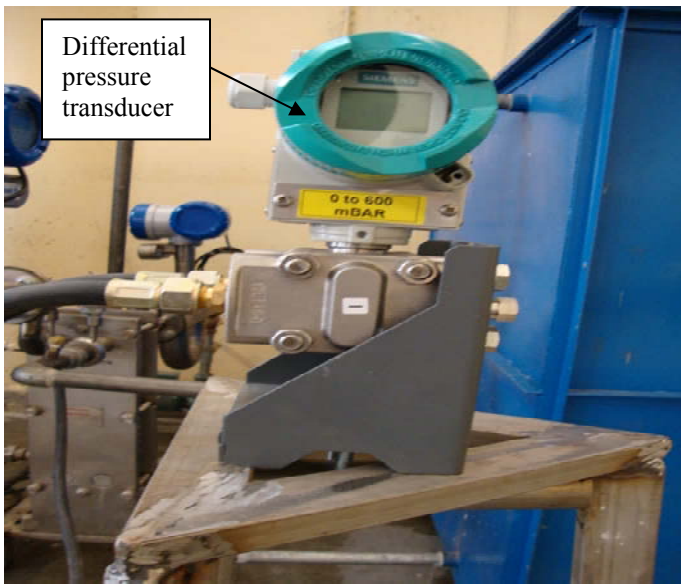

Fig.5.9 Photograph of differential pressure transducer

5.2. EXPERIMENTAL PROCEDURE AND DATA COLLECTION

Experimental runs were performed using chilled water (at approximately 4 ºC) at flow rates starting from 0.3 m^3/h to 3.0 m^3/h. The hot water flow rate was adjusted to obtain a fixed flow rate of 0.7 m^3/h. The pressure drop and heat transfer results from these runs would form the bases for validating and comparing the ice slurry results.

Initially 10 % of PG solution (66.6 kg of water and 7.4 kg of PG) is prepared and filled in ice slurry generator. Vapour compression system of ice slurry generator and scraper motor are started. The operating data at inlet and outlet of all the components are stored in Data Acquisition System. Sample of PG solution having ice crystal is taken and ice percentage is measured. The ice slurry generation system was shut down and the ice slurry was collected in a storage tank. Stirr is used for mixing of ice slurry in the storage tank. This allowed good mixing of the ice slurry /liquid solution, producing a homogeneous mixture throughout the tests. The hot water, at 17.4 ° C, was then allowed to flow through the heat exchanger and the flow rate was adjusted to 0.7 m^3/h of primary fluid flow. During each test the ice fraction was measured. The flowing mixture was sampled near the inlet (17) and outlet (16) of the heat exchanger (Fig.5.1). The ice crystals were separated from the mixture in separate container and the ice fraction was

determined from the corresponding weight of the ice crystals collected separately. The ice fraction was kept 10% for all the runs. The secondary fluid (ice slurry) was circulated through the heat exchanger by ice slurry circulation pump initially at a flow rate of 0.3 m^3/h adjusted using valve 3 (Figure 5.1).Data are collected at a frequency of 30 seconds and the criteria for steady state condition was observed when the parametric value is independent of time. Simultaneously the data of temperatures and pressures across the PHE are collected at different flow rates upto maximum flow rate of 3.0 m^3/h. The same procedure is repeated for 20%, 30% and 40% of PG solution. The whole procedure is repeated for MEG as depressant.

The various experimental data taken are given in following Table:

Table 5.2 (a) The various experimental data for chilled water

Run	hot water stream			Chilled water stream		
	Temperature (^{0}C)		Flow rate (LPH)	Temperature (^{0}C)		Flow rate (LPH)
	Inlet	outlet		Inlet	outlet	
CH1	17.400	13.142	700	4.000	13.901	300
CH2	17.400	10.653	700	4.000	11.847	600
CH3	17.400	8.951	700	4.000	10.549	900
CH4	17.400	8.267	700	4.000	9.3098	1200
CH5	17.400	7.807	700	4.000	8.462	1500
CH6	17.400	7.562	700	4.000	7.813	1800
CH7	17.400	7.025	700	4.000	7.446	2100
CH8	17.400	6.917	700	4.000	7.047	2400
CH9	17.400	6.890	700	4.000	6.715	2700
CH10	17.400	6.688	700	4.000	6.491	3000

5.3. RESULTS AND DISCUSSIONS

Experimental results of chilled water vs hot water flowing in plate heat exchanger and ice slurry vs hot water flowing in plate heat exchanger are described below:

5.3.1. CHILLED WATER VS HOT WATER

Heat transfer and pressure Drop

Based on the observation data given in Table 5.2 (a), experimental values of overall heat transfer coefficient, cooling duty and pressure drop are given in Table 5.2 (b) and compared with predicted values using thermo-hydraulic modeling. Table 5.2 also represents the predicted values of heat transfer coefficients (h_1, and h_2) for both the streams. The last column represents the values of Reynolds number for chilled water side. The overall heat transfer coefficient, cooling duty and pressure drop are predicted using equations 4.34, 4.34a and 4.32 given in Chapter 4. Cooling duty is calculated by equation: $Q = M.c_p.\Delta T$, where M is the mass flow rate of chilled water in kg/s, c_p is the specific heat and ΔT is the temperature difference.

Figure 5.10 (a) shows the comparison of experimental and predicted valued of overall heat transfer coefficients w.r.t. flow rates. Predicted values matches satisfactory with the experimental ones for with range of flow rates. Variation of predicted values of heat transfer coefficients are shown in Figure 5.10 (b). Predicted and experimental values of cooling duties are compared in Fig. 5.11. Overall heat transfer coefficient and cooling duty are slightly underpredicted for flow rates more than 2 m^3/hr. comparison of experimental and predicted values of pressure drop with variation of flow rate and Reynolds number is shown in Figures 5.12 and 5.13 respectively. Experimental data matches satisfactorily for the entire range of flow rate. Further, the pressure drop increases proportional to flow rate.

Table 5.2 (b) Variation of overall heat transfer coefficient, heat transfer coefficient, cooling duty and pressure drop of chilled water with flow rate and pressure drop of chilled water with Reynolds number

Chilled water flow rate (m^3/h)	Overall heat transfer coefficient (KW/ m^2K)		Predicted Heat transfer coefficient (kW/ m^2K)		Cooling Duty (KW)		Pressure drop for Stream1(kPa)		Reynolds number
	Prediction	Experimental	h_1	h_2	Prediction	Experimental	Prediction	Experimental	
0.30	2.0154	1.9801	3.4885	5.7920	3.7098	3.4620	5.3059	5.1237	77.4859
0.60	2.2982	2.3996	4.4966	5.6853	5.7578	5.4860	7.2233	7.9002	154.9718
0.90	2.4968	2.3923	5.3779	5.6277	6.7264	6.8700	9.9482	9.9871	232.4670
1.20	2.6523	2.7022	6.1992	5.5913	7.2624	7.4260	13.3240	13.9230	309.9528
1.50	2.7789	2.8120	6.9768	5.5660	7.5973	7.8002	17.2681	17.3001	387.4387
1.80	2.8844	2.9012	7.7191	5.5473	7.8245	8.0002	21.7278	21.1071	464.9339
2.10	2.9741	3.0112	8.4295	5.5330	7.9880	8.4366	26.6638	26.9030	542.4198
2.40	3.0515	3.1256	9.1130	5.5216	8.1108	8.5240	32.0428	32.7008	619.8499
2.70	3.1191	3.1890	9.7736	5.5124	8.2064	8.5460	37.8540	37.0042	697.4009
3.00	3.1789	3.2432	10.412	5.5047	8.2826	8.7100	44.0590	44.9588	774.8588

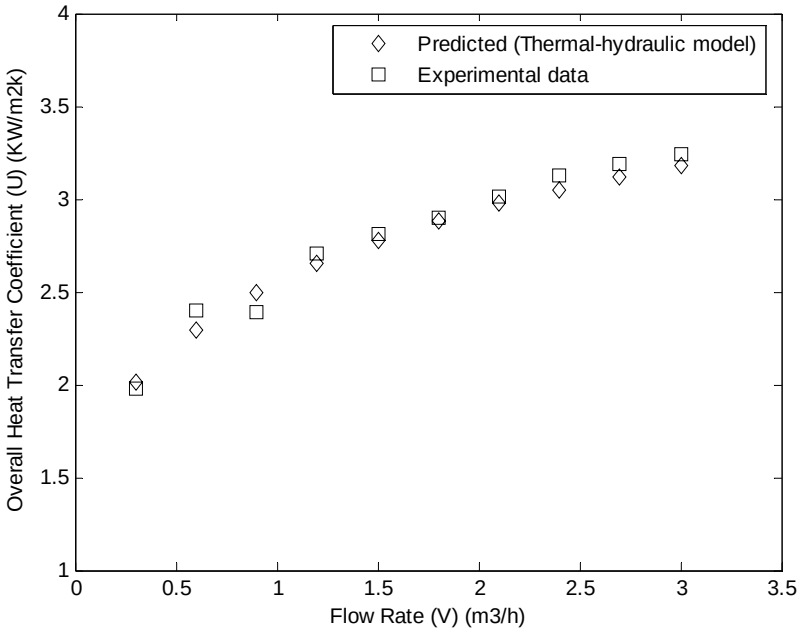

Figure 5.10 (a) Variation of overall heat transfer coefficient with flow rate

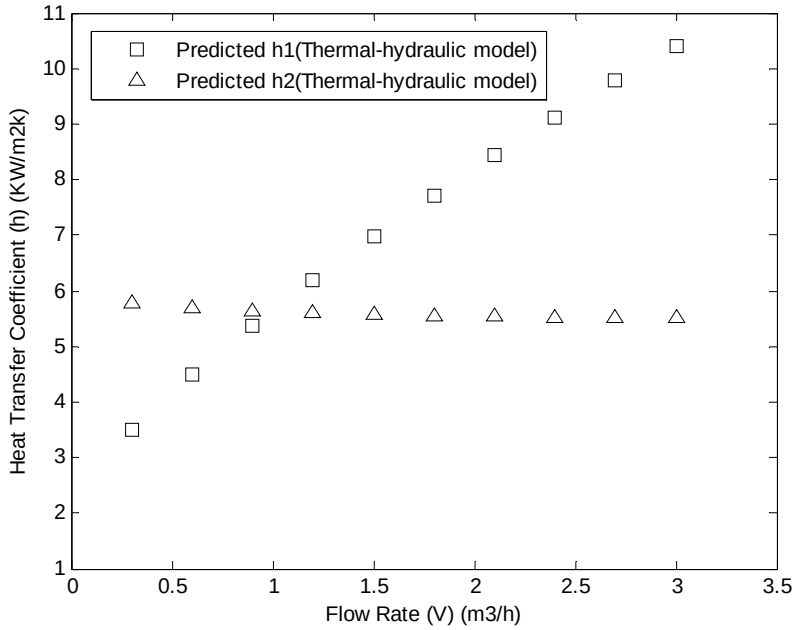

Figure 5.10 (b) Variation of stream heat transfer coefficients with flow rate

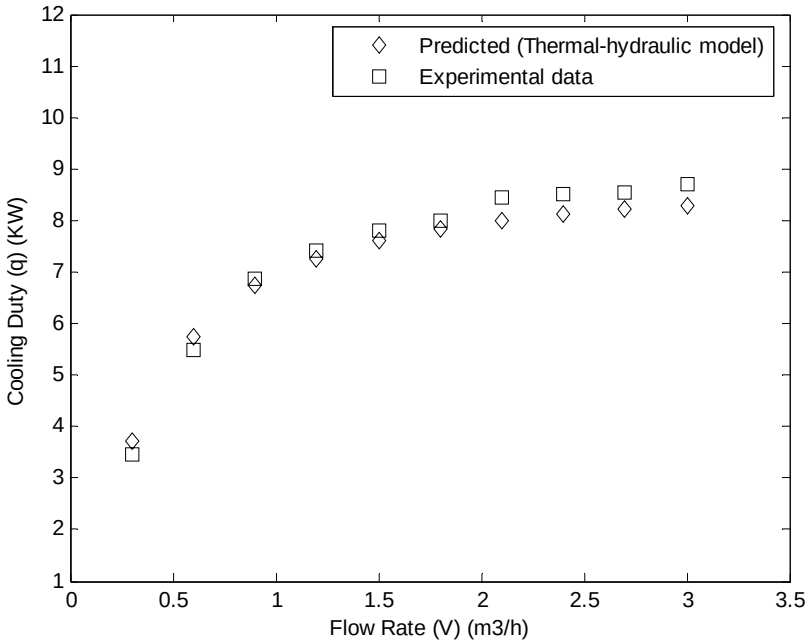

Figure 5.11 Flow Rate Vs Cooling Duty of Chilled Water

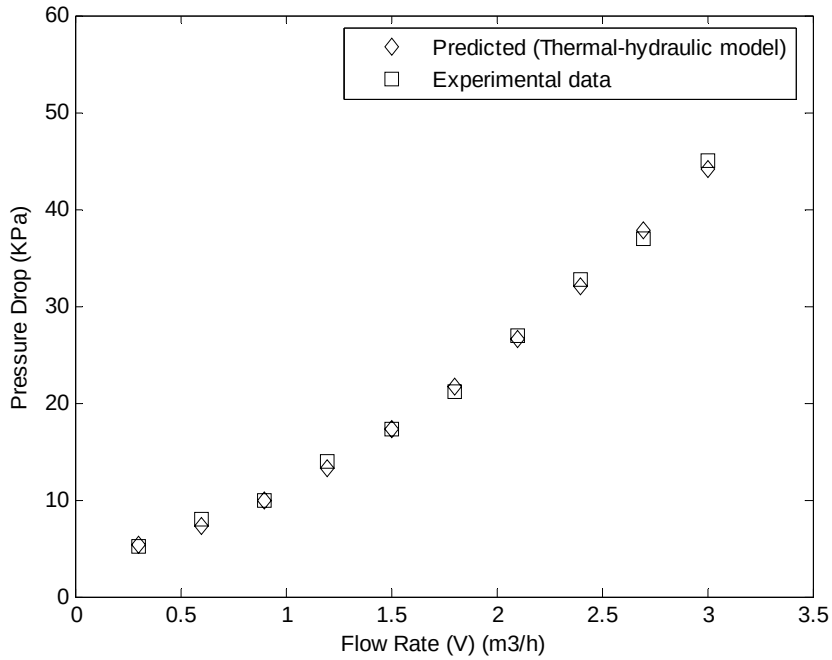

Figure 5.12. Variation of pressure drop with flow rate

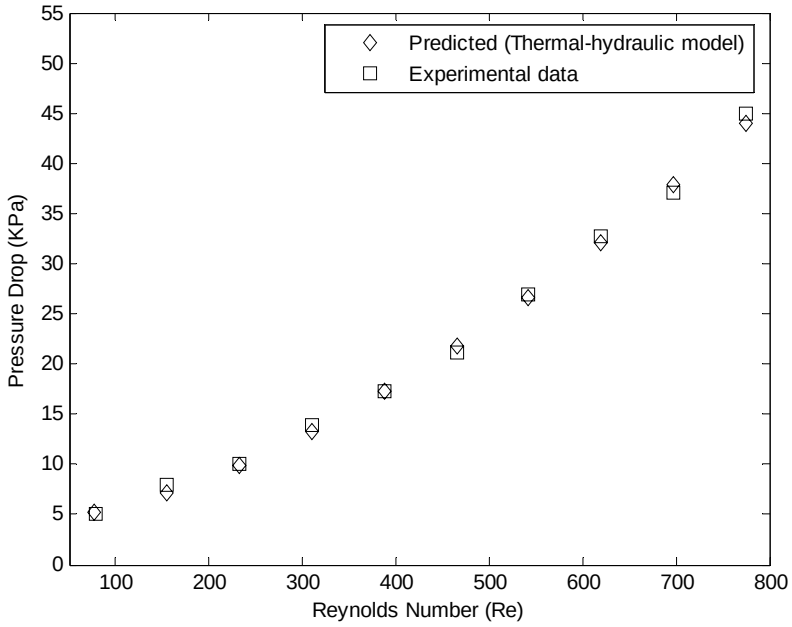

Figure 5.13. Pressure drop versus Reynolds number

5.3.2. ICE SLURRY VS HOT WATER

Table 5.3 summarizes the calculated thermophysical properties of Ice Slurry at 10%, 20%, 30% and 40% concentrations of PG and MEG respectively for 10% ice fraction. With increase in concentrations of PG and MEG, density, dynamic viscosity and Prandtl number increases whereas specific heat and thermal conductivity decreases with increase in concentrations. As compare to water, PG and MEG solutions having higher density, higher dynamic viscosity, higher thermal conductivity and higher Prandtl number whereas lower specific heat.

Table 5.3 Calculated thermophysical properties of Ice Slurry at various concentrations of PG and MEG

Thermophysical Properties	Concentration of PG					Concentration of MEG				
	0%	10%	20%	30%	40%	0%	10%	20%	30%	40%
Density (Kg/m^3)	990.54	996.45	1001.9	1007.5	1013.1	990.54	996.46	1002.00	1007.5	1013.1
Dynamic viscosity (Kg/m-s)	0.0013	0.0029	0.0043	0.0066	0.0099	0.0013	0.0029	0.0047	0.0076	0.0121
Thermal conductivity (W/m-K)	0.5881	0.6605	0.6402	0.6183	0.5951	0.5881	0.6601	0.6384	0.6151	0.5896
Specific heat (J/Kg-K)	4196.00	4140.40	4077.40	4010.60	3939.50	4196.00	4140.60	4077.60	4009.50	3935.9
Prandtl number	9.09	17.91	27.26	42.73	65.78	9.09	18.21	29.79	49.34	76.49

Heat transfer and pressure drop at various concentrations of PG

Table 5.4 shows the comparison of experimental and predicted valued of overall heat transfer coefficients w.r.t. flow rates. Predicted values matches satisfactory with the experimental ones for with range of flow rates. Variation of predicted values of heat transfer coefficients are shown in Figure 5.14. Experimental data matches satisfactorily for the entire range of flow rate. Predicted and experimental values of cooling duties are compared in Fig. 5.15. Comparison of experimental and predicted values of pressure drop with variation of flow rate and Reynolds number is shown in Figures 5.16 and 5.17 respectively. Experimental data matches satisfactorily for the entire range of flow rate. Further, the pressure drop increases proportional to flow rate.

Table 5.4 Variation of overall heat transfer coefficient, cooling duty and pressure drop of ice slurry with flow rate and pressure drop of ice slurry with Reynolds number using PG as antifreeze with 10% concentration

Ice Slurry flow rate (m^3/h)	Overall heat transfer coefficient (KW/ m^2K)		Cooling Duty (KW)		Pressure drop for Stream1 (kPa)		Reynolds number
	Prediction	Experimental	Prediction	Experimental	Prediction	Experimental	
0.30	1.9800	1.8860	5.2947	5.1030	5.6275	5.0200	34.5678
0.60	2.1868	2.0820	8.1029	8.0020	6.7630	6.1224	69.1107
0.90	2.3434	2.4640	9.4095	9.6430	8.7997	9.2100	103.7075
1.20	2.4743	2.5660	10.1443	10.3460	11.6380	11.9480	138.2629
1.50	2.5863	2.6662	10.6164	10.9100	15.2747	15.8200	172.8182
1.80	2.6831	2.7660	10.9456	11.1200	19.7171	20.9980	207.4151
2.10	2.7670	2.8880	11.1872	11.3802	24.9565	25.3920	241.9704
2.40	2.8403	2.9602	11.3716	11.5916	30.9996	31.3460	276.5258
2.70	2.9048	3.0002	11.5169	11.7880	37.8566	38.8700	311.1226
3.00	2.9619	3.0708	11.6338	11.9020	45.5122	46.4230	345.6780

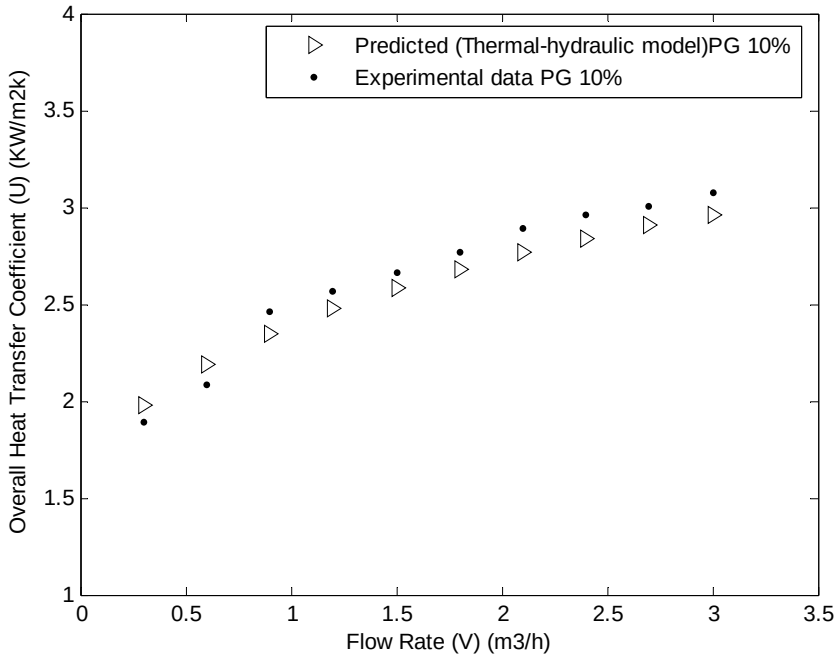

Figure 5.14 Variation of overall heat transfer coefficient with flow rate using PG as antifreeze with 10% concentration

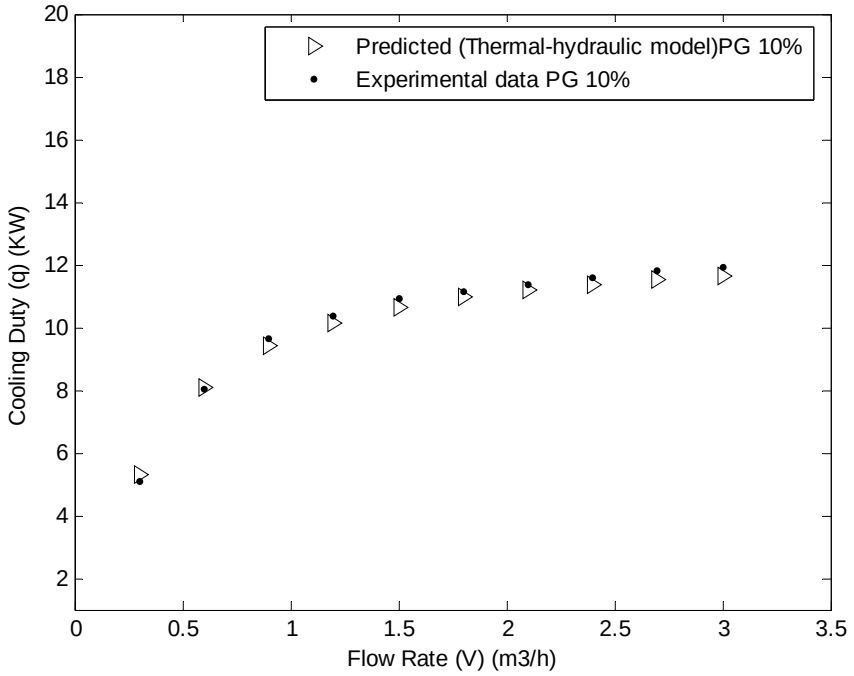

Figure 5.15 Flow Rate Vs Cooling Duty of Ice Slurry using PG as antifreeze with 10% concentration

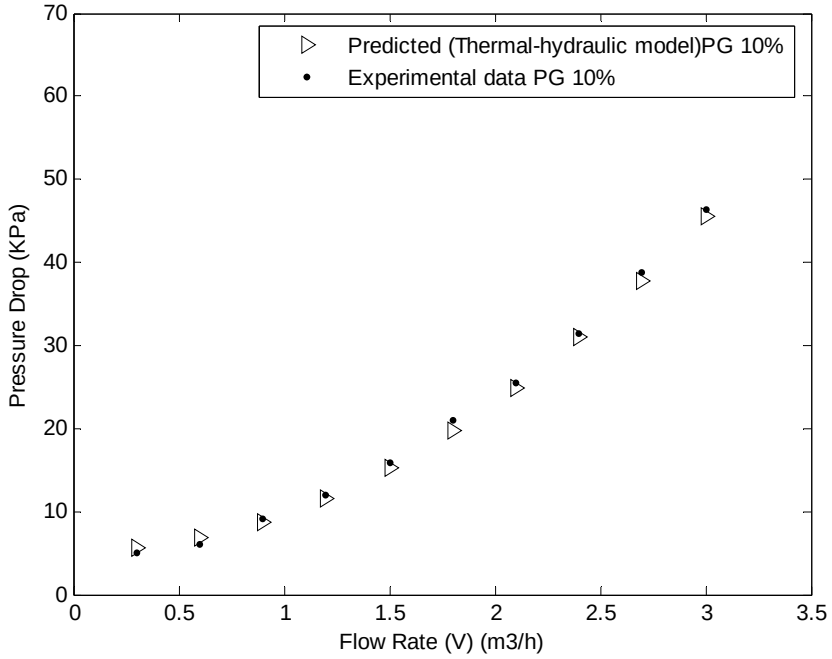

Figure 5.16 Variation of pressure drop with flow rate using PG as antifreeze with 10% concentration

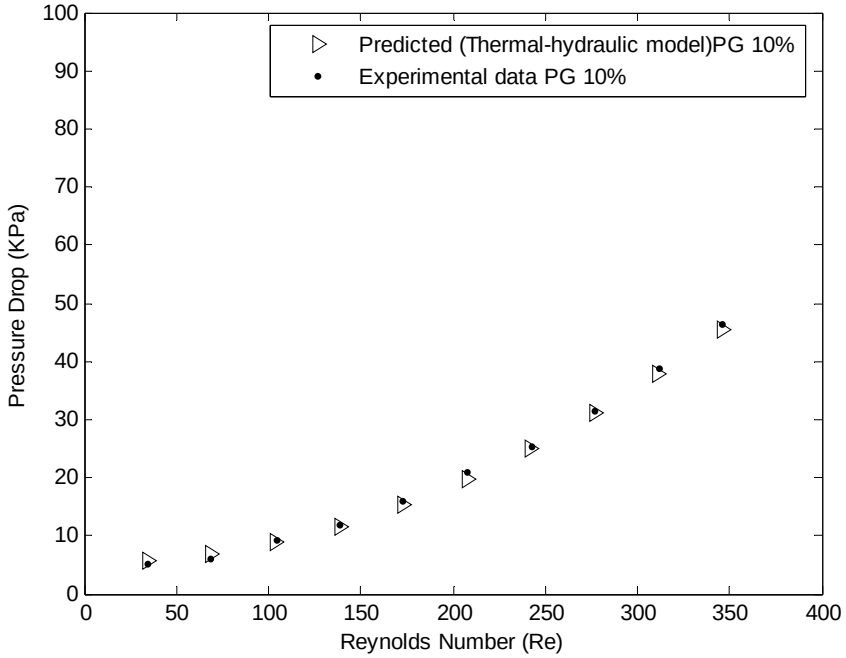

Figure 5.17 Pressure drop versus Reynolds number using PG as antifreeze with 10% concentration

Model prediction with validation for ice slurry to hot water is shown in Table 5.5 and Fig.5.18 for overall heat transfer coefficient, Fig.5.19 for cooling duty, Fig.5.20 for pressure drop and Fig.5.21 for Reynolds number for PHE using PG as antifreeze with 20% concentration. The predicted and experimental data matches satisfactorily. Similarly the prediction for other antifreezes for different concentrations are validated with experimental data.

Table 5.5 Variation of overall heat transfer coefficient, heat transfer coefficient, cooling duty and pressure drop of ice slurry with flow rate and pressure drop of ice slurry with Reynolds number using PG as antifreeze with 20% concentration

Ice Slurry flow rate (m^3/h)	Overall heat transfer coefficient (KW/ m^2K)		Cooling Duty (KW)		Pressure drop for Stream1 (kPa)		Reynolds number
	Prediction	Experimental	Prediction	Experimental	Prediction	Experimental	
0.30	1.9554	1.8566	6.0247	5.9112	6.9131	6.3600	23.0743
0.60	2.1286	2.0466	9.1531	9.0326	7.3433	7.0224	46.1320
0.90	2.2755	2.3868	10.6112	10.8668	9.2481	9.0810	69.2257
1.20	2.4013	2.4898	11.4399	11.6282	11.9831	12.2330	92.2917
1.50	2.5109	2.5780	11.9789	12.1630	15.5045	15.8860	115.3577
1.80	2.6069	2.6790	12.3592	12.5060	19.8123	21.8600	138.4514
2.10	2.6912	2.7800	12.6411	12.8334	24.8966	25.2040	161.5174
2.40	2.7655	2.8720	12.8583	12.9868	30.7643	31.0040	184.5834
2.70	2.8315	2.9264	13.0307	13.3208	37.4259	38.4600	207.6771
3.00	2.8903	2.9788	13.1702	13.4200	44.8674	46.0062	230.7431

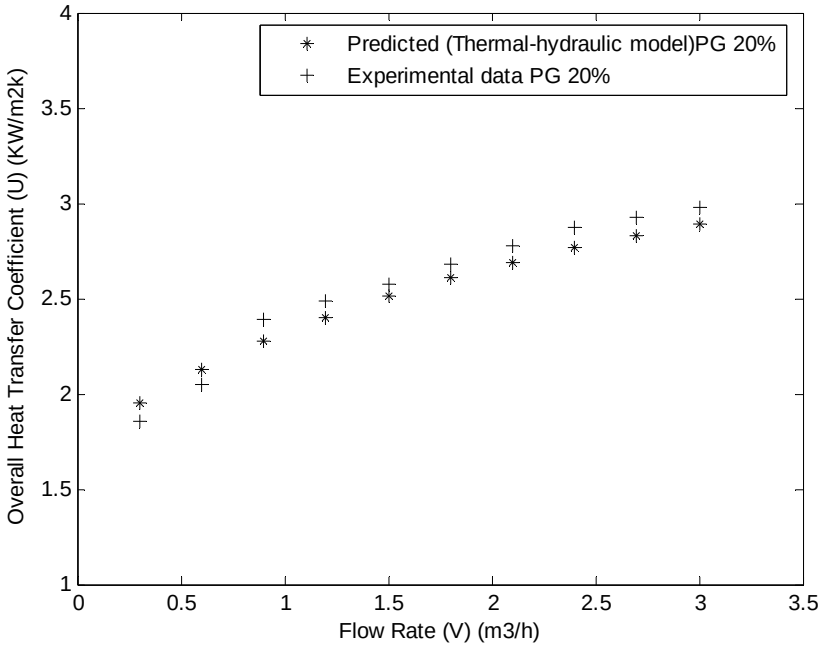

Figure 5.18 Variation of overall heat transfer coefficient with flow rate using PG as antifreeze with 20% concentration

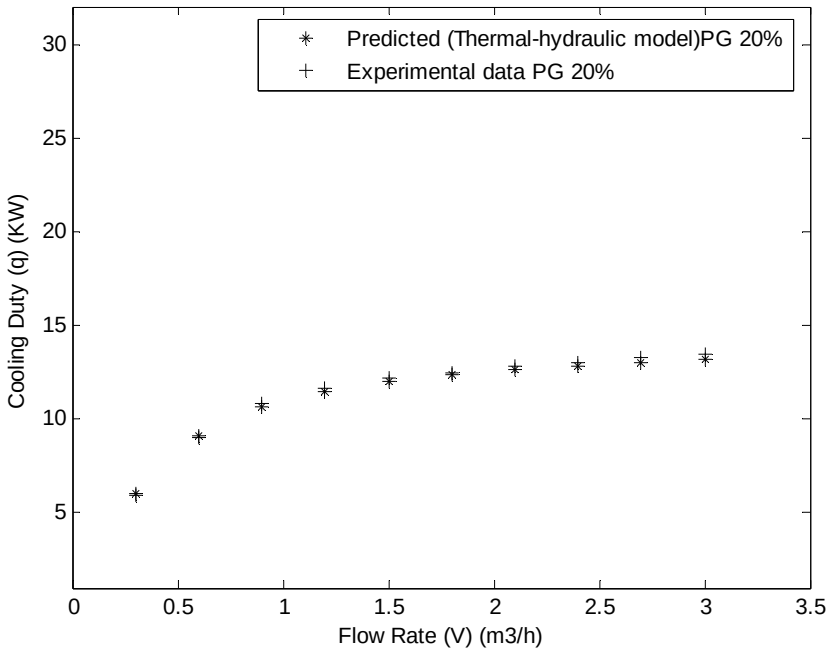

Figure 5.19 Flow Rate Vs Cooling Duty of Ice Slurry using PG as antifreeze with 20% concentration

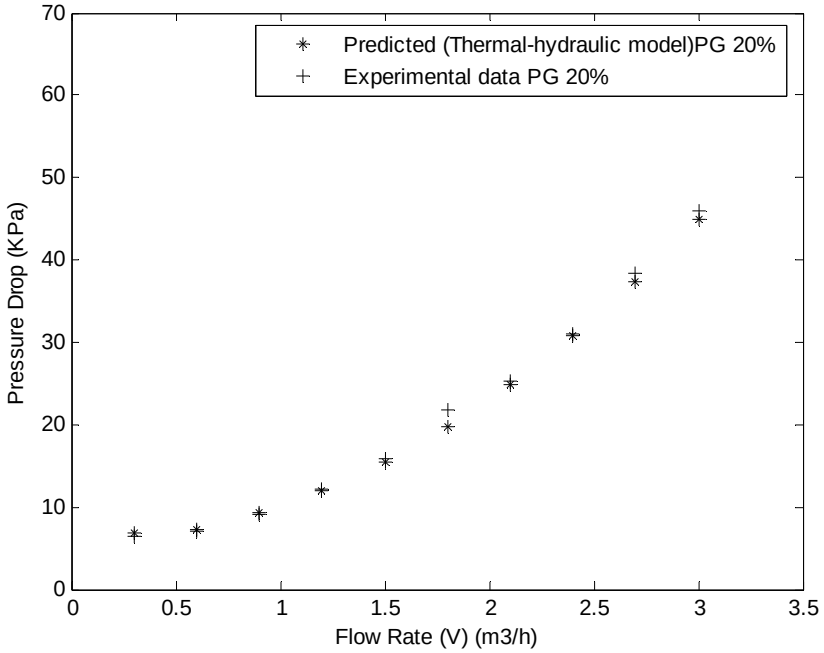

Figure 5.20 Variation of pressure drop with flow rate using PG as antifreeze with 20% concentration

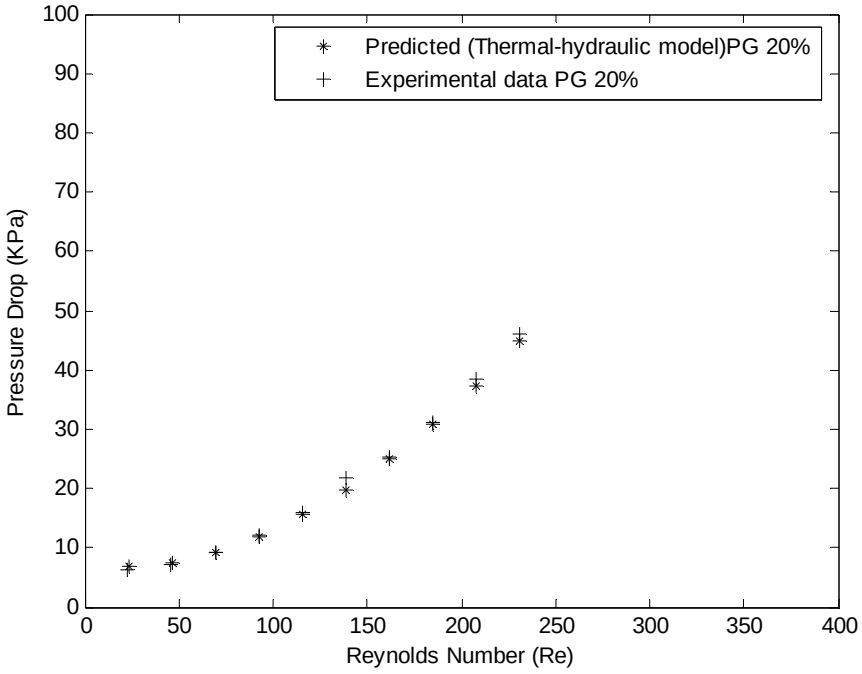

Figure 5.21 Pressure drop versus Reynolds number using PG as antifreeze with 20% concentration

Model prediction with validation for ice slurry to hot water is shown in Table 5.6 and Fig.5.22 for overall heat transfer coefficient, Fig.5.23 for cooling duty, Fig.5.24 for pressure drop and Fig.5.25 for Reynolds number for PHE using PG as antifreeze with 30% concentration. The predicted and experimental data matches satisfactorily. Similarly the prediction for other antifreezes for different concentrations are validated with experimental data.

Table 5.6 Variation of overall heat transfer coefficient, heat transfer coefficient, cooling duty and pressure drop of ice slurry with flow rate and pressure drop of ice slurry with Reynolds number using PG as antifreeze with 30% concentration

Ice Slurry flow rate (m^3/h)	Overall heat transfer coefficient (KW/ m^2K)		Cooling Duty (KW)		Pressure drop for Stream1 (kPa)		Reynolds number
	Prediction	Experimental	Prediction	Experimental	Prediction	Experimental	
0.30	2.0858	1.9644	6.9687	6.7800	16.7028	10.8860	14.9927
0.60	2.1039	1.9960	10.4354	10.3210	9.1831	8.9020	29.9746
0.90	2.2260	2.4280	12.0467	12.2322	10.5036	10.8640	44.9800
1.20	2.3400	2.4520	12.9705	13.1666	13.0022	13.6200	59.9673
1.50	2.4426	2.4940	13.5783	13.6820	16.3408	16.7642	74.9546
1.80	2.5344	2.6300	14.0124	14.1884	20.4640	21.0820	89.9599
2.10	2.6165	2.7280	14.3381	14.5020	25.3469	25.8644	104.9472
2.40	2.6900	2.7520	14.5918	14.6800	30.9908	31.3688	119.9346
2.70	2.7560	2.8620	14.7947	14.9882	37.4044	38.0800	134.9399
3.00	2.8154	2.9220	14.9607	15.1828	44.5740	46.4620	149.9272

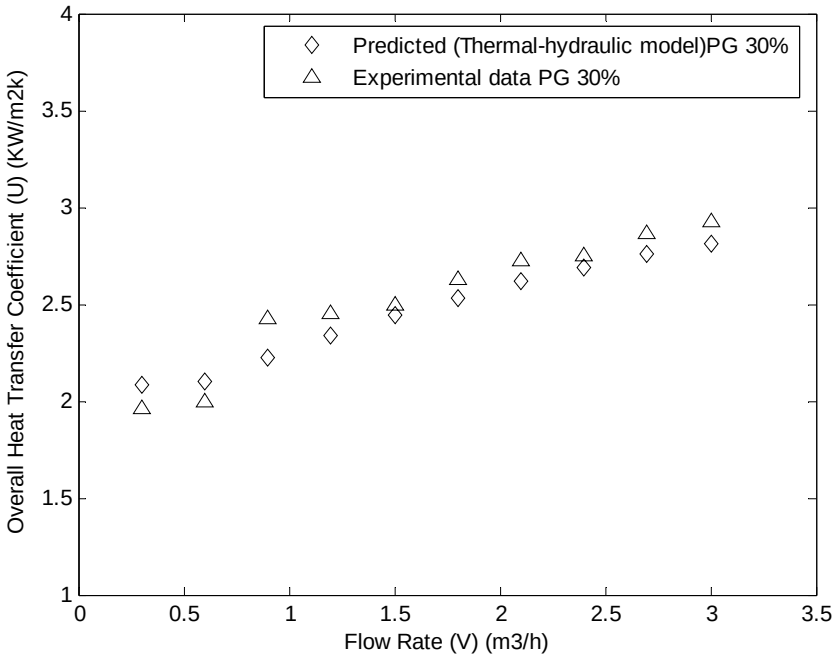

Figure 5.22 Variation of overall heat transfer coefficient with flow rate using PG as antifreeze with 30% concentration

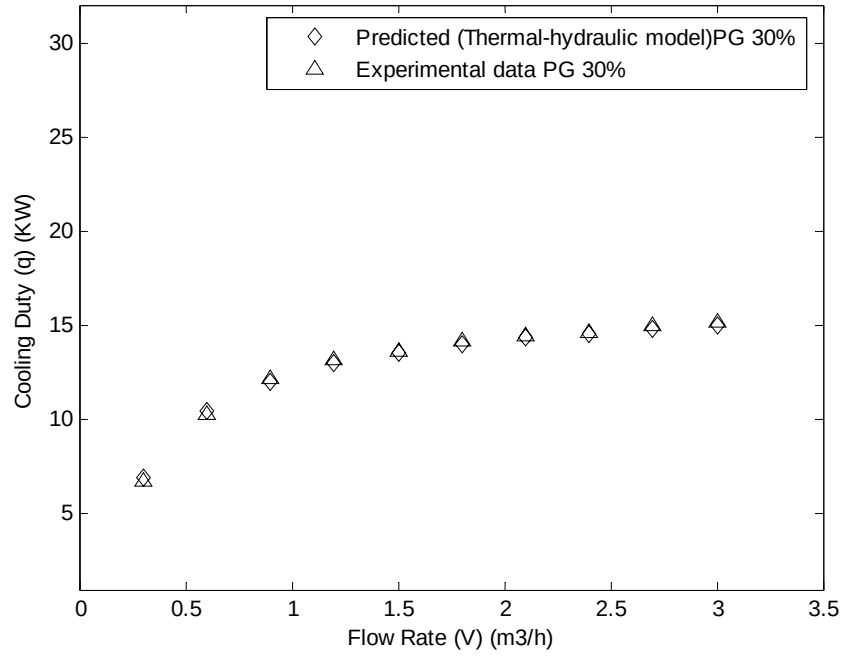

Figure 5.23 Flow Rate Vs Cooling Duty of Ice Slurry using PG as antifreeze with 30% concentration

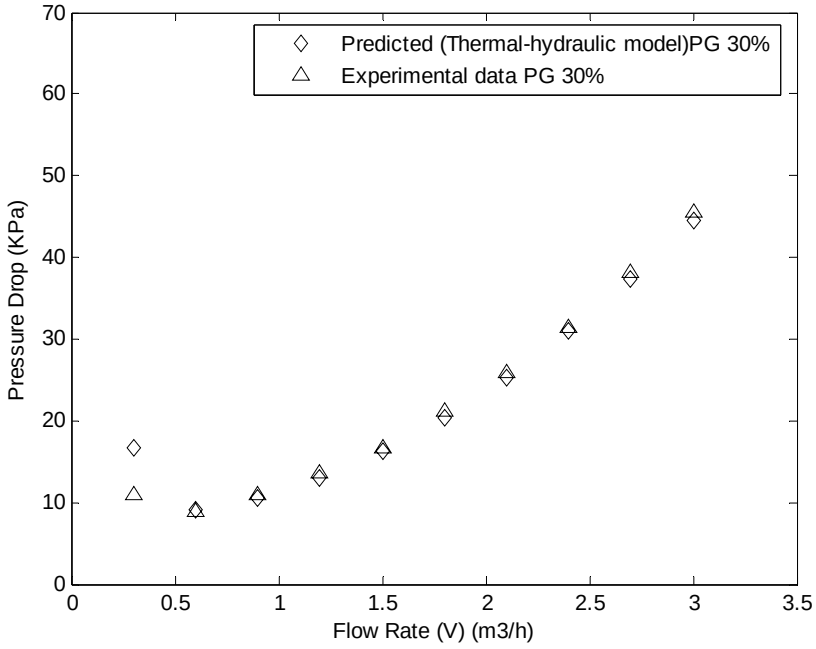

Figure 5.24 Variation of pressure drop with flow rate using PG as antifreeze with 30% concentration

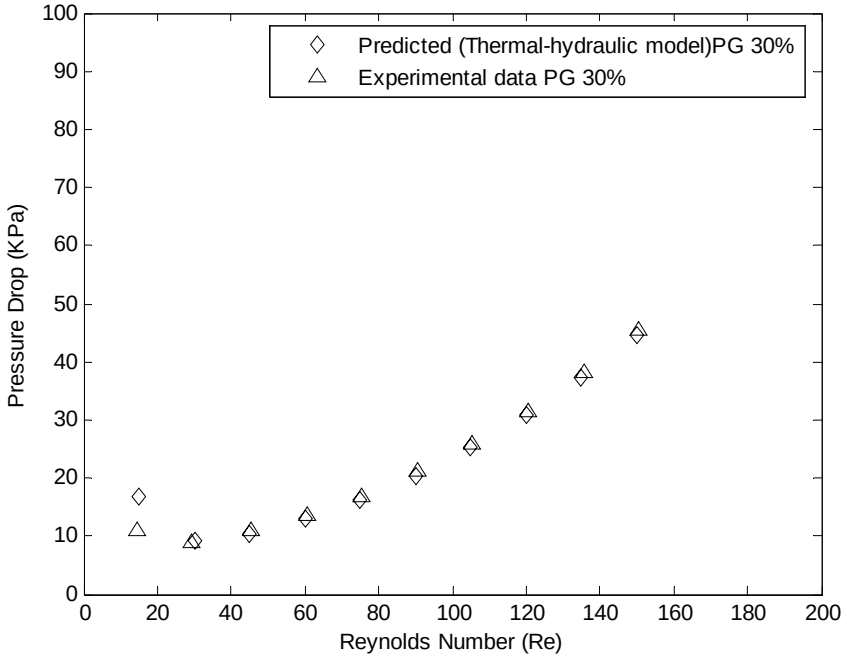

Figure 5.25 Pressure drop versus Reynolds number using PG as antifreeze with 30% concentration

Model prediction with validation for ice slurry to hot water is shown in Table 5.7 and Fig.5.26 for overall heat transfer coefficient, Fig.5.27 for cooling duty, Fig.5.28 for pressure drop and Fig.5.29 for Reynolds number for PHE using PG as antifreeze with 40% concentration. The predicted and experimental data matches satisfactorily. Similarly the prediction for other antifreezes for different concentrations are validated with experimental data.

Table 5.7 Variation of overall heat transfer coefficient, heat transfer coefficient, cooling duty and pressure drop of ice slurry with flow rate and pressure drop of ice slurry with Reynolds number using PG as antifreeze with 40% concentration

Ice Slurry flow rate (m^3/h)	Overall heat transfer coefficient (KW/ m^2K)		Cooling Duty (KW)		Pressure drop for Stream1 (kPa)		Reynolds number
	Prediction	Experimental	Prediction	Experimental	Prediction	Experimental	
0.30	2.6652	2.2680	8.0700	7.9268	26.2168	19.6888	9.9397
0.60	2.1734	2.0610	11.8584	11.7464	16.8763	15.8882	19.8722
0.90	2.2220	2.3340	13.5298	13.7188	14.1630	14.5200	29.8203
1.20	2.3090	2.4122	14.5060	14.6998	15.7059	16.0060	39.7564
1.50	2.3969	2.4888	15.1585	15.3238	18.5892	19.0360	49.6925
1.80	2.4796	2.5620	15.6314	15.8878	22.3919	22.7620	59.6406
2.10	2.5556	2.6660	15.9911	16.1998	26.9918	27.3686	69.5767
2.40	2.6253	2.7322	16.2748	16.3686	32.3541	32.8866	79.5128
2.70	2.6889	2.7912	16.5046	16.6868	38.4723	38.9698	89.4609
3.00	2.7470	2.8680	16.6941	16.8112	45.3264	45.9688	99.3970

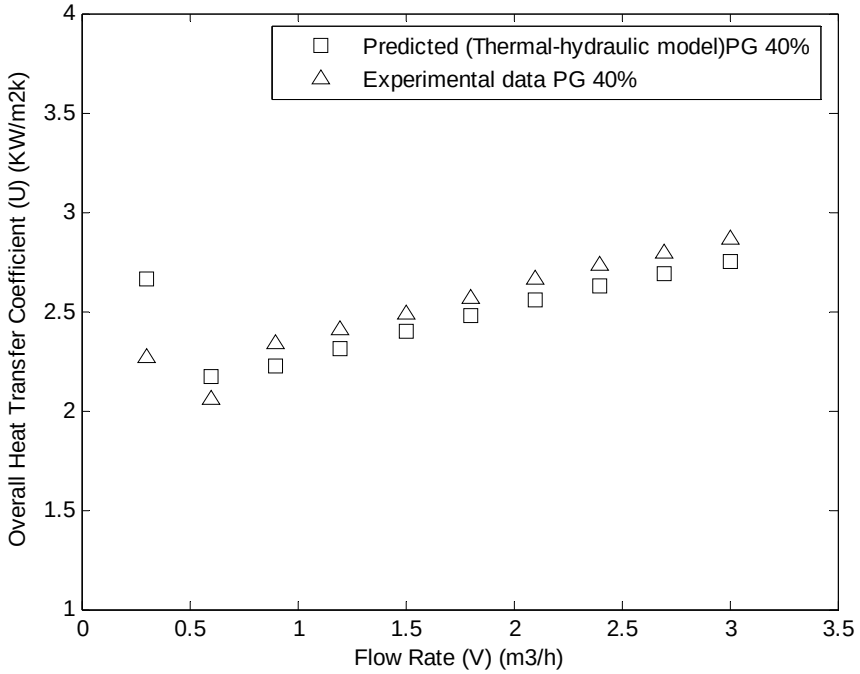

Figure 5.26 Variation of overall heat transfer coefficient with flow rate using PG as antifreeze with 40% concentration

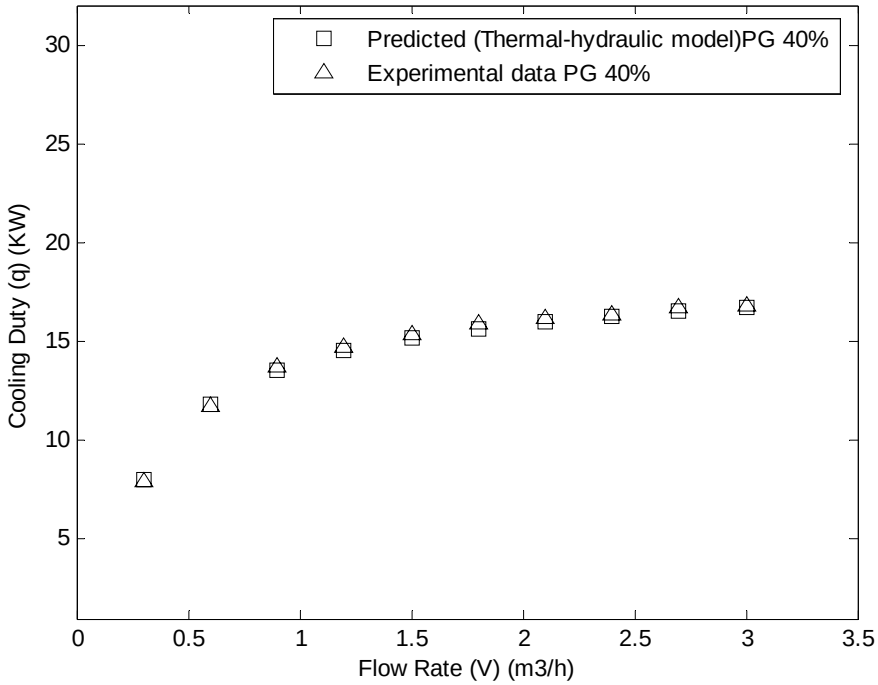

Figure 5.27 Flow Rate Vs Cooling Duty of Ice Slurry using PG as antifreeze with 40% concentration

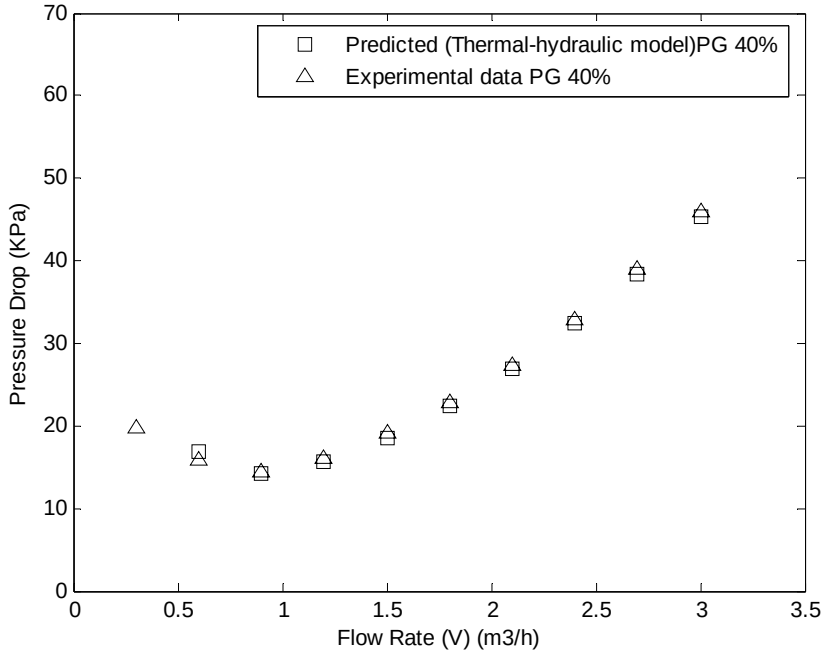

Figure 5.28 Variation of pressure drop with flow rate using PG as antifreeze with 40% concentration

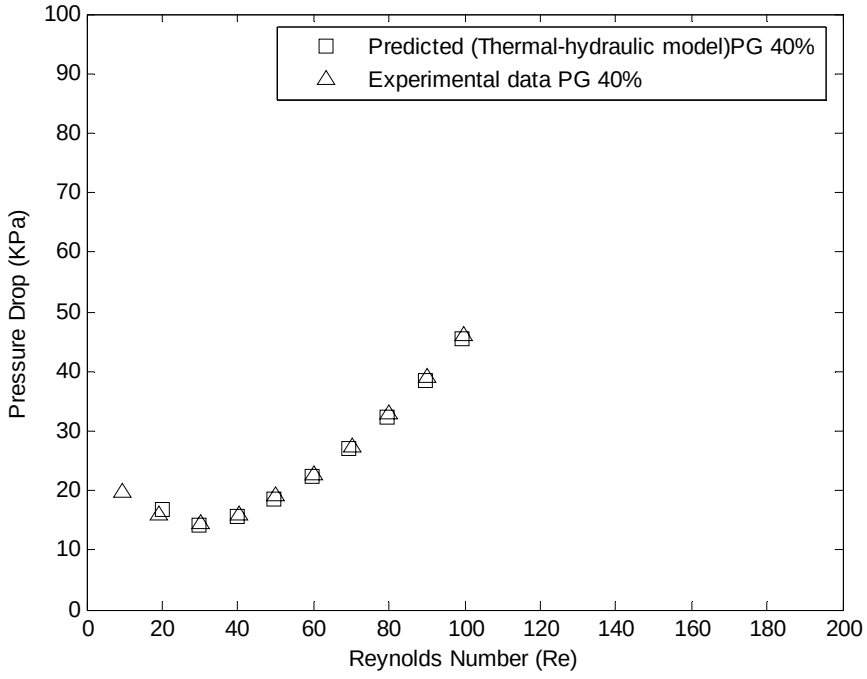

Figure 5.29 Pressure drop versus Reynolds number using PG as antifreeze with 40% concentration

Heat transfer

Variation of overall heat transfer coefficient with flow rate is shown in Figure 5.30. using PG as antifreeze with 10%, 20%, 30% and 40% concentration. Overall heat transfer coefficient increases with increase in flow rate. The predicted and experimental data matches satisfactorily.

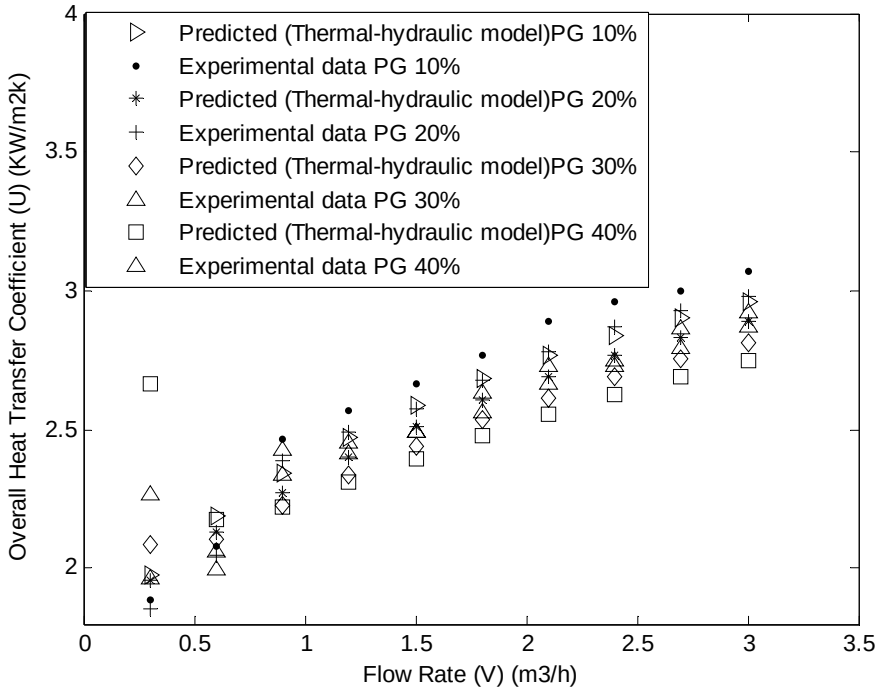

Figure 5.30 Variation of overall heat transfer coefficient with flow rate using PG as antifreeze with 10%, 20%, 30% and 40% concentration

Figure 5.31.using PG as antifreeze with 10%, 20%, 30% and 40% concentration shows the variation of cooling duty with flow rate of ice slurry. Cooling duty increases with increase in flow rate. Experimental data is compared with the prediction of the present formulation. It can be seen that predicted ice slurry cooling duty matches reasonably well with the experimental data.

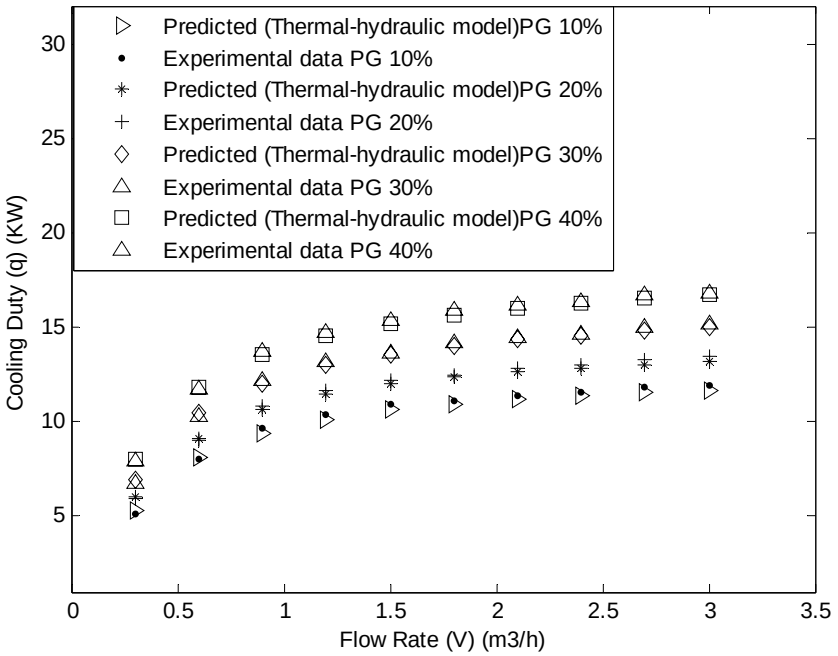

Figure 5.31 Flow Rate Vs Cooling Duty of Ice Slurry using PG as antifreeze with 10%, 20%, 30% and 40% concentration

Pressure Drop

Figure 5.32.using PG as antifreeze with 10%, 20%, 30% and 40% concentration shows the variation of pressure drop with flow rate of ice slurry. Pressure drop increases with increase in flow rate. Experimental data is compared with the prediction of the present formulation. It can be seen that predicted ice slurry pressure drop matches reasonably well with the experimental data.

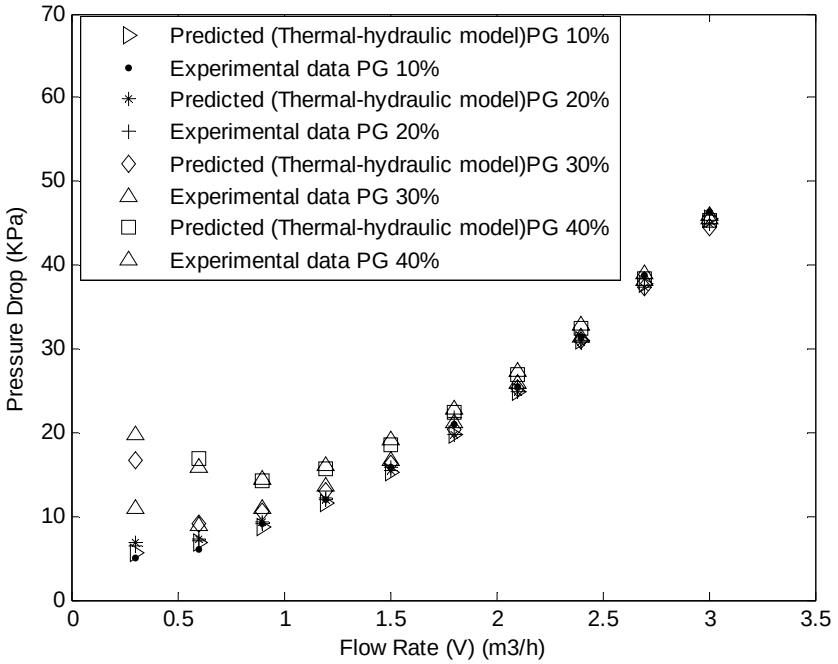

Figure 5.32 Variation of pressure drop with flow rate using PG as antifreeze with 10%, 20%, 30% and 40% concentration

Variation of pressure drop vs Reynolds Number is shown in Figure 5.33. using PG as antifreeze with 10%, 20%, 30% and 40% concentration. The predicted and experimental data matches satisfactorily.

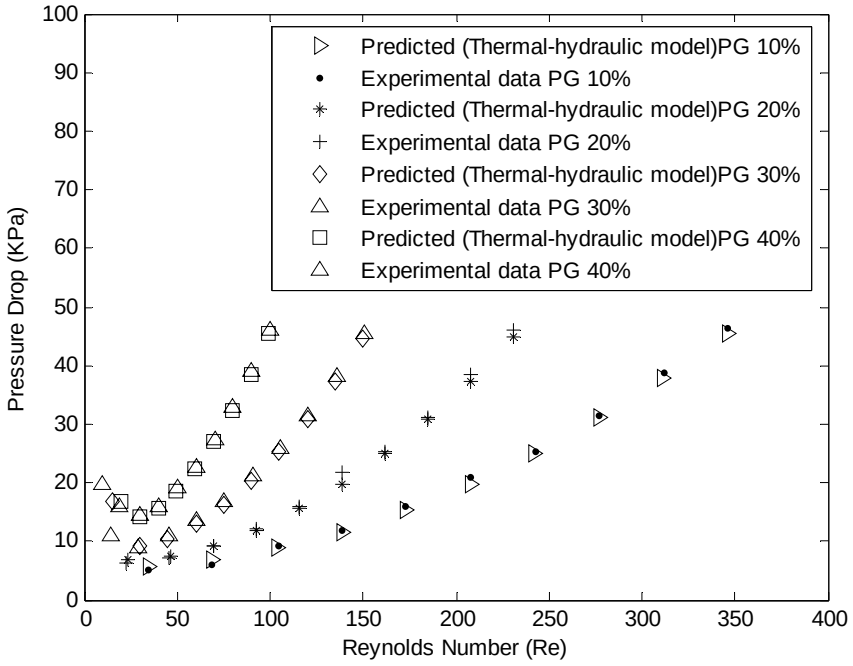

Figure 5.33 Pressure drop versus Reynolds number using PG as antifreeze with 10%, 20%, 30% and 40% concentration

Heat transfer and pressure drop at various concentrations of MEG

Table 5.8 shows the comparison of experimental and predicted valued of overall heat transfer coefficients w.r.t. flow rates. Predicted values matches satisfactory with the experimental ones for with range of flow rates. Variation of predicted values of heat transfer coefficients are shown in Figure 5.34. Experimental data matches satisfactorily for the entire range of flow rate. Predicted and experimental values of cooling duties are compared in Fig. 5.35. Comparison of experimental and predicted values of pressure drop with variation of flow rate and Reynolds number is shown in Figures 5.36 and 5.77 respectively. Experimental data matches satisfactorily for the entire range of flow rate. Further, the pressure drop increases proportional to flow rate.

Table 5.8 Variation of overall heat transfer coefficient, cooling duty and pressure drop of ice slurry with flow rate and pressure drop of ice slurry with Reynolds number using MEG as antifreeze with 10% concentration

Ice Slurry flow rate (m^3/h)	Overall heat transfer coefficient (KW/ m^2K)		Cooling Duty (KW)		Pressure drop for Stream1 (kPa)		Reynolds number
	Prediction	Experimental	Prediction	Experimental	Prediction	Experimental	
0.30	1.9787	1.8720	5.3930	5.2064	5.6516	5.0800	34.0161
0.60	2.1847	2.0932	8.2513	8.1436	6.7771	6.1380	68.0078
0.90	2.3410	2.4520	9.5812	9.7826	8.8109	9.0126	102.0525
1.20	2.4718	2.5580	10.3294	10.5064	11.6463	11.9520	136.0563
1.50	2.5838	2.6560	10.8103	10.9992	15.2797	15.7780	170.0602
1.80	2.6806	2.7600	11.1458	11.8268	19.7182	20.8600	204.1049
2.10	2.7645	2.8790	11.3920	11.5890	24.9531	25.1926	238.1088
2.40	2.8379	2.9506	11.5801	11.7766	30.9910	31.2460	272.1127
2.70	2.9024	2.9960	11.7283	11.9880	37.8423	38.8600	306.1574
3.00	2.9596	3.0510	11.8476	12.1462	45.4918	46.3202	340.1612

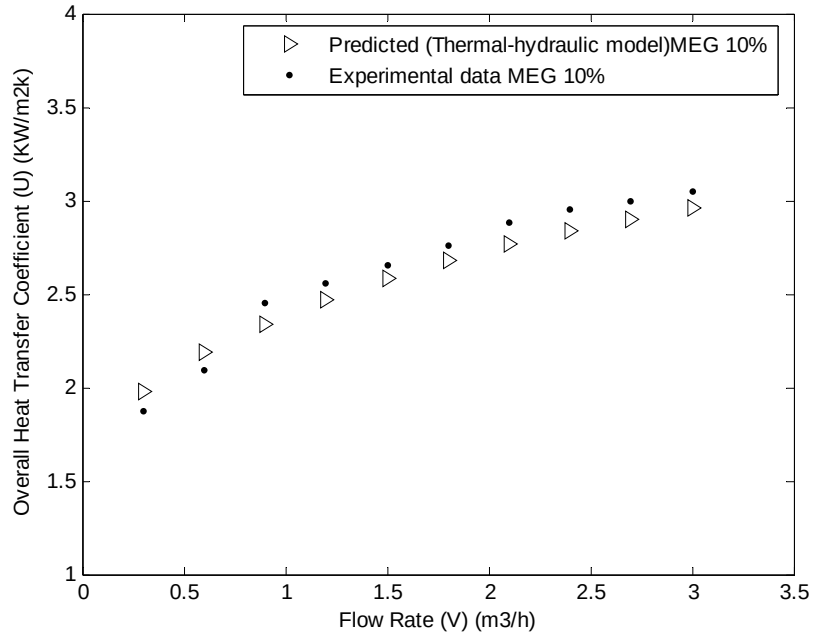

Figure 5.34 Variation of overall heat transfer coefficient with flow rate using MEG as antifreeze with 10% concentration

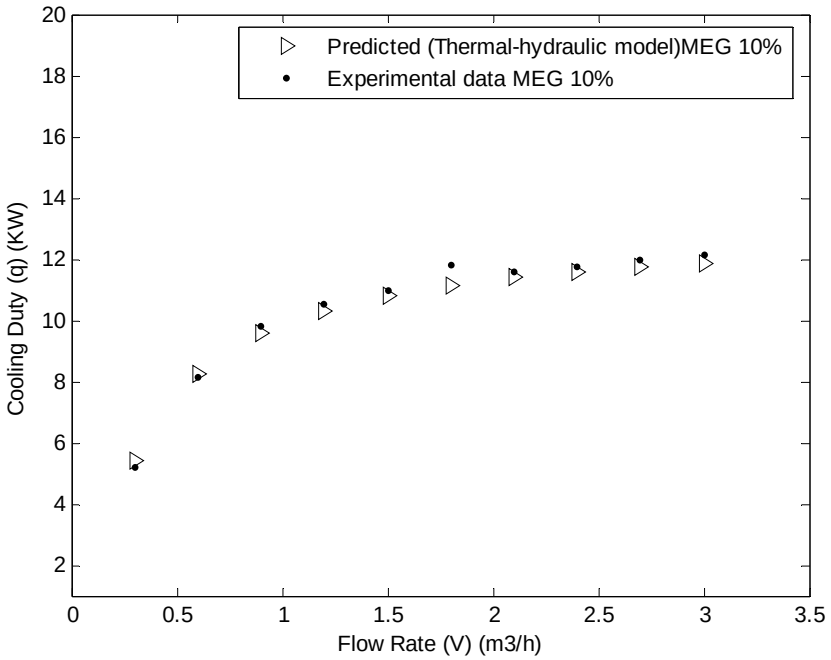

Figure 5.35 Flow Rate Vs Cooling Duty of Ice Slurry using MEG as antifreeze with 10% concentration

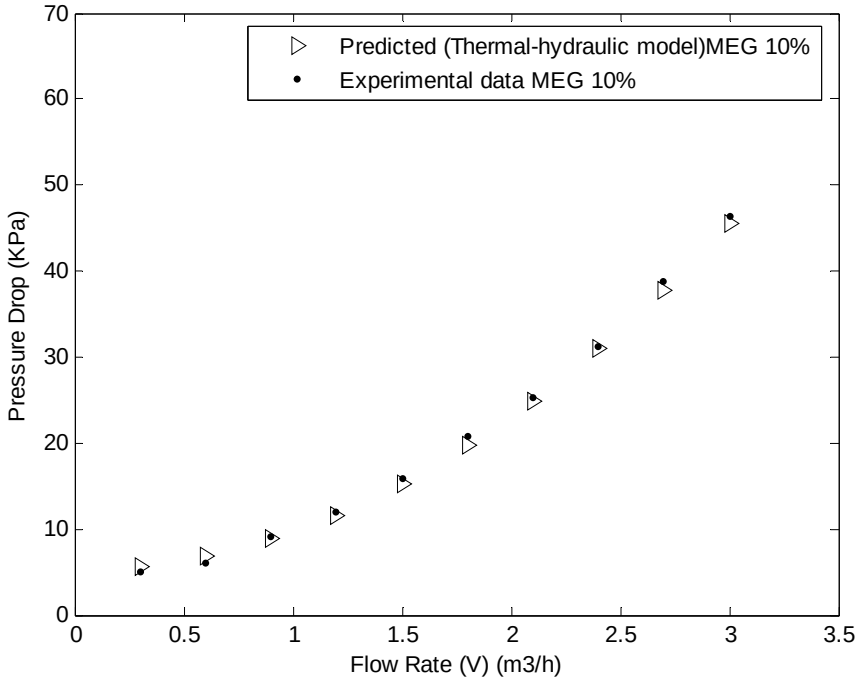

Figure 5.36 Variation of pressure drop with flow rate using MEG as antifreeze with 10% concentration

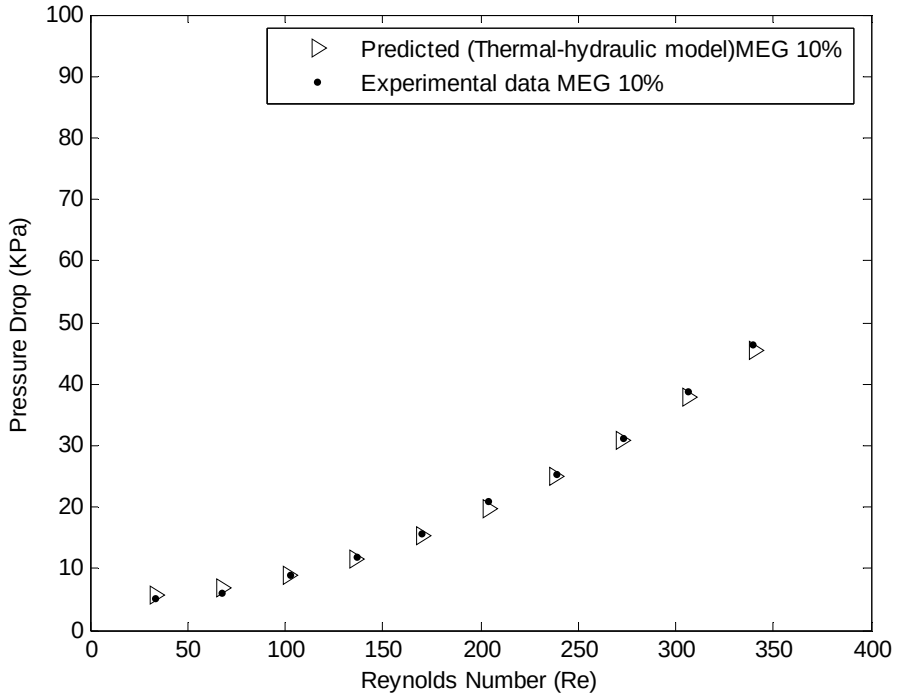

Figure 5.37 Pressure drop versus Reynolds number using MEG as antifreeze with 10% concentration

Model prediction with validation for ice slurry to hot water is shown in Table 5.9 and Fig.5.38 for overall heat transfer coefficient, Fig.5.39 for cooling duty, Fig.5.40 for pressure drop and Fig.5.41 for Reynolds number for PHE using MEG as antifreeze with 20% concentration. The predicted and experimental data matches satisfactorily. Similarly the prediction for other antifreezes for different concentrations are validated with experimental data.

Table 5.9 Variation of overall heat transfer coefficient, heat transfer coefficient, cooling duty and pressure drop of ice slurry with flow rate and pressure drop of ice slurry with Reynolds number using MEG as antifreeze with 20% concentration

Ice Slurry flow rate (m^3/h)	Overall heat transfer coefficient (KW/ m^2K)		Cooling Duty (KW)		Pressure drop for Stream1 (kPa)		Reynolds number
	Prediction	Experimental	Prediction	Experimental	Prediction	Experimental	
0.30	1.9650	1.8620	6.4254	6.1286	7.5598	6.9980	21.1724
0.60	2.1232	2.0422	9.7439	9.6236	7.5553	7.2800	42.3297
0.90	2.2670	2.3690	11.2894	11.4994	9.4083	9.1938	63.5199
1.20	2.3911	2.4766	12.1688	12.3560	12.1160	12.9890	84.6847
1.50	2.4997	2.5620	12.7417	12.9316	15.6122	15.6732	105.8495
1.80	2.5951	2.6740	13.1467	13.2870	19.8924	21.6800	127.0398
2.10	2.6791	2.7764	13.4476	13.6374	24.9455	25.1966	148.2046
2.40	2.7533	2.8602	13.6798	13.8084	30.7782	31.0060	169.3694
2.70	2.8194	2.9032	13.8643	14.0602	37.4010	38.3820	190.5597
3.00	2.8783	2.9390	14.0139	14.2246	44.8000	46.0800	211.7245

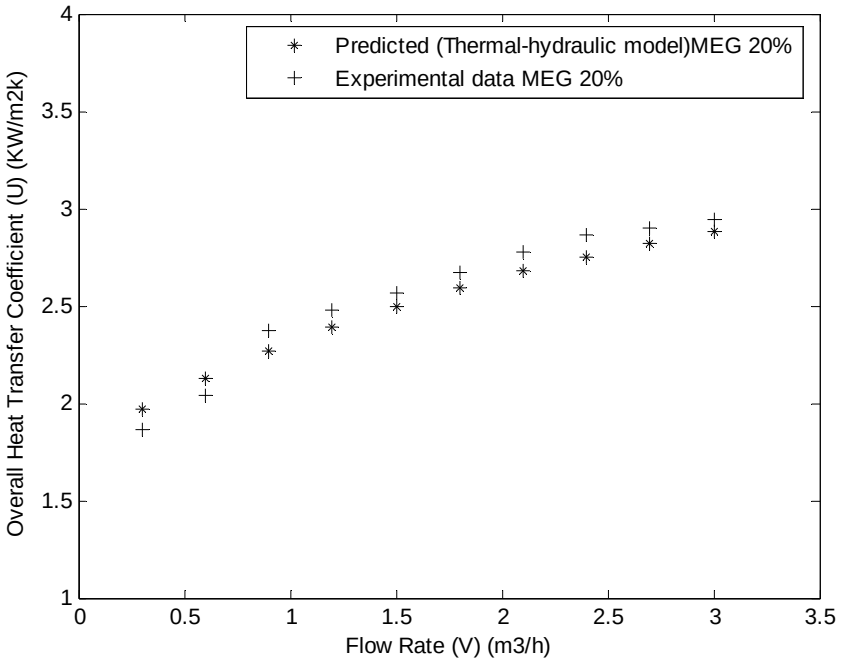

Figure 5.38 Variation of overall heat transfer coefficient with flow rate using MEG as antifreeze with 20% concentration

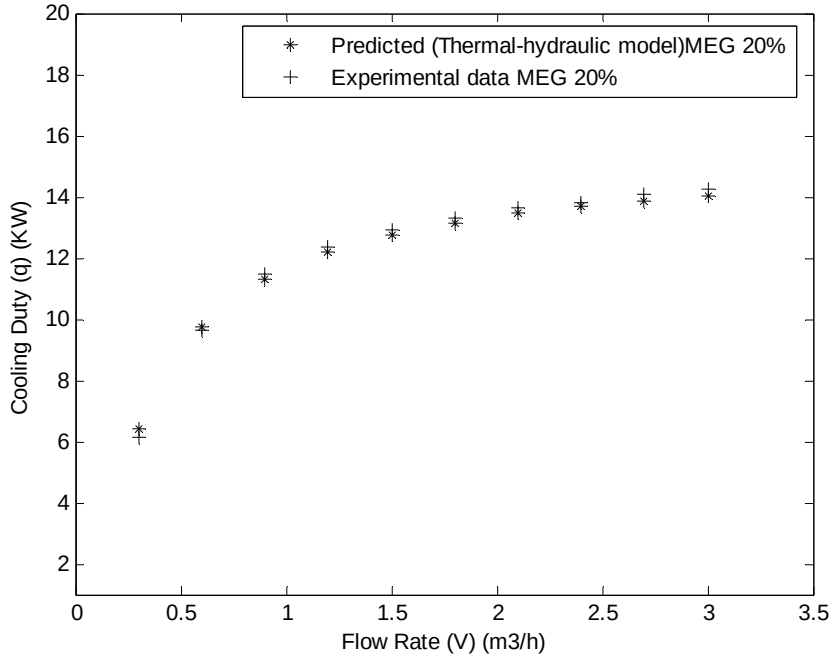

Figure 5.39 Flow Rate Vs Cooling Duty of Ice Slurry using MEG as antifreeze with 20% concentration

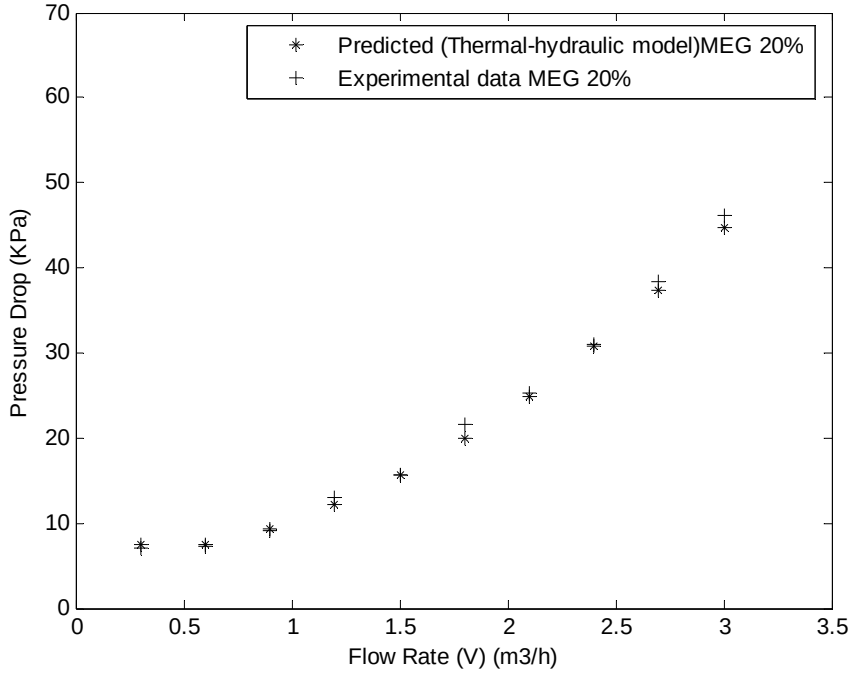

Figure 5.40 Variation of pressure drop with flow rate using MEG as antifreeze with 20% concentration

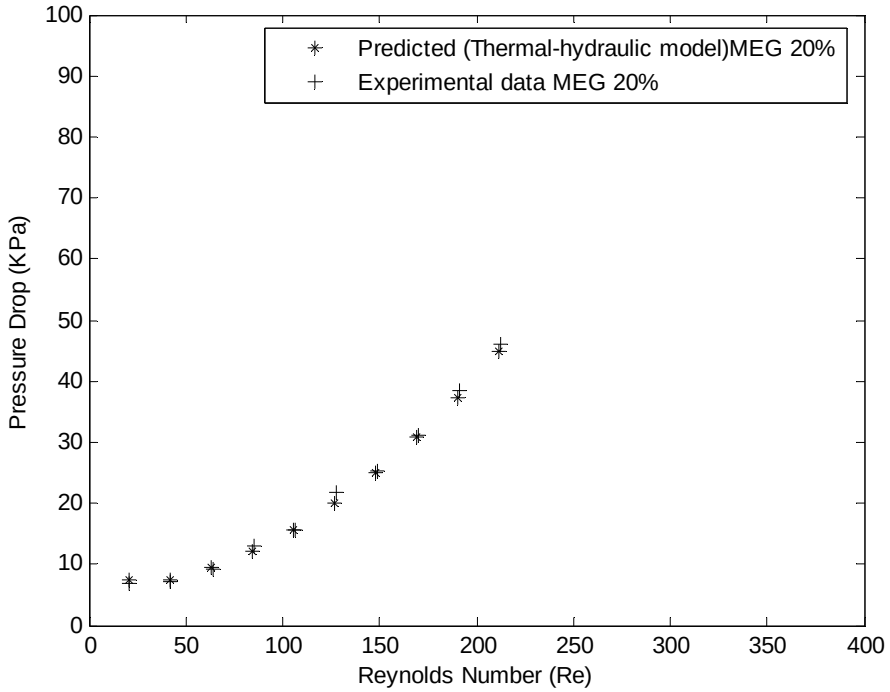

Figure 5.41 Pressure drop versus Reynolds number using MEG as antifreeze with 20% concentration

Model prediction with validation for ice slurry to hot water is shown in Table 5.10 and Fig.5.42 for overall heat transfer coefficient, Fig.5.43 for cooling duty, Fig.5.44 for pressure drop and Fig.5.45 for Reynolds number for PHE using MEG as antifreeze with 30% concentration. The predicted and experimental data matches satisfactorily. Similarly the prediction for other antifreezes for different concentrations are validated with experimental data.

Table 5.10 Variation of overall heat transfer coefficient, heat transfer coefficient, Cooling duty and pressure drop of ice slurry with flow rate and pressure drop of ice slurry with Reynolds number using MEG as antifreeze with 30% concentration

Ice Slurry flow rate (m^3/h)	Overall heat transfer coefficient (KW/ m^2K)		Cooling Duty (KW)		Pressure drop for Stream1 (kPa)		Reynolds number
	Prediction	Experimental	Prediction	Experimental	Prediction	Experimental	
0.30	2.2221	2.1890	7.6205	7.5820	22.1710	12.2640	13.0483
0.60	2.1186	1.9912	11.3334	11.2220	10.5537	11.0082	26.0873
0.90	2.2248	2.4240	13.0481	13.2370	11.3000	11.6520	39.1466
1.20	2.3322	2.4380	14.0339	14.1808	13.6325	13.9860	52.1902
1.50	2.4309	2.4860	14.6848	14.6700	16.8793	17.2100	65.2339
1.80	2.5204	2.6220	15.1508	14.7998	20.9290	21.4620	78.2932
2.10	2.6008	2.6998	15.5019	15.6466	25.7411	26.1968	91.3368
2.40	2.6733	2.7290	15.7762	15.9120	31.3108	31.7066	104.3805
2.70	2.7387	2.8380	15.9966	16.9200	37.6445	38.0060	117.4398
3.00	2.7978	2.9120	16.1770	16.2886	44.7275	45.6260	130.4834

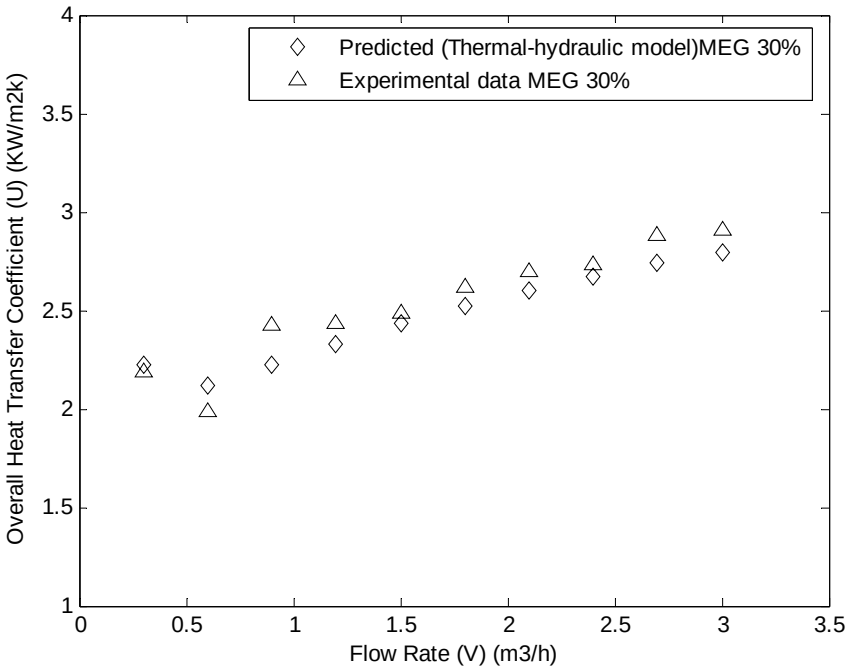

Figure 5.42 Variation of overall heat transfer coefficient with flow rate using MEG as antifreeze with 30% concentration

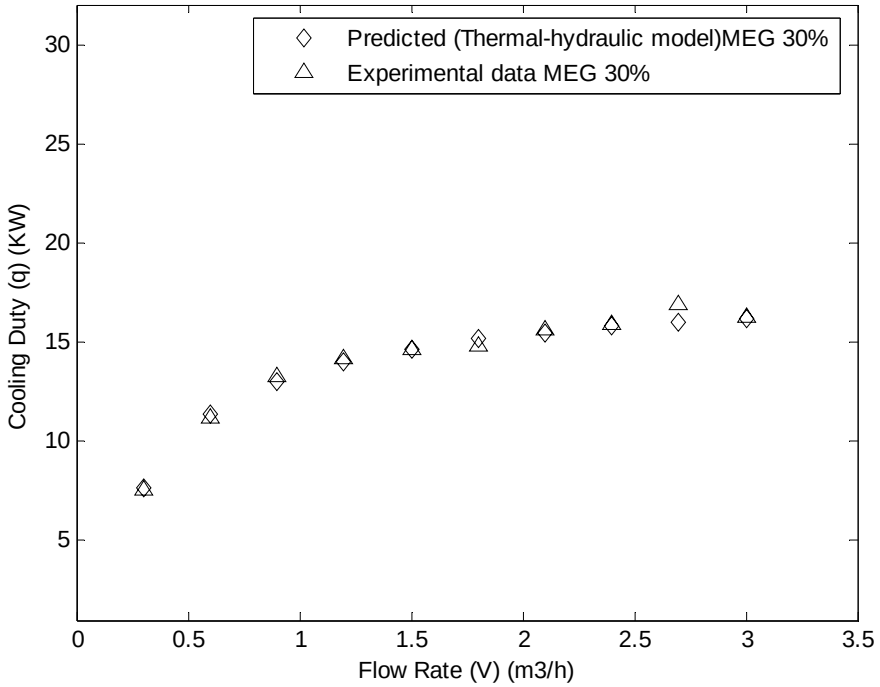

Figure 5.43 Flow Rate Vs Cooling Duty of Ice Slurry using MEG as antifreeze with 30% concentration

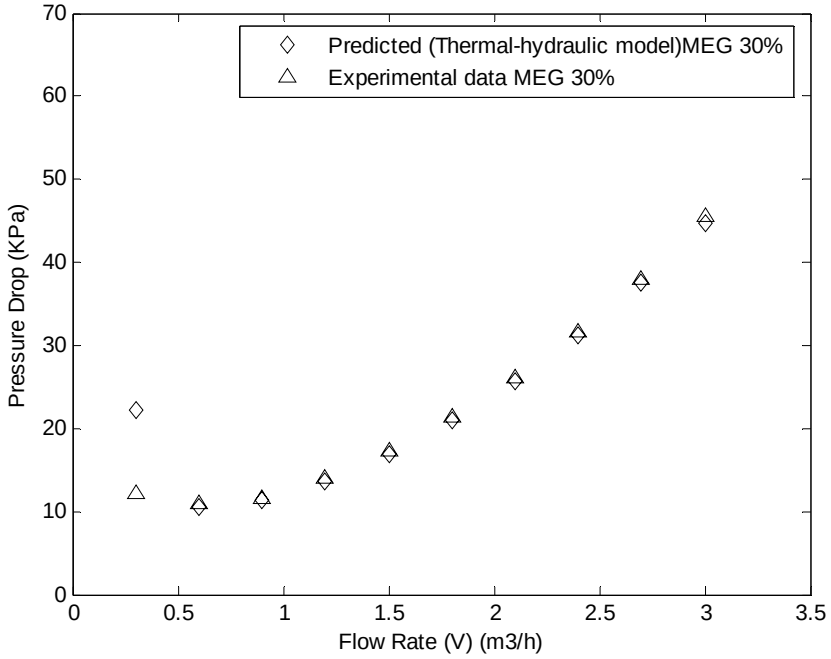

Figure 5.44 Variation of pressure drop with flow rate using MEG as antifreeze with 30% concentration

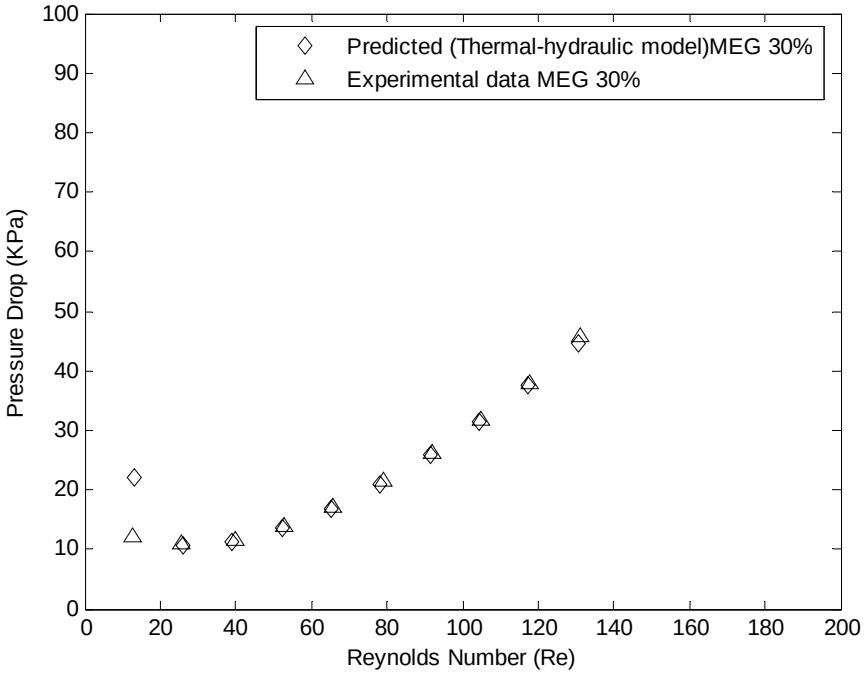

Figure 5.45 Pressure drop versus Reynolds number using MEG as antifreeze with 30% concentration

Model prediction with validation for ice slurry to hot water is shown in Table 5.11 and Fig.5.46 for overall heat transfer coefficient, Fig.5.47 for cooling duty, Fig.5.48 for pressure drop and Fig.5.49 for Reynolds number for PHE using MEG as antifreeze with 40% concentration. The predicted and experimental data matches satisfactorily. Similarly the prediction for other antifreezes for different concentrations are validated with experimental data.

Table 5.11 Variation of overall heat transfer coefficient, heat transfer coefficient, cooling duty and pressure drop of ice slurry with flow rate and pressure drop of ice slurry with Reynolds number using MEG as antifreeze with 40% concentration

Ice Slurry flow rate (m^3/h)	Overall heat transfer coefficient (KW/ m^2K)		Cooling Duty (KW)		Pressure drop for Stream1 (kPa)		Reynolds number
	Prediction	Experimental	Prediction	Experimental	Prediction	Experimental	
0.30	3.1694	2.3980	9.0345	9.8320	25.0500	24.9802	8.1773
0.60	2.2910	2.3290	13.3195	13.2030	30.8817	20.2600	16.3487
0.90	2.2612	2.3566	15.0313	15.2680	18.6156	18.9268	24.5329
1.20	2.3228	2.4180	16.0464	16.1866	18.5579	19.0026	32.7072
1.50	2.3980	2.4860	16.7340	16.8890	20.8406	21.0620	40.8816
1.80	2.4729	2.5588	17.2372	17.3560	24.3227	25.5660	49.0657
2.10	2.5438	2.6530	17.6231	17.8960	28.7011	29.2180	57.2401
2.40	2.6099	2.7080	17.9297	16.8992	33.8811	34.2022	65.4144
2.70	2.6710	2.7812	18.1796	18.3280	39.8307	40.2360	73.5986
3.00	2.7273	2.8488	18.3867	18.8650	46.5185	46.9980	81.7729

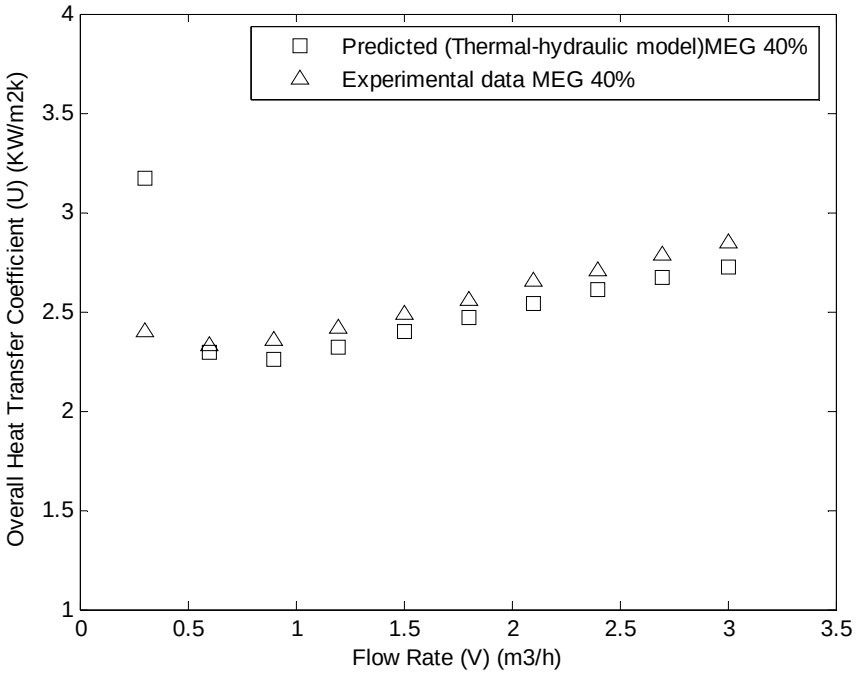

Figure 5.46 Variation of overall heat transfer coefficient with flow rate using MEG as antifreeze with 40% concentration

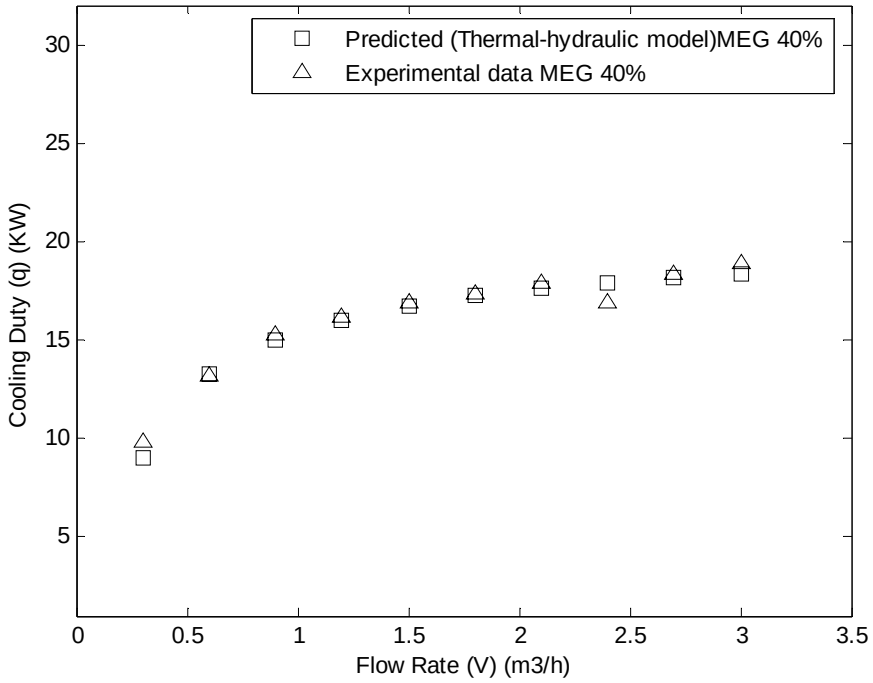

Figure 5.47 Flow Rate Vs Cooling Duty of Ice Slurry using MEG as antifreeze with 40% concentration

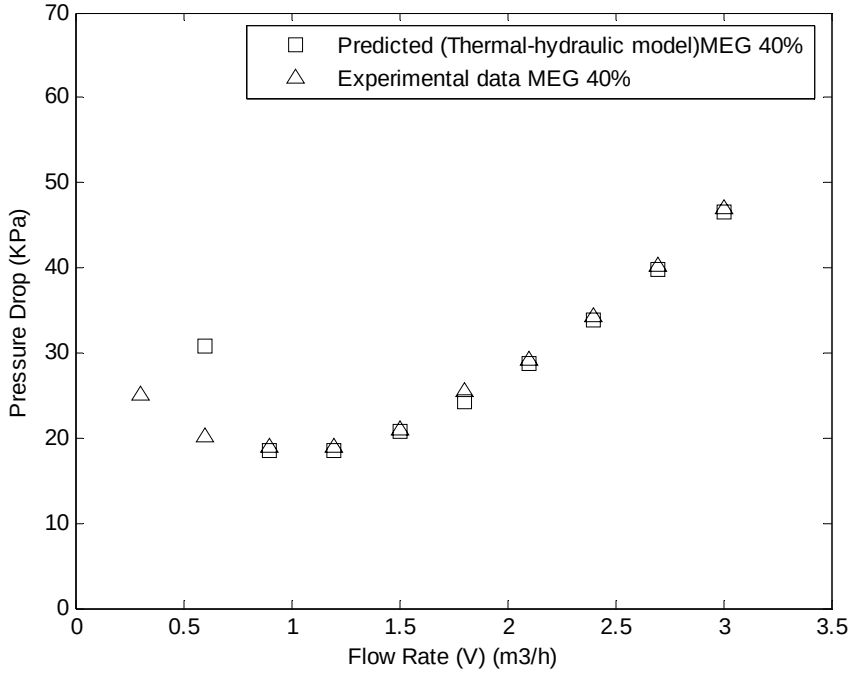

Figure 5.48 Variation of pressure drop with flow rate using MEG as antifreeze with 40% concentration

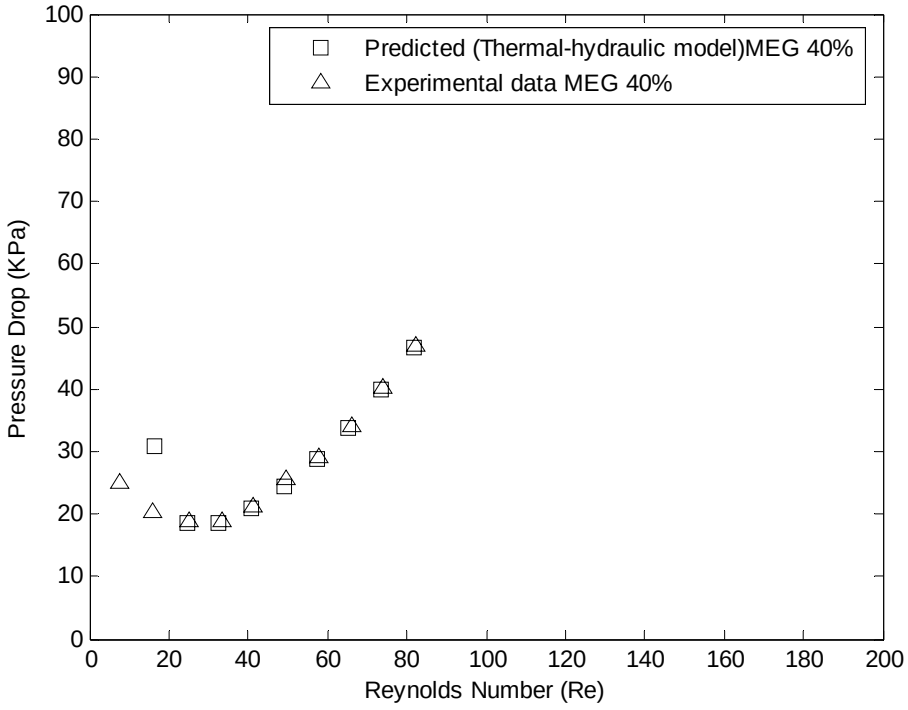

Figure 5.49 Pressure drop versus Reynolds number using MEG as antifreeze with 40% concentration

Heat transfer

Variation of overall heat transfer coefficient with flow rate is shown in Figure 5.50. using MEG as antifreeze with 10%, 20%, 30% and 40% concentration. Overall heat transfer coefficient increases with increase in flow rate. The predicted and experimental data matches satisfactorily.

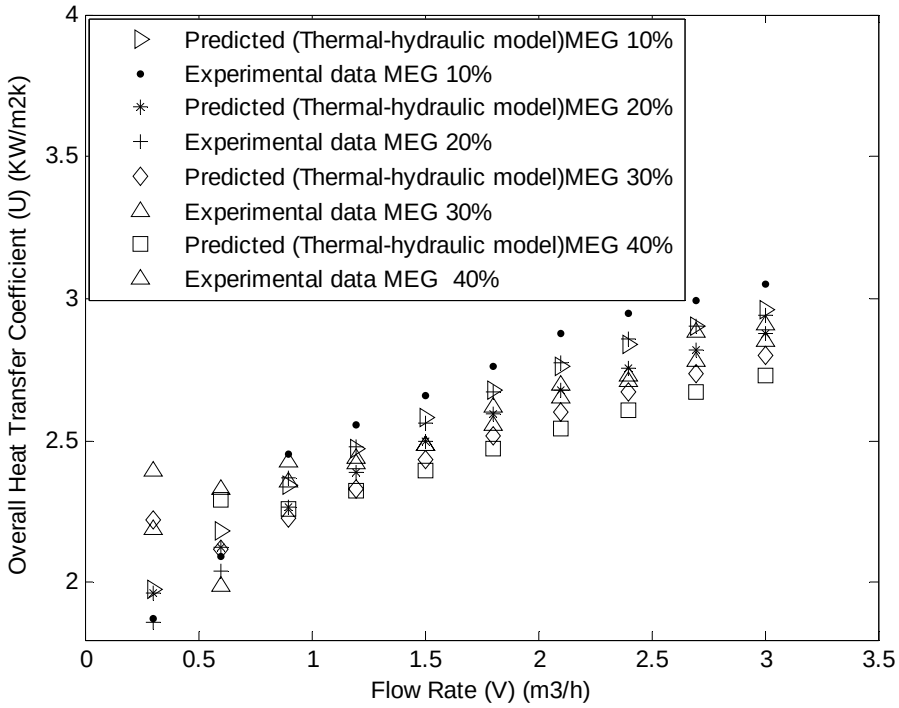

Figure 5.50 Variation of overall heat transfer coefficient with flow rate using MEG as antifreeze with 10%, 20%, 30% and 40% concentration

Figure 5.51.using MEG as antifreeze with 10%, 20%, 30% and 40% concentration shows the variation of cooling duty with flow rate of ice slurry. Cooling duty increases with increase in flow rate. Experimental data is compared with the prediction of the present formulation. It can be seen that predicted ice slurry cooling duty matches reasonably well with the experimental data.

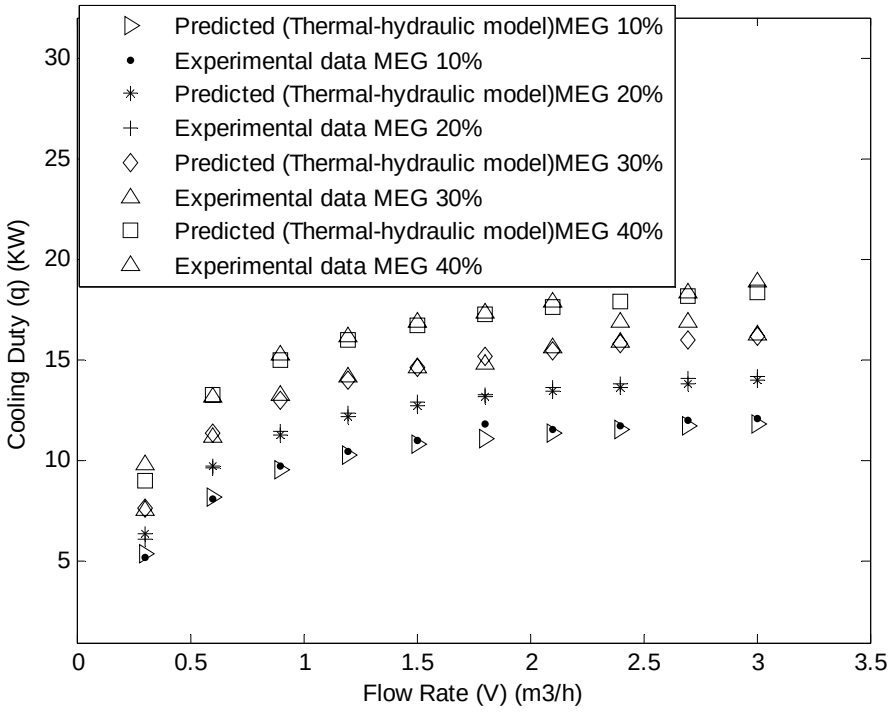

Figure 5.51 Flow Rate Vs Cooling Duty of Ice Slurry using MEG as antifreeze with 10%, 20%, 30% and 40% concentration

Pressure Drop

Figure 5.52.using MEG as antifreeze with 10%, 20%, 30% and 40% concentration shows the variation of pressure drop with flow rate of ice slurry. Pressure drop increases with increase in flow rate. Experimental data is compared with the prediction of the present formulation. It can be seen that predicted ice slurry pressure drop matches reasonably well with the experimental data.

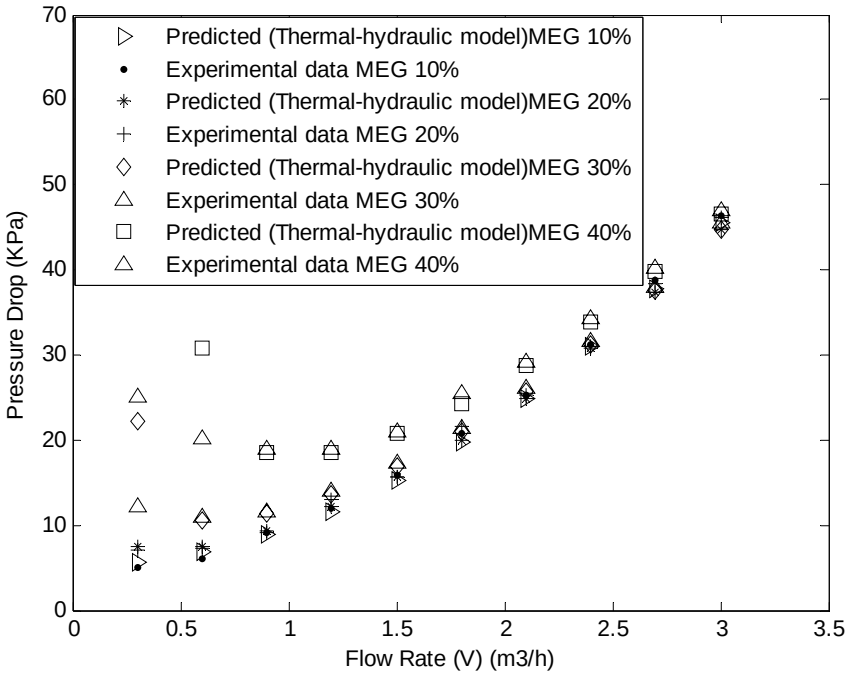

Figure 5.52 Variation of pressure drop with flow rate using MEG as antifreeze with 10%, 20%, 30% and 40% concentration

Variation of pressure drop vs Reynolds Number is shown in Figure 5.53. using MEG as antifreeze with 10%, 20%, 30% and 40% concentration. The predicted and experimental data matches satisfactorily.

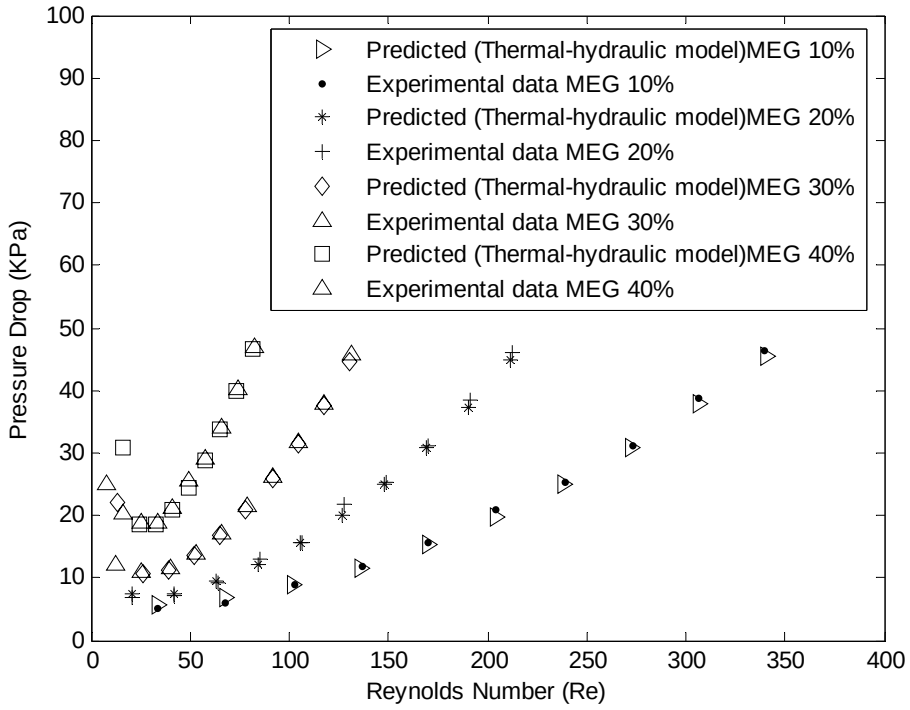

Figure 5.53 Pressure drop versus Reynolds number using MEG as antifreeze with 10%, 20%, 30% and 40% concentration

5.4. COMPARISON OF ICE SLURRY AND CHILLED WATER

By using ice slurry in place of chilled water in plate heat exchanger, cooling duty found to be higher and pressure drop is slightly higher in case of ice slurry. Cooling duty of ice slurry increases with increase in antifreeze concentrations 10%, 20%, 30% and 40%. By using ice slurry in plate heat exchanger cooling duty found to be increased by 50% at 0.3m^3/h and increased by 37 % at 3.0 m^3/h of 10% ice crystal PG ice slurry and pressure drop increased by 10% at 0.3m^3/h and increased by 7 % at 3.0 m^3/h.

REFERENCES

1. Åke Melinder, (2007) Thermophysical Properties of Aqueous Solutions Used as Secondary Working Fluids, Doctoral Thesis, Division of Applied Thermodynamics and Refrigeration Dept. of Energy Technology School of Industrial Engineering and Management Royal Institute of Technology, KTH Stockholm, Sweden.

2. Cecilia Hagg, (2005) Ice Slurry as Secondary Fluid in Refrigeration Systems Fundamentals and Applications in Supermarkets, Licentiate Thesis, Stockholm, School of Industrial Engineering and Management Department of Energy Technology Division of Applied Thermodynamics and Refrigeration.

3. Kauffeld M, Wang M.J, Goldstein V, Kasza K.E, (2010) Ice Slurry Applications, International Journal of Refrigeration, 33, 1491-1505.

4. Michael Kauffeld, Masahiro Kawaji, Peter W. Egolf, Handbook on Ice Slurries-Fundamentals and Engineering, International Institute of Refrigeration (IIR), 2005.

5. Saraceno L, Boccardi G, Celata G.P, Lazzarini R, Trinchieri R, (2011) Development of two heat transfer correlations for a scraped surface heat exchanger in an ice-cream machine, Applied Thermal Engineering, 31, 4106-4112.

6. Mourad Yataghene, Fayolle Francine, Legrand Jack, (2011) Flow patterns analysis using experimental PIV technique inside scraped surface, Applied Thermal Engineering, 31, 2855-2868.

7. Solano J.P, García A, Vicente P.G, Viedma A, (2011) Flow pattern assessment in tubes of reciprocating scraped surface heat exchangers, International Journal of Thermal Sciences, 50, 803-815.

8. Rodriguez Pascual M, Derksen J.J, VanRosmalen G.M, Witkamp G.J, (2009) Flow and particle motion in scraped heat exchanger crystallizers, Chemical Engineering Science, 64, 5153-5161.

9. Qin Frank , Xiao Dong Chen, Shashini Ramachandra , Kevin Free, (2006) Heat transfer and power consumption in a scraped-surface heat exchanger while freezing aqueous solutions, Separation and Purification Technology, 48, 150-158.

10. Lakhdar Mohamed Ben , Rosalia Cerecero , Graciela Alvarez , Jacques Guilpart , Denis Flick , Andr Lallemand, (2005) Heat transfer with freezing in a scraped surface heat exchanger, Applied Thermal Engineering, 25, 45-60.

11. Stamatiou E, Meewisse J.W, Kawaji M, (2005) Ice slurry generation involving moving parts, International Journal of Refrigeration, 28, 60-72.

12. Vaessen R.J.C, Seckler M.M, Witkamp G.J, (2004) Heat transfer in scraped eutectic

crystallizers, International Journal of Heat and Mass Transfer, 47, 717-728.

13. Qin Frank G.F, Chen Xiao Dong, and Andrew B. Russell, (2003) Heat Transfer at the Subcooled-Scraped Surface, with/without Phase Change, AIChE Journal, 49(8), 1947-1955.

14. Eric Dumon, Francine Fayolle, Jack Legrand, {2000) Flow regimes and wall shear rates determination within a scraped surface heat exchanger, Journal of Food Engineering, 45, 195-207.

15. Mounir Baccar , Mohamed Salah Abid, (1997) Numerical analysis of three-dimensional flow and thermal behaviour in a scraped-surface heat exchanger, Rev Gt!n Therm Elsevier, 36, 782-790.

16. Lim Hyo-Mook [KR], (2004) Ice slurry generator, European Patent number: WO2004046624 (A1).

17. Doetsch Christian [DE], (2000) Ice generator for providing ice slurry uses stripping devices for removing ice from inside walls of parallel pipes for aqueous medium within heat exchanger, European Patent number: DE19938044 (C1).

18. Lee Seung Kee [KR], (2000) Slurry ice generator for cool thermal storage system, European Patent number: KR20000017696 (A).

19. Goldstein Vladimir [CA] (2000) Ice making machine and heat exchanger, U.S. Patent number: 6056046 (A).

20. Tatsunori Asaoka, Akio Saito, Seiji Okawa, Hiroyuki Kumano, Tsutomu Hozumi, (2009) Vacuum freezing type ice slurry production using ethanol solution 2nd report: Investigation on evaporation characteristics of ice slurry in ice production, International Journal of Refrigeration, 32, 394-401.

21. Koji Matsumoto, Yutaka Suzuki, Masashi Okada, Yoshikazu Teraoka, Tetsuo Kawago, (2006) Study on continuous ice slurry formation using functional fluid for ice storage Discussion of optimal operating conditions, International Journal of Refrigeration, 29, 1208-1217.

22. Hawlader M.N.A, Wahed M.A, (2009) Analyses of ice slurry formation using direct contact heat transfer, Applied Energy, 86, 1170-1178.

23. Thongwik S, Vorayos N, Kiatsiriroat T, Nuntaphan A, (2008) Thermal analysis of slurry ice production system using direct contact heat transfer of carbon dioxide and water mixture, International Communications in Heat and Mass Transfer, 35, 756-761.

24. Didier Vuarnoz, D.Ata-Caesar, Osmann Sari, Peter William Egolf, (2004) Ultrasonic measurements in ice slurry generation by direct contact evaporation, 4th International Symposium on Ultrasonic Doppler Method for Fluid Mechanics and

Fluid Engineering Sapporo, 6-8 September.

25. Xiu-Wei Li, Xiao-Song Zhang , Rong-Quan Cao, Xiu-Zhang F, (2009) A novel ice slurry producing system: Producing ice by utilizing inner waste heat, Energy Conversion and Management, 50, 2893-2904.

26. Jean Castaing-Lasvignottes , Thomas David, Jean-Pierre Be´de´carrats Franc¸oise Strub (2006) Dynamic modelling and experimental study of an ice generator heat exchanger using supercooled water, Energy Conversion and Management, 47, 3644-3651.

27. Pronk P, Meewisse J.W, Infante Ferreira C.A, (2001) Heat transfer model for a fluidised bed ice slurry generator, Presented at the 4th Workshop on Ice Slurries of the IIR, 12-13 November Osaka (Japan).

28. M. Haid, (1997) Correlations for the prediction of heat transfer to liquid-solid fluidized beds, Chemical Engineering and Processing, 36, 143-147.

29. Melinder A, Handbook on indirect refrigeration and heat pump systems Dept. of Energy Technology, KTH Sweden Publisher: Svenska Kyltekniska Föreningen, KTF, Banvallen 11, 429 30 Kullavik, Swedan.

30. Melinder A, (2010) Properties and other aspects of aqueous solutions used for single phase and ice slurry applications, International Journal of Refrigeration, 33, 1506-1512.

31. Hiroyuki Kumano, Tatsunori Asaoka, Akio Saito, Seiji Okawa, (2007) Study on latent heat of fusion of ice in aqueous solutions, International Journal of Refrigeration, 30, 267-273.

32. Jacques Guilpart, Evangelos Stamatiou, Anthony Delahaye, Laurence Fournaison, (2006) Comparison of the performance of different ice slurry types depending on the application temperature, International Journal of Refrigeration, 29, 781-788.

33. .Melinder A, Granryd E, (2005) Using property values of aqueous solutions and ice to estimate ice concentrations and enthalpies of ice slurries, International Journal of Refrigeration, 28, 13-19.

34. Vincent Ayel , Olivier Lottin , Elena Popa , Hassan Peerhossaini, (2005) Using undercooling to measure the freezing points of aqueous solutions, International Journal of Thermal Sciences, 44, 11-20.

35. Shu-Shen Lua, Takaaki Inadab,, Akira Yabeb, Xu Zhangb, Svein Grandumc, (2002) Microscale study of poly(vinyl alcohol) as an effective additive for inhibiting recrystallization in ice slurries, International Journal of Refrigeration, 25, 262-268.

36. Illa´n F, Viedma A, (2012) Heat exchanger performance modeling using ice slurry as secondary refrigerant, International Journal of Refrigeration, 35, 1275-1283.

37. Ma Z.W, Zhang P, (2011) Pressure drop and heat transfer characteristics of clathrate hydrate slurry in a plate heat exchanger, International Journal of Refrigeration, 34, 796-806.

38. Kalaiselvam S, Karthik P, Ranjit Prakash S, (2009) Numerical investigation of heat transfer and pressure drop characteristics of tube–fin heat exchangers in ice slurry HVAC system, Applied Thermal Engineering, 29, 1831-1839.

39. Warnakulasuriya F.S.K, Worek W.M, (2008) Heat transfer and pressure drop properties of high viscous solutions in plate heat exchangers, International Journal of Heat and Mass Transfer, 51, 52-67.

40. Hao Peng, Xiang Ling, (2008) Optimal design approach for the plate-fin heat exchangers using neural networks cooperated with genetic algorithms, Applied Thermal Engineering, 28, 642-650.

41. Pronk P, Infante Ferreira C.A, Witkamp G.J, (2008) Superheating of ice slurry in melting heat exchangers, International Journal of Refrigeration, 31, 911-920.

42. Dong Ho, Yu-Jui, Chii-Chuang, Jr-Wei Tu, (2007) Double-pass flow heat transfer in a parallel-plate channel for improved device performance under uniform heat fluxes, International Journal of Heat and Mass Transfer, 50, 2208-2216.

43. Garcı´a-Cascales J.R, Vera-Garcı´a F, Corber_an-Salvador J.M, Gonz_alvez-Maci'a J., (2007) Assessment of boiling and condensation heat transfer correlations in the modelling of plate heat Exchangers, International Journal of Refrigeration, 30, 1029-1041.

44. Nørgaard E, Sørensena T.A, Hansena T.M, Kauffeld M, (2005) Performance of components of ice slurry systems: pumps, plate heat exchangers, and fittings, International Journal of Refrigeration, 28, 83-91.

45. Jorge A.W. Gut , Jose M. Pinto, (2004) Optimal configuration design for plate heat exchangers, International Journal of Heat and Mass Transfer, 47, 4833-4848.

46. Jialing Zhu, Wei Zhang, (2004) Optimization design of plate heat exchangers (PHE) for geothermal district heating systems, Geothermics, 33, 337-347.

47. Lieke Wang, Bengt Sunden, (2003) Optimal design of plate heat exchangers with and without pressure drop specifications, Applied Thermal Engineering, 23, 295-311.

48. Bellas J, Chaer I, Tassou S.A, (2002) Heat transfer and pressure drop of ice slurries in plate heat exchangers, Applied Thermal Engineering, 22, 721-732.

49. Kousksou T, Jamil A, Arid A, Jegadheeswaran S, Zeraouli Y, (2012) Crystallisation kinetics with nucleation phenomenon: Ice slurry system, International Journal of Refrigeration,

50. Lu W, Tassou S.A, (2012) Experimental study of the thermal characteristics of phase change slurries for active cooling, Applied Energy; 91, 366-374.

51. Che´gnimonhan V, Josset C, Peerhossaini H, (2010) Ice slurry crystallization based on kinetic phase-change modeling, International Journal of Refrigeration, 33, 1559-1568.

52. Zhang X.J, Qiu L.M, Zhang P, Liu L, Gan Z.H, (2008) Performance improvement of vertical ice slurry generator by using bubbling device, Energy Conversion and Management, 49, 83-88.

53. Sathaporn Thongwik , Tanongkiat Kiatsiriroat, Atipoang Nuntaphan, (2008) Heat transfer model of slurry ice melting on external surface of helical coil, International Communications in Heat and Mass Transfer, 35, 1335-1339.

54. Hiroyuki Kumano, Tatsunori Asaoka, Akio Saito, Seiji Okawa, (2007) Study on latent heat of fusion of ice in aqueous solutions, International Journal of Refrigeration, 30, 267-273.

55. Takaaki Inada, Poly Rani Modak, (2006) Growth control of ice crystals by poly(vinyl alcohol) and antifreeze protein in ice slurries, Chemical Engineering Science, 61, 3149-3158.

56. Jacques Guilpart, Evangelos Stamatiou, Anthony Delahaye, Laurence Fournaison, (2006) Comparison of the performance of different ice slurry types depending on the application temperature, International Journal of Refrigeration, 29, 781-788.

57. Vincent Ayel, Olivier Lottin, Elena Popa, Hassan Peerhossaini, (2005) Using undercooling to measure the freezing points of aqueous solutions, International Journal of Thermal Sciences, 441, 1-20.

58. Melinder A, Granryd E, (2005) Using property values of aqueous solutions and ice to estimate ice concentrations and enthalpies of ice slurries, International Journal of Refrigeration, 28, 13-19.

59. Frank G.F. Qin, Xiao Dong Chen, Mohammed M. Farid, (2004) Growth kinetics of ice films spreading on a subcooled solid surface, Separation and Purification Technology, 39, 109-121.

60. Frank G.F. Qin, Jian Chao Zhao , Andrew B. Russell, Xiao Dong Chen, John J. Chen, Lindsay Robertson, (2003) Simulation and experiment of the unsteady heat transport in the onset time of nucleation and crystallization of ice from the subcooled solution, International Journal of Heat and Mass Transfer, 46, 3221-3231.

61. Svein Grandum, Akira Yabe, Kazuya Nakagomi, Makoto Tanaka, Fumio Takemura, Yasunori Kobayashi, Per-Erling Frivik, (1999) Analysis of ice crystal growth for a crystal surface containing adsorbed antifreeze proteins, Journal of

Crystal Growth, 205, 382-390.

62. Hiroyuki Kumano, Tetsuo Hirata, Yosuke Hagiwara, Fumets Tamura, Effects of storage on flow and heat transfer characteristics of ice slurry, International Journal of Refrigeration 35 (2012) 122–129.

63. Ma Z.W, Zhang P, (2012) Pressure drops and loss coefficients of a phase change material slurry in pipe fittings, International Journal of Refrigeration, 35, 992–1002.

64. Mellari S, Boumaza M, Egolf P.W, (2012) Physical modeling, numerical simulations and experimental investigations of Non-Newtonian ice slurry flows, International Journal of Refrigeration, 35, 1284–1291.

65. Hiroyuki Kumano, Tetsuo Hirata, Michito Shirakawa , Ryouta Shouji, Yosuke Hagiwara, (2012) Flow characteristics of ice slurry in narrow tubes, International Journal of Refrigeration, 35, 1513–1522.

66. Mourad Yataghene, Fayolle Francine, Legrand Jack, (2011) Flow patterns analysis using experimental PIV technique inside scraped surface, Applied Thermal Engineering, 31, 2855-2868.

67. Langlois V, Gautherin W, Laurent J, Royon L, Fournaison L, Delahaye A, Jia X, (2011) Ultrasonic determination of the particle concentration in model suspensions and ice slurry, International Journal of Refrigeration, 34, 1972–1979.

68. Mika L, (2011) Energy losses of ice slurry in pipe sudden contractions, Experimental Thermal and Fluid Science, 35, 939–947.

69. Patrick J. Rensing, Matthew W. Liberatore, Amadeu K. Sum, Carolyn A. Koh, E. Dendy Sloan, (2011) Viscosity and yield stresses of ice slurries formed in water-in-oil emulsions, Journal of Non-Newtonian Fluid Mechanics, 166, 859–866.

70. Hiroyuki Kumano, Tetsuo Hirata, Yasuyuki Izumi, (2010) Study on specific enthalpy of ice including solute in aqueous solution, International Journal of Refrigeration, 33, 480–486.

71. Jose´ Ferna´ndez-Seara, Rube´n Diz, Francisco J. Uhı´a, J. Alberto Dopazo, (2010) Experimental analysis on pressure drop and heat transfer of a terminal fan-coil unit with ice slurry as cooling medium, International Journal of Refrigeration, 33, 1095–1104.

72. Ashley C.S. Monteiro, Pradeep K. Bansal, (2010) Pressure drop characteristics and rheological modeling of ice slurry flow in pipes, International Journal of Refrigeration, 33, 1523–1532.

73. Hiroyuki Kumano, Tetsuo Hirata, Ryouta Shouji, Michito Shirakawa, (2010) Experimental study on heat transfer characteristics of ice slurry, International Journal of Refrigeration, 33, 1540–1549.

74. Illa´n F, Viedma A, (2009) Experimental study on pressure drop and heat transfer in pipelines for brine based ice slurry. Part I: Operational parameters correlations, International Journal of Refrigeration, 32, 1015–1023.

75. Illa´n F, Viedma A, (2009) Experimental study on pressure drop and heat transfer in pipelines for brine based ice slurry Part II: Dimensional analysis and rheological model, International Journal of Refrigeration, 32, 1024–1031.

76. Marino Grozdek, Rahmatollah Khodabandeh, Per Lundqvist, (2009) Experimental investigation of ice slurry flow pressure drop in horizontal tubes, Experimental Thermal and Fluid Science, 33, 357–370.

77. Evans T.S, Quarini G.L, Shire G.S.F, (2008) Investigation into the transportation and melting of thick ice slurries in pipes, International Journal of Refrigeration,. 31, 145– 151.

78. Beata Niezgoda Z elasko , Jerzy Z elasko, (2008) Melting of ice slurry under forced convection conditions in tubes, Experimental Thermal and Fluid Science, 32, 1597–1608.

79. Wissam Racheda, Fre´deric Sicarda,, Alain Lafarguea, Delphine Thorel, (2007) Ice slurry: Pressure drop and deposition velocity, International Journal of Refrigeration, 30, 1-8.

80. Koji Matsumotoa,, Takahiro Suzuki, (2007) Measurement of thermal conductivity of ice slurry made from solution by transient line heat-source technique (analytical discussion on influence of latent heat of fusion), International Journal of Refrigeration, 30, 187-194.

81. Koji Matsumotoa,, Tomoastu Kobayashi, (2007) Fundamental study on adhesion of ice to cooling solid surface, International Journal of Refrigeration, 30, 851-860.

82. Constantin Ionescua, Philippe Haberschillb,, Ildiko¨ Kissc, Andre´ Lallemand, (2007) Local and global heat transfer coefficients of a stabilized ice slurry in laminar and transitional flows, International Journal of Refrigeration, 30, 970-977.

83. Beata Niezgoda- ˙ Zelasko , Jerzy ˙ Zelasko, (2007) Generalized non-Newtonian flow of ice-slurry, Chemical Engineering and Processing, 46, 895–904.

84. Jorge L. Alvarado a, Charles Marsh , Chang Sohn , Gary Phetteplace , Ty Newell, (2007) Thermal performance of microencapsulated phase change material slurry in turbulent flow under constant heat flux, International Journal of Heat and Mass Transfer, 50, 1938–1952.

85. Beata Niezgoda-Zelasko, Wojciech Zalewski, (2006) Momentum transfer of ice slurry flows in tubes, experimental investigations, International Journal of Refrigeration, 29, 418–428.

86. Beata Niezgoda-Z˙ elasko, Wojciech Zalewski, (2006) Momentum transfer of ice slurry flows in tubes, modeling, International Journal of Refrigeration, 29, 429–436.

87. Beata Niezgoda-Z˙ elasko, (2006) Heat transfer of ice slurry flows in tubes, International Journal of Refrigeration, 29, 437–450.

88. Dong Won Lee, Eung Sang Yoon, Moon Chang Joo, Atul Sharma, (2006) Heat transfer characteristics of the ice slurry at melting process in a tube flow, International Journal of Refrigeration, 29, 451–455.

89. Stamatiou E, Kawaji M , (2005) Thermal and flow behavior of ice slurries in a vertical rectangular channel—Part II. Forced convective melting heat transfer, International Journal of Heat and Mass Transfer, 48, 3544–3559.

90. Ayel V, Lottin O, Peerhossaini H, (2003) Rheology, flow behaviour and heat transfer of ice slurries: a review of the state of the art, International Journal of Refrigeration, 26, 95–107.

91. Andrej Kitanovski, Alojz Poredos, (2002) Concentration distribution and viscosity of ice-slurry in heterogeneous flow, International Journal of Refrigeration, 25, 827–835.

92. Knodela B.D, Franceb D.M, Choic U.S, Wambsganssc M.W, (2000) Heat transfer and pressure drop in ice-water slurries, Applied Thermal Engineering, 20, 671-685.

93. Paul J, (2002) Innovative applications of pumpable ice slurry, Paper given at Institute of Refrigeration, 7 Feb, London, UK.

94. Paul J, (1992) Binary ice-technologies for the production of pumpable ice slurries, Proceedings of the International Institute of Refrigeration, pp. 5.1-5.10.

95. Sarit K.Das,Process Heat Transfer, Narosa Publishing House Pvt.Ltd.,2006 (Chapter 7).

96. Doebelin EO. (1990) Measurement systems.New York: Mcgraw-Hill.

97. Sabatelli V, Marano D, Braccio G, Sharma VK. (2002) Efficiency test of solar collectors: uncertainty in the estimation of regression parameters and sensitivity analysis. Energy Convers Manage, 43, 2287-2295.

APPENDIX-I

SAMPLE CALCULATIONS

Measured Thermodynamic Properties (PG as Antifreeze in Ice Slurry Generator) taken from Table 3.6(a)

Refrigerating Effect, $N = m_r (h_1 - h_5)$

$= 0.03334(4.2466\times10^5 - 3.1000\times10^5)$

$= 3822.7644$ W

Compressor Work, $W = m_r (h_2 - h_1)$

$= 0.03334(4.5909\times10^5 - 4.2466\times10^5)$

$= 1147.8962$ W

Heat Rejected in Condenser, $Qc = m_r (h_2 - h_4)$

$= 0.03334(4.5909\times10^5 - 3.1000\times10^5)$

$= 4970.6606$ W

Coefficient of Performance (COP=N/W)

$= 3822.7644 / 1147.8962$

$= 3.3302$

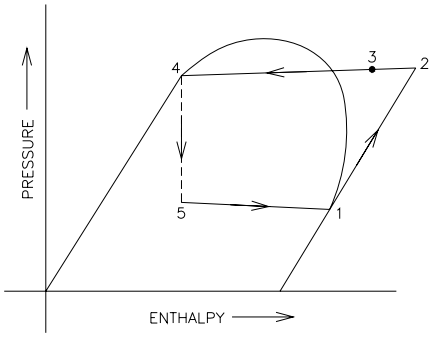

Fig. Pressure-enthalpy diagram

APPENDIX-II

UNCERTAINTY ANALYSIS

Using the experimental data thermodynamic heat and work calculations of ice slurry generation system are done. The errors in the results are introduced because of the equation of state or correlations used for the property calculations. The correlations are based on the experimental data having percentage deviation caused due to experimentation. Uncertainty analysis of thermodynamic heat and work calculations of ice slurry generation system are shown in Table 3.5 and Table 3.11. (a), (b) and (c).

To compute the overall uncertainty due to combined effect of uncertainties of different variables, let us consider the following equation in most general form.

$$y = f\ (x_1, x_2, \ldots\ldots x_i, \ldots\ldots x_n) \tag{1}$$

Where y is a parameter that depends on independent variables, x_1, x_2,……x_i,…..x_n.

Thus Uy is the uncertainty in y due to combine effect of different variables is given by [96,97].

$$Uy^2 = \pm\left\{(\delta y/\delta x_1)^2(Ux_1)^2 + (\partial y/\partial x_2)^2(Ux_2)^2 + \ldots(\partial y/\partial x_i)^2(Ux_i)^2 + \ldots(\partial y/\partial x_n)^2(Ux_n)^2\right\} \tag{2}$$

Where Ux is the uncertainty in the measurement of x and x_1, x_2,……x_i,…..x_n are temperature, pressure and mass flow rate of refrigerant at different state points.

Based on above, at design point, the uncertainty in values of refrigerating effect, (N), compressor work, (W), heat rejected in condenser, (Qc) and coefficient of performance (COP) is calculated.

APPENDIX-III

PUBLICATIONS OUT OF RESEARCH WORK

A) PAPER PUBLISHED IN INTERNATIONAL JOURNAL:

1 Rajinder Singh and Surendra Singh Kachhwaha, 'Experimental Studies on a Scraped Surface Ice Slurry Generator' International Journal of Engineering Science and Innovative Technology (IJESIT) Vol.2, Issue 4, July 2013, PP. 117-131.

2 Rajinder Singh and Surendra Singh Kachhwaha, 'Thermal hydraulic analysis of a plate heat exchanger' Journal of Scientific and Industrial Research (JSIR) Vol. 69, February 2010, PP. 121-124.

B) PAPER PUBLISHED IN PROCEEDINGS OF INTERNATIONAL CONFERENCES:

1. Rajinder Singh and Surendra Singh Kachhwaha, 'Experimental Performance of an Indigenously Developed Scraped Surface Ice Slurry Generator for Refrigeration and Air-conditioning industry', Proceedings of the 5th International Conference On Energy Research & Development (ICERD-5), 9-11 April,2012, State Of Kuwait.

2. Rajinder Singh and Surendra Singh Kachhwaha, 'Heat Transfer and Pressure Drop Analysis in a Plate Heat Exchanger', Proceedings of the 20th National and 9th International Conference ISHMT-ASME heat and Mass Transfer January 4-6, 2010, Mumbai, India.

3. Rajinder Singh and Surendra Singh Kachhwaha, 'Heat Transfer and Pressure Drop Analysis of a Plate Heat Exchanger Using Ice Slurry', Proceedings of the 22th National and 11th International ISHMT-ASME Heat and Mass Transfer Conference Dec 28-31, 2013, IIT Kharagpur, India (Accepted for Publication).

4. Rajinder Singh and Surendra Singh Kachhwaha, 'Experimental Performance of a Scraped Surface Ice Slurry Generator Using PG, MEG and DEG as Antifreezes', Proceedings of the 22th National and 11th International ISHMT-ASME Heat and Mass Transfer Conference Dec 28- 31, 2013, IIT Kharagpur, India (Accepted for Publication).

5. Rajinder Singh and Surendra Singh Kachhwaha, 'Experimental Study of Ice Slurries in Plate Heat Exchanger', Proceedings of the 3rd National Conference on Refrigeration and Air Conditioning (NCRAC-2013) 12-14 December 2013, IIT Madras, Chennai, India (Accepted for Publication).

AWARDS

Awarded with Ist position in innovation in Refrigeration &Air-Conditioning category of the "7Th Bry-Air Awards for Excellence in HVAC&R 2011-12" All India Basis on" Development of Scraped Surface Ice Slurry Generator for Refrigeration &Air-Conditioning Industry"

SOME STUDIES ON ICE SLURRY REFRIGERATION SYSTEM

By

RAJINDER SINGH
(Enrolment Number: Ph.D (DP-145/92)

Submitted

In partial fulfillment of the requirement of the degree of

DOCTOR OF PHILOSOPHY

To the

DEPARTMENT OF MECHANICAL ENGINEERING
DELHI COLLEGE OF ENGINEERING (NOW DTU)
UNIVERSITY OF DELHI
DELHI
NOVEMBER 2013

CHAPTER-VI
CONCLUSIONS AND SCOPE FOR FUTURE WORK

Chapter 6 describes conclusions of results of experimental data observed during ice slurry formation in ice slurry generator, collection of heat transfer and pressure drop data on a PHE test rig and scope for future work.

6.1. CONCLUSIONS

A summary of conclusions drawn from the present research study is given below:

1. A scraped surface ice slurry generator (74 litre capacity) through commonly used cost effective manufacturing processes (employed by small and medium scale industries) is successfully fabricated for collection of ice slurry data.
2. Refrigerant R410A (having zero ODP) is used as primary refrigerant in the primary circuit of scraped surface ice slurry generator.
3. The minimum ice slurry temperatures achieved are -5.7 ^{0}C, -10.2 ^{0}C, -15.5 and -20.7 ^{0}C for PG, -6.3 ^{0}C, -12.6 ^{0}C, -19.0 ^{0}C and -25.6 ^{0}C for MEG and -5.1 ^{0}C, -10.0 ^{0}C, -14.6 ^{0}C and -19.9 ^{0}C for DEG at 10%, 20%, 30% and 40% depressant concentrations respectively.
4. The thermo-physical properties of ice slurry are significantly different as compared to chilled water.
5. It is observed that the freezing temperature reduces with increase in antifreeze mass fraction for PG, MEG and DEG.
6. Three distinct stages- cool down or chilling period, nucleation or unstable ice slurry generation period and stable ice slurry generation period were observed through historical time dependence curves.
7. The time required for 50% measured volumetric ice concentration increases with increase in concentrations of PG, MEG and DEG.

8. For different concentrations of additives PG, MEG and DEG, the COP of the ice slurry generation system (74 litre capacity) is between 2.92 to 3.33 for PG, 2.75 to 2.88 for MEG and 2.30 to 2.55 for DEG.

9. The price of 74 litre capacity scraped surface ice slurry generator per TR comes out to be Rs.3858.

10. For water to water experiments in PHE, overall heat transfer coefficient, cooling duty and pressure drop for chilled water stream increase with increase in flow rate of chilled water. Thermo-hydraulic modeling gives satisfactory results for water to water heat transfer and pressure drop calculations and therefore, readily used for design and analysis of PHEs.

11. With increase in concentrations of PG and MEG, density, dynamic viscosity and Prandtl number increases whereas specific heat and thermal conductivity decreases with increase in concentrations. As compare to water, PG and MEG solutions having higher density, higher dynamic viscosity, higher thermal conductivity and higher Prandtl number whereas lower specific heat.

12. By flowing ice slurry in place of chilled water in plate heat exchanger, cooling duty found to be higher and pressure drop is slightly higher in case of ice slurry. Cooling duty of ice slurry increases with increase in antifreeze concentrations 10%, 20%, 30% and 40%. Cooling duty found to be increased by 50% at 0.3m^3/h and increased by 37 % at 3.0 m^3/h of 10% ice crystal PG ice slurry and pressure drop increased by 10% at 0.3m^3/h and increased by 7 % at 3.0 m^3/h.

13. It can be concluded that the present formulation provides the relationship to predict heat transfer based on the allowable pressure drops are reasonably matching with experimental data. The thermo-hydraulic model is useful for the design of individual PHEs. The model can be extended for the optimization of plate heat exchanger networks; this is because the optimization of plate heat exchanger networks requires the consideration of pressure drops at the initial stage.

6.2. SCOPE OF FUTURE WORK

The present scraped surface ice slurry generator can be further optimized by variations and modifications to the present design. Present technique can be analyzed for cost reduction and the product reliability can be reevaluated.